POLITECNICO
MILANO 1863

SCUOLA DI INGEGNERIA INDUSTRIALE
E DELL'INFORMAZIONE

Hydrogen production exploiting biomass: An industrial case study

TESI DI LAUREA MAGISTRALE IN
ENERGY ENGINEERING – TRACK "POWER GENERATION"

Author: **Francesco Campesi**

Student ID: 10598131
Advisor: Dr. Paolo Colbertaldo
Co-advisors: Prof. Stefano Campanari (PoliMi), Dr. Eleonora Cordioli (FBK)
Academic Year: 2021-2022

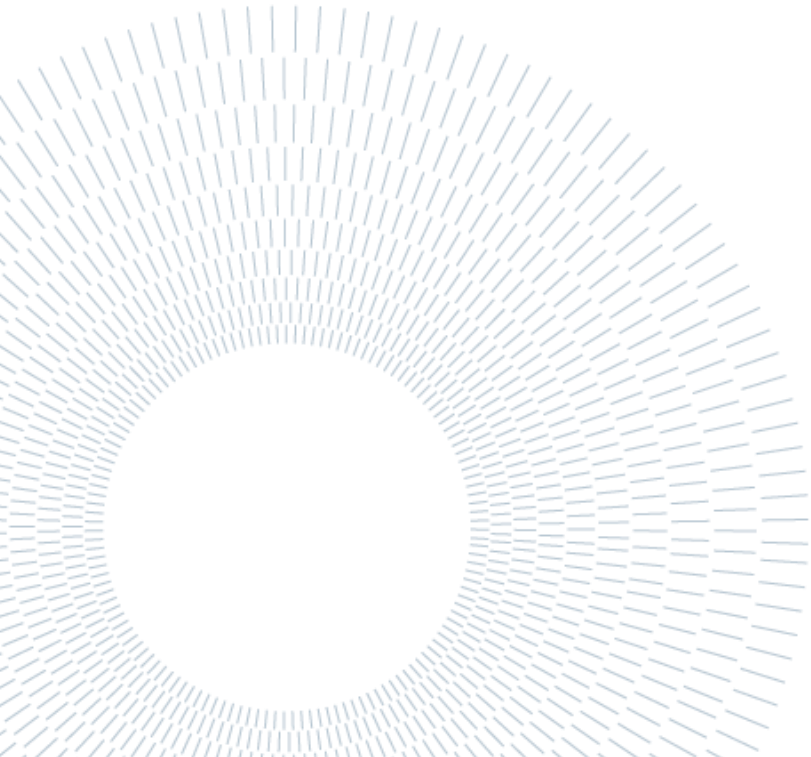

Abstract

Green hydrogen represents a relevant energy carrier that can help to face climate change challenges, as well as it may lead to greater energy independency of European countries. The thesis aims to analyze the hydrogen production exploiting biomasses according to an industrial case study. A fraction of the biomasses considered are byproducts of the vegetable oil production that is the main activity of the company, while the remaining part is procured on the market. Processes in the industrial area require high- and low-pressure vapor, as well as electricity. To satisfy these demands two CHP plants fed by biomass are operated according to vapors demands. The power plant is oversized in order to exploit the green certificates incentives on the excess electricity sold on the wholesale market. However, the company wants to evaluate new ways to valorize this electricity, since the incentives are ending in 2026. Therefore, according to the case study features, after a deep review of the state of the art of biomass-to-H_2 processes, a techno-economic assessment is performed on two configurations based on the most promising technologies. The first configuration is based on biomass steam gasification with syngas upgrading and purification processes. Gasification is modeled by literature experimental data, coupling the biomasses processed in the company with biomasses for which experimental data are available. Furthermore, gasification plant is assumed to operate at the nominal point for a target number of yearly hours. The second process is based on electrolysis which exploits the excess electricity of the industrial site. Given the dynamic features of electrolyzers, an hourly production logic is adopted according to process efficiency, electricity and H_2 prices. The analysis of the case study shows optimal sizes for both technologies, 20-30 MW_{th} of biomass input for gasification and 4.0-4.5 MW_e for electrolysis, at which correspond respectively a maximum hydrogen production of 2,558 t/y and 630 t/y. The LCOH according to 2019 energy prices are respectively about 5.0 €/kg and 3.5 €/kg, considering sizes of 30 MW_{th} and 4.5 MW_e. Gasification results to have a lower dependency on electricity price than electrolysis and it produces a valuable tail gas that is used to substitute NG in the industrial area. On the other side, electrolysis is more mature, and it requires a significantly smaller investment, hence it is less risky. Nevertheless, it is not possible to identify the best solution since the results vary according to electricity, NG, H_2 and biomasses prices. Since today's energy markets instability, sensitivity analysis is performed according to several energy markets conditions, showing when investment is feasible for each technology. Results show the need of incentives to invest in green hydrogen production according to technology features and H_2 end application, unless NG and H_2 prices are above 120 €/MWh and 6.67 €/kg, for which gasification configuration is already competitive.

Keywords: Hydrogen, biomass, electrolysis, gasification, tecno-economic assessment

Abstract in italiano

L'idrogeno verde rappresenta un importante vettore energetico che può aiutare ad affrontare le sfide del cambiamento climatico e a rendere i paesi europei più indipendenti dal punto di vista energetico. La tesi si propone di trattare la produzione di idrogeno sfruttando delle biomasse, basandosi su un caso studio industriale. Le biomasse sono in parte sottoprodotti della produzione di olio vegetale che è l'attività principale nel sito industriale, mentre la restante parte viene reperita esternamente. I processi nell'area industriale richiedono vapore ad alta e bassa pressione, oltre che elettricità. Per soddisfare queste esigenze vengono utilizzati due impianti di cogenerazione alimentati da biomasse che vengono gestiti in base alle richieste di vapore. Questi ultimi sono sovradimensionati in quanto l'eccesso di energia elettrica immesso nella rete nazionale è attualmente incentivato attraverso i certificati verdi. Tuttavia, l'azienda vuole valutare nuove modalità per valorizzare l'eccesso di elettricità, dal momento che l'incentivo scadrà nel 2026. Pertanto, secondo le caratteristiche del caso studio, e dopo un'approfondita revisione dello stato dell'arte dei processi di produzione di H_2 da biomassa, viene effettuata una valutazione tecno-economica per le configurazioni basate sulle due tecnologie più promettenti. La prima si basa sulla gassificazione della biomassa con vapore seguita da processi di upgrading e purificazione del syngas. La gassificazione è stata modellata da dati sperimentali di letteratura, accoppiando, secondo la composizione CHNOS, le biomasse trattate in azienda con quelle per le quali sono disponibili dati sperimentali. Inoltre, si assume che l'impianto lavori al punto nominale per un numero target di ore annue. La seconda configurazione si basa sull'elettrolisi, che utilizza l'elettricità in eccesso del sito industriale. Date le caratteristiche dinamiche degli elettrolizzatori, viene adottata una logica di produzione oraria in funzione dell'efficienza del processo e dei prezzi dell'elettricità e dell'idrogeno. L'analisi mostra che le dimensioni ottimali per questo caso studio sono di 20-30 MW_{th} di biomassa in ingresso al gassificatore e 4.0-4.5 MW_e per l'elettrolizzatore, a cui corrispondono rispettivamente una produzione massima di H_2 di 2,558 t/a e 630 t/a. Considerando taglie di 30 MW_{th} e 4.5 MW_e secondo i prezzi dei mercati energetici del 2019, il LCOH è rispettivamente di circa 5.0 €/kg e 3.5 €/kg. Tuttavia, la gassificazione risulta avere una minore dipendenza dal prezzo dell'elettricità rispetto all'elettrolisi e produce come sottoprodotto un syngas che viene valorizzato come sostituto del gas naturale attualmente utilizzato nell'area industriale. D'altra parte, l'elettrolisi è più matura e richiede un investimento notevolmente inferiore, quindi meno rischioso. Tuttavia, non è possibile identificare la soluzione migliore poiché i risultati sono legati ai prezzi dell'elettricità, del gas naturale, dell'H_2 e delle biomasse. Data l'instabilità dei mercati energetici odierni, viene eseguita un'analisi di sensibilità in base a diverse possibili condizioni dei mercati energetici, che mostra per ogni tecnologia quando l'investimento è fattibile. I risultati mostrano che, a meno di prezzi del GN e H_2 superiori a 120 €/MWh e 6.67 €/kg per i quali la gassificazione è già competitiva, sono necessari incentivi per investire nella produzione di idrogeno verde.

Parole chiave: Idrogeno, biomasse, elettrolisi, gassificazione, analisi tecno-economica

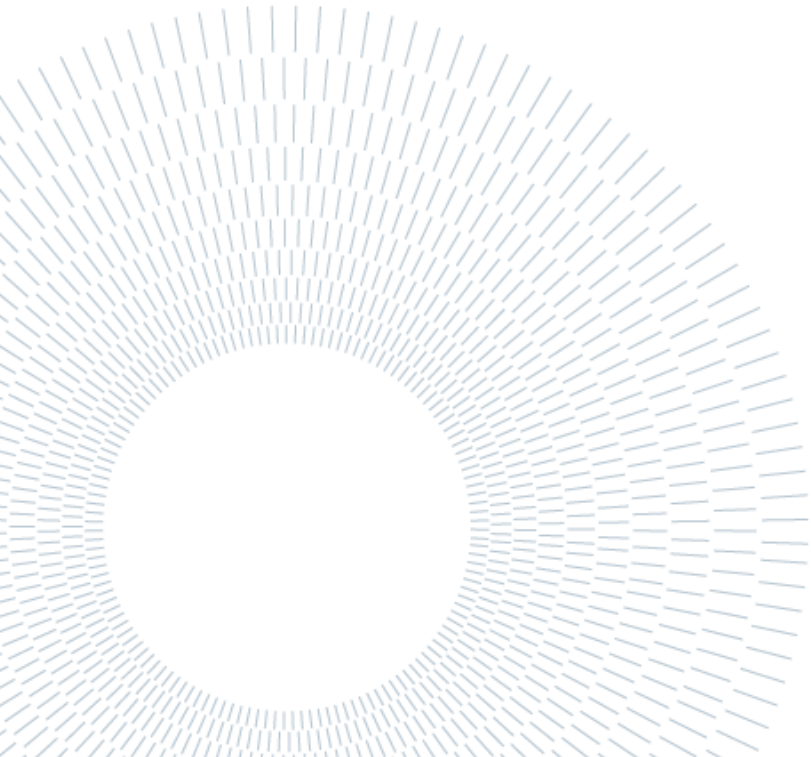

Contents

Introduction

The 21st century has several challenges to face, including the one against climate change, which is further complicated by the increase in global energy demand, partially due to increased demand by developing countries. The Paris agreement, adopted in 2015 and involving most of the nations around the world, aims to keep global temperature increase below 2° C in order to contrast climate change consequences. The European "net zero" goal, hence carbon neutrality achievement, set for 2050, has a similar target with further implications. Green hydrogen results as one of the energy carriers through which the energy transition can be achieved. In fact, green hydrogen represents the route to decarbonize the current hydrogen demand as well as a substitute for fossil fuels, helping the greenhouse gases (GHG) emissions reduction in several industries where electrification is not feasible, the so-called "hard-to-abate" sectors. Finally, green hydrogen production allows to improve the use of resources in the European countries, leading to an improved resilience and energy independency from other countries.

Nowadays, world hydrogen consumption is divided in three main industries. The oil refining sector accounts for 33%, where hydrogen is used mainly as reactant in hydrotreating and hydrocracking processes. Ammonia production rates for 27%, while methanol production is about 11% [1], [2]. The remaining fraction (29%) comprises several applications, such as steel production, food, and semi-conductor industries, as well as the manufacturing of chemicals [3].

Currently, world hydrogen production derives almost totally from fossil fuels. In fact, the 76% of the production is based on steam reforming processes of natural gas to which 10 t_{CO_2}/t_{H_2} CO_2 equivalent emission are associated. The 22% is ensured by coal gasification to which correspond GHG emissions of 19 t_{CO_2}/t_{H_2} [2]. Finally, only less than 2% is provided by electrolysis, which has GHG emissions accounted as zero if renewable electricity is used to carry out the process. Since 98% of today's hydrogen production is based on fossil fuels and carbon capture and storage (CCS) is not significantly utilized, hydrogen production has associated a great amount of GHG emissions, despite its consumption does not directly produce them.

Figure 1 shows current hydrogen value chain highlighting that, beyond dedicated hydrogen production, hydrogen is partially provided as mixture of gases since some applications do not need pure hydrogen. It also shows the amount of hydrogen currently supplied and consumed in the value chain, remarking how green and blue hydrogen production has an extremely minor role nowadays.

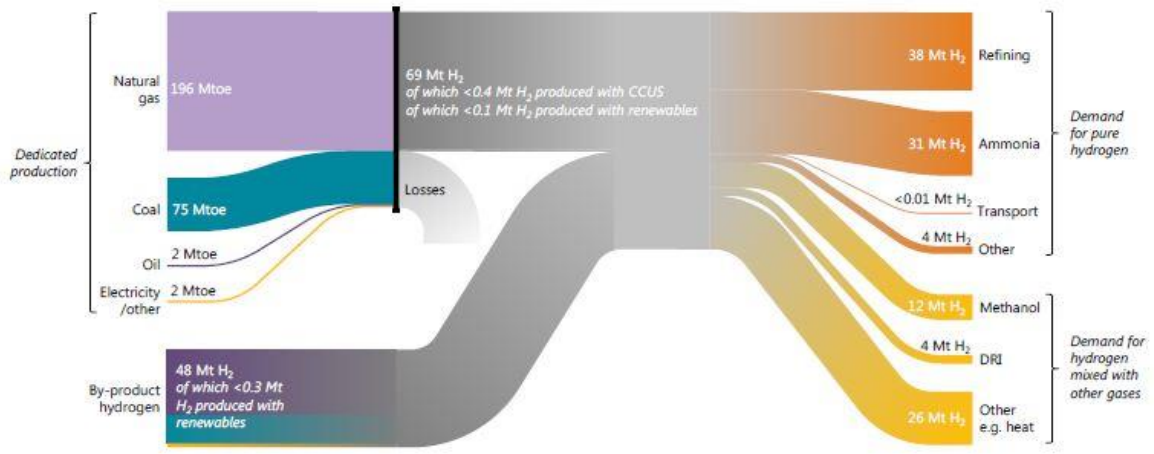

Notes: Other forms of pure hydrogen demand include the chemicals, metals, electronics and glass-making industries. Other forms of demand for hydrogen mixed with other gases (e.g. carbon monoxide) include the generation of heat from steel works arising gases and by-product gases from steam crackers. The shares of hydrogen production based on renewables are calculated using the share of renewable electricity in global electricity generation. The share of dedicated hydrogen produced with CCUS is estimated based on existing installations with permanent geological storage, assuming an 85% utilisation rate. Several estimates are made as to the shares of by-products and dedicated generation in various end uses, while input energy for by-product production is assumed equal to energy content of hydrogen produced without further allocation. All figures shown are estimates for 2018. The thickness of the lines in the Sankey diagram are sized according to energy contents of the flows depicted.

Figure 1: 2018 hydrogen value chain, adapted from [2]

However, hydrogen consumption is already growing in the industries where is currently utilized and its consumption should relevantly increase in the next future because new end applications for green and blue hydrogen will start according to the GHG emissions reduction objectives. Some likely new end uses are:

- Hydrogen injection into the natural gas (NG) grid in order to progressively reduce emissions related to NG consumption for industrial or household heating needs
- Hydrogen as reactant for synthetic fuel production
- Power generation via fuel cells as well as H_2 gas turbines
- Transport applications for which electrification is not feasible, like heavy and light duty vehicles that require long kilometric range and quick refueling time; maritime and aviation applications; railroad applications, for trains that are currently operated with diesel since there is no profitability in building electric infrastructures.

Furthermore, hydrogen production via electrolysis might help the electric grid to manage electricity fluctuations given by the increase of intermittent and aleatory renewables in the energy mix. In fact, electrolyzers may transform excess of electricity into hydrogen that could be stored for longer periods, as weeks or months, compared to storage with batteries. Afterward, it can provide electricity back to the grid, when it is needed, by means of fuel cells or it could be utilized in other applications.

The increase in hydrogen use must be coupled to a great increase in green hydrogen production in order to abate emissions related to current hydrogen demand and to give the possibility of helping the decarbonization of the sectors mentioned above. To reach this challenging target the main technology considered is electrolysis since it gives high feasibility to scale up the hydrogen production. At the same time, also production via fossil fuels coupled with carbon capture and storage could play a relevant role in the next 20 years. However, this technology cannot guarantee a complete emission reduction since 85-95% of CO_2 is captured as best, and some GHG emissions derive from the natural gas value chain [4]–[7]. The use of other possible and feasible solutions must be taken into account in order to achieve the final goals. Therefore, green hydrogen production from biomasses via thermochemical and biological processes might play a relevant role and provide local low hydrogen price spots, despite they cannot cover the main demand of hydrogen due to limited and regionally heterogeneous availability of biomasses. Hydrogen production from biomass will account for 8% of total demand in 2050, according to forecast [3].

Nowadays, hydrogen price depends strongly on natural gas and CO_2 prices because of today's production volumes. Therefore, according to the recent increase of the prices of both markets, the hydrogen price has become greater too. However, as reported in Figure 2, grey and blue H_2 are typically cheaper than green hydrogen in most of the cases. Electricity price increased as well, hence proper policies must be adopted in order to stimulate investor and commercial demand, and to limit investment risks related to uncertainty of energy markets.

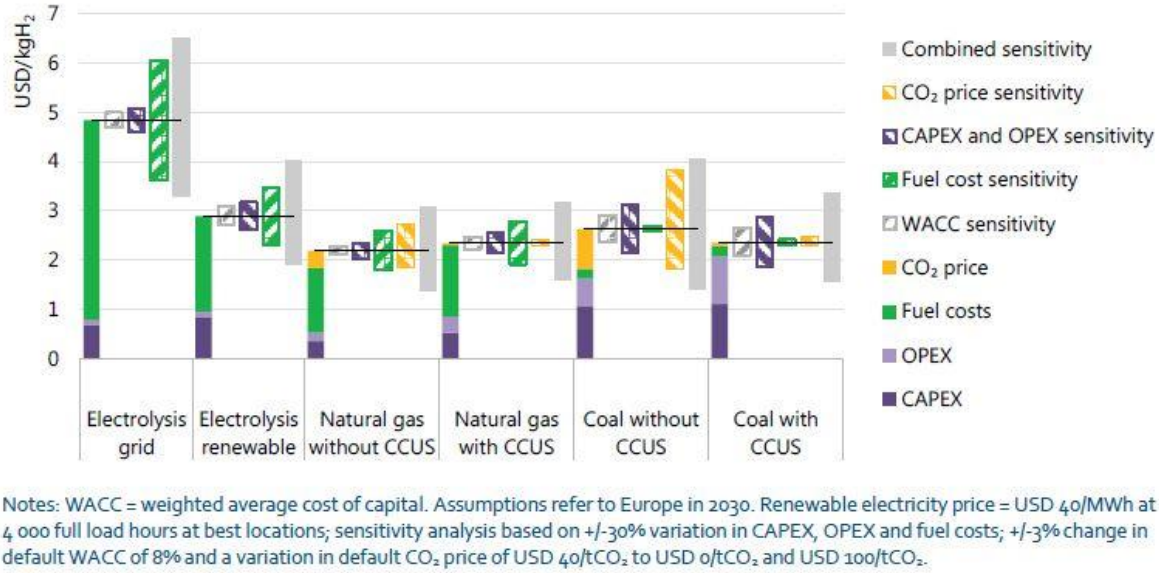

Notes: WACC = weighted average cost of capital. Assumptions refer to Europe in 2030. Renewable electricity price = USD 40/MWh at 4 000 full load hours at best locations; sensitivity analysis based on +/-30% variation in CAPEX, OPEX and fuel costs; +/-3% change in default WACC of 8% and a variation in default CO_2 price of USD 40/tCO_2 to USD 0/tCO_2 and USD 100/tCO_2.

Figure 2: LCOH vs main hydrogen production technologies, adapted from [2]

This thesis aims to firstly analyze the available biomass to hydrogen routes. Afterward, it wants to identify the most promising processes to produce hydrogen according to the

considered industrial case study features. Hence, the final purpose is to provide a techno-economic assessment for the most promising technologies in order to discuss general features of each configuration as well as to show for which of them and in which markets conditions bio-hydrogen production could be feasible for the analyzed case study.

1 State of the art

1.1. Overview of hydrogen production routes exploiting biomass

Hydrogen can be produced from biomass via thermochemical, biological, and electrochemical processes, hence there are several pathways to produce green hydrogen. Main routes are summarized in Figure 3. Thermochemical processes, that include gasification and pyrolysis, are processes that use heat to promote the chemical transformation of biomass into a useful product (syngas); biological processes involve the use of microorganisms for breaking down biodegradable material into biogas (mixture of mainly H_2 and CO_2); and electrochemical processes refer to water electrolysis, that leads to H_2 production using as inputs water and electricity. Starting from biomass, the electricity used for powering the electrolyzer can be generated by a power plant fed by biomasses.

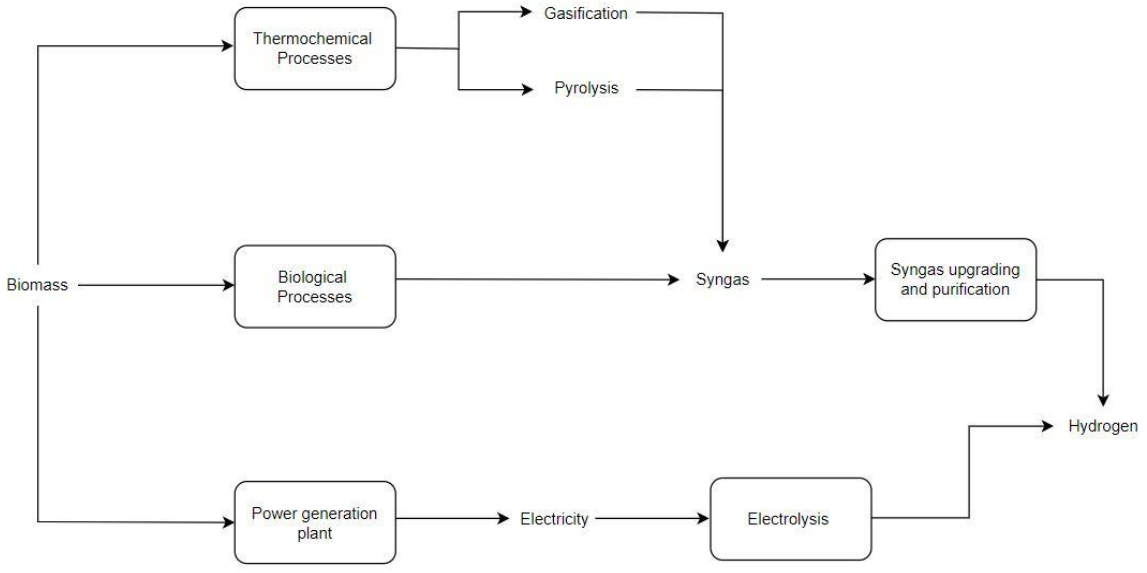

Figure 3: Overview of investigated biomass-to-H_2 routes

In the following sections these routes are briefly described, afterwards the most promising technologies for the industrial case study will be explained in detail.

1.1.1. Thermochemical processes

The two main processes characterized by a thermochemical conversion are gasification and pyrolysis. Both give as output a syngas with a hydrogen fraction that depends on the technology and its operating conditions. After a thermochemical process an upgrading section is always needed if the objective is to produce nearly pure H_2.

Gasification

Gasification is an endothermic process that is conducted at high temperature in an oxygen deficient ambient. This process can be used with different feedstock, from coal to different types of biomasses. Process maximum temperature is in the range of 700-1200°C and it depends on several aspects such as reactor type, gasifying agent, feedstock. The main distinction that must be done is according to the gasification agent: air, pure oxygen, steam or even a mixture of steam and O_2. Each of these options leads to completely different results, both at technical and economic level, hence it is relevant to describe their characteristics in order to be able to select the best configuration according to the application.

Furthermore, it is possible to distinguish "direct gasification" where the gasification agent works also as oxidant to partially oxidize the feedstock in order to supply the energy required from the endothermic process. On the other side, there is the so called "indirect gasification" in which the gasifying agent does not work as oxidant, for instance steam, therefore an external source of energy is needed.

The following equation (Eq. 1) represents general overall reaction for gasification:

$$Biomass + Steam/Air/O_2 \rightarrow H_2 + CO + CO_2 + LHC + tar + char + N_2 + H_2O \quad \text{Eq. 1}$$

The so called "char" is the resulting solid from biomass gasification, while "tar" represents the viscous liquid hydrocarbons created during the process. It is common to define tars as all organic compounds with a molecular weight higher than benzene. Every biomass gasification plant is subjected to problems related to tar, since it could condense, leading to plugging of downstream "cold" components in the upgrading section. In fact, tars typically have a dew point between 350°C and 150°C that is well above the minimum temperature in the plant that is close to ambient one [8][9]. Tar is also commonly distinguished into GC-MS tar and gravimetric tar. The first one is given by the sum of all single compounds that can be measured by gas chromatography coupled with mass spectrometry, while the gravimetric tars are heavy polycyclic aromatic hydrocarbons which cannot be detected by the previous equipment. The latter is the most difficult to reduce and it represents the main reason for fouling that impacts on downstream equipment. Therefore, it is crucial to understand how to reduce those components content and how to get reliable measures of the dew point.

Air, as gasification agent, is cheap and it works also as oxidant (direct gasification), but on the other side leads to a poor syngas quality since it is very diluted by nitrogen, hence the syngas is characterized by a smaller lower heating value (LHV). Moreover, the problem of nitrogen removal is added compared to the other configurations and at the moment there is not an economical way to separate the nitrogen from the gas stream, since the only technology to reach the requirement of pure hydrogen is a cryogenic process that exploits the lower boiling temperature of H_2 with respect to N_2 and other gases. Considering that the goal is to produce hydrogen, it must be underlined that gasification with air leads to lower gas and hydrogen yields. If compared with other options, it also shows a higher amount of tar and char that are detrimental for the equipment in the upgrading section. For all these reasons air as gasification agents is not typically considered for this application.

Oxygen still is a gasifying and oxidizing agent as air (direct gasification), but it provides better results in terms of gas yield and syngas quality since the stream is nitrogen free, so the LHV is higher; moreover, tar and char production decrease importantly. On the other side, it is extremely expensive since pure O_2 is produced by cryogenic process separating it from the ambient air. Despite the better performance, also this option is not the most investigated due to the very high cost associated with pure oxygen. It could have an economic sense just on some type of large-scale gasification plant.

Steam is just a gasifying agent (indirect gasification), and it represents a compromise between air and oxygen, in fact it is cheap if compared with pure O_2 but more expensive than air, since water has a low cost, but some energy is required to heat up and obtain superheated vapor needed for the process. Moreover, it has the advantage, as for the pure oxygen, to provide a syngas nearly free of nitrogen, and the presence of vapor enhances steam reforming reactions decreasing the amount of light hydrocarbons (LHC) and increasing H_2 fraction in the syngas.

Steam, compared to air, leads to have N_2 free syngas, typically lower content of tar and char, higher gas yield and H_2 fraction, hence it maintains some advantages of pure oxygen. Furthermore, on a dry basis the syngas LHV per mass unit is the highest since the H_2 yield increases thanks to reforming reactions [10]. Afterwards, the unreacted vapor can be used for water gas shift (WGS) reaction in following reactors to increase H_2 content. Finally, it is separated by condensation. Another advantage of using steam as gasification agent is the possibility to treat biomass with higher humidity, until 35 wt% [9], so in general costs to dry the biomass are reduced compared to other configurations in which a drier biomass is required.

Nowadays steam gasification looks as the most promising thermochemical process when the objective is to produce pure hydrogen in medium-size plants.

Table 1 shows differences in relevant parameters of biomass gasification, reported according to gasifying agent.

Table 1: Process features vs gasification agent [10]

Gasification agent	Air	Oxygen	Steam
Syngas LHV [MJ/Nm³]	4-6	10-15	15-20
Average syngas composition [vol%]	H_2: 15% CO: 20% CO_2: 15% CH_4: 2% N_2: 48%	H_2: 40% CO: 40% CO_2: 20%	H_2: 40% CO: 25% CO_2: 25% CH_4: 8% N_2 < 2%
Reactor temperature [°C]	900-1100	1000-1400	700-1200
Cost	Cheap	Costly	Medium

Pyrolysis

Pyrolysis is another thermochemical way to convert biomass into hydrogen, the main difference with respect to gasification is the absence of a gasification agent, consequently, since the process is endothermic, the heat required for the process must be provided indirectly. Typically, it works in a temperature range of 400-600°C at low pressure, until 5 bar [9], [11]. The overall reaction is reported in the following equation Eq. 2.

$$Biomass + heat \rightarrow H_2 + CO + CO_2 + CH_4 + H_2O + bio\_oil + char \qquad \text{Eq. 2}$$

It is possible to differentiate pyrolysis according to the operating temperature.

Conventional pyrolysis has an operating temperature under 450°C and this leads to high char production and a relevant part of bio-oil.

Fast pyrolysis occurs at 450-600°C and it is characterized by short residence time and therefore high heating rate that results in a higher bio-oil yield.

Flash pyrolysis has the objective of maximizing the gas yield therefore is similar to fast pyrolysis, but operating temperature is further increased above 600°C, and residence time become shorter and consequently the heating rate greater.

The lower operating temperature of pyrolysis is translated into lower gas and hydrogen yields and a higher production of char than in gasification processes. Moreover, bio-oil is a relevant product since after pyrolysis condensation can occur due to the lower temperature. The bio-oil is divided in soluble and insoluble in water. The latter has already a market, in

fact it can be destined to a cracking process to produce desired components, which may be used for instance in adhesive sector [9]; whereas the soluble bio-oil can be exploited via steam reforming reactions in order to improve the hydrogen yield [9], [11].

Pyrolysis is mostly indicated for bio-oil production and the hydrogen yield is much smaller if compared to steam gasification. Moreover, the high presence of tar and char makes the upgrading processes more complex with a high risk of fouling and plugging of downstream equipment [9],[10].

1.1.2. Biological processes

Biological processes produce a gas (biogas) with a different composition and a different H_2 yield compared to thermochemical processes. The main products of biological conversion of biomass are hydrogen and carbon dioxide, and the biogas yield is lower than the syngas yield in gasification as well as the H_2 content. These processes are operated at low temperature (30-80°C) and typically at ambient pressure, hence the energy required is lower as well as the associated cost. There are several possibilities of process according to the enzymes and microorganisms used to catalyze hydrogen formation, some interesting examples, allowing to directly produce a high H_2 content biogas, are "Dark fermentation, Biological WGS, and Photo-fermentation"[9], [12]–[14].

Biological processes have more potential if feedstocks are waste biomasses such as municipal, industrial, and agricultural organic waste. These feedstocks give typically better performances and the low or negative cost associated to them makes these technologies more feasible also at economical level [9], [12], [13], [15].

It is possible to distinguish biological pathways according to the need of sunlight for the processes as reported in Figure 4 together with representative reactions for each process. In particular, the most promising light dependent process is the so called "Photo-fermentation". This process uses as main reactant organic acids or volatile fatty acids (VFAs) or also glucose, and by the action of photosynthetic non-sulfur (PNS) bacteria hydrogen is produced. The main PNS organisms used to catalyze H_2 formation can be found in [13]. Photo-fermentation occurs in anerobic condition, and it is strongly affected by available sunlight, therefore is fundamental to guarantee a sufficient area through which light can be absorbed. Other parameters that affect process yield are Ph value and temperature, and typical optimal values are in the range of 6.8-7.5 and 31-36°C, respectively [13].

The most promising light independent process is "Dark fermentation". It occurs in a no light and anerobic environment where rich carbohydrate substrates, like glucose, are decomposed thanks to several possible microorganisms, some of them are listed in [12]. More in detail, hydrogen is produced exploiting the excess of electrons generated during oxidation of the organic substrate. Hence, through the catalytic activity of the hydrogenase enzyme, under anerobic condition protons work as electron acceptors and consequently H_2

is produced. As shown in Figure 4 the products of dark fermentation are hydrogen, carbon dioxide and VFAs. Several studies proposed a two steps solution, so a dark fermentation section followed by a photo fermentation one, since this latter process can exploit the generated VFAs from the previous section to enhance the hydrogen yield [12]–[14].

The optimal temperature range for dark fermentation is between 25°C and 80°C according to the type of microorganisms adopted to carry out the process. In a similar way Ph values can typically vary between 5.5 and 8.5 according to the feedstock as well as microorganisms' characteristics.

One of the main challenges related to dark fermentation is caused by hydrogen-consuming bacteria (HCB) that significantly affect the hydrogen yield. Hence, a pretreatment process is needed in order to inhibit activity of HCB to improve the H_2 production.

Compared with other biological processes, dark fermentation is the most studied and promising technology since it has the highest hydrogen production rate, and it can treat a wider spectrum of biomasses. Other advantages compared to photo-fermentation are due to the no light requirement, which is translated into continuous operation (day and night) and a simplified design of the equipment [12], [13].

Biological conversion of biomass directly into hydrogen is still under development therefore all the discussed configurations are under research and just few pilot plants are present, in fact the technology readiness level (TRL) of this type of technology is low (4-5), hence far from commercialization. The main factors that are limiting the development and scaling of this technology are the low H_2 yield and the time-consuming production (months) since the reactions occur typically inside batch reactors. Furthermore, compared to thermochemical conversion, this technology requires specific feedstock that can react with the enzymes, hence it is less flexible to the inputs.

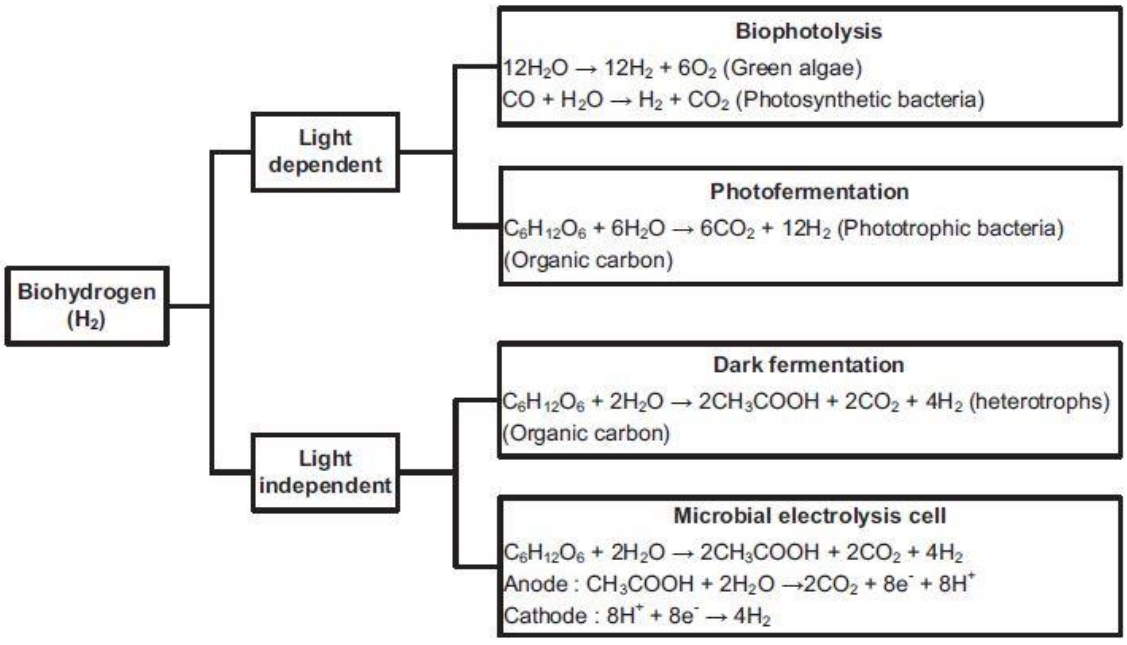

Figure 4: Biological processes for biomass-to-H_2, reprinted from [12]

A mention about anerobic digestion must be done, although it does not directly produce hydrogen. This process occurs in a closed reactor (digester) where no air or oxygen are present. It typically processes waste biomasses defined as organic, for instance animal manure, sewage sludge, food waste and other industrial organic residuals. Anerobic digestion leads to biogas production, which is mostly methane and carbon dioxide with very small amounts of water vapor and other gases. Therefore, if the objective is to produce hydrogen, after a CO_2 separation, the purified bio-methane must undergo a steam reforming process as for hydrogen production from natural gas. To conclude, anerobic digestion preserves some features of other biological processes, such as the low flexibility due to the specific biomass required as well as the relatively slow production in low temperature batch reactors. However, it is a commercial process, therefore much more mature and so potentially competitive compared to the biological processes described previously.

1.1.3. Electrochemical processes

The main electrochemical process is water electrolysis, but it requires a double process to produce hydrogen from biomass. In fact, biomass must be firstly transformed into electricity by a proper power generation plant, and afterwards the electricity is fed to the electrolyzer in order to produce hydrogen.

Although two transformations are needed, this solution could have a techno-economic sense for several reasons. It has lower complexity since it does not require upgrading and purification processes as mentioned for the above thermochemical and biological processes. In fact, delivered hydrogen from an electrolyzer might be already compliant to the requirements. Finally, compared to the previous technologies it results to be the one with the highest readiness, despite a lot of research and development is still going on nowadays.

Water electrolysis is a relatively simple process that is based on two electrodes, the anode (positive electrode) where oxidation reaction occurs leading to the generation of electrons, and the cathode (negative electrode) where reduction reaction occurs consuming electrons. The electrodes are kept in two separated environments by a membrane or diaphragm in order to have two half cells in which different reactions can occur, hence it has the aim of preventing gas crossover between half-cells. The electrolyte, which could be even part of the membrane, is the media that enables transport of chemical ions and between the two half-cells [4], [16], [17].

Given the endothermic nature of the electrolysis process, a supply of electricity is required, in fact reactions take place only if a sufficient electrodes voltage difference is applied. If so, hydrogen is produced at the cathode, while oxygen at the anode, as shown in Figure 5. Electrolyzers work with direct current (DC) supply, therefore it is typically needed a power

supply equipment that comprises a transformer and a rectifier that coverts alternated current (AC) into a DC supply [17].

Electrolyzers as well as fuel cells have a relevant peculiarity compared to typical processes or components. In fact, electrolyzer efficiency increases at partial load thanks to the reduction of ohmic losses because of lower current, and thanks to lower mass transport losses.

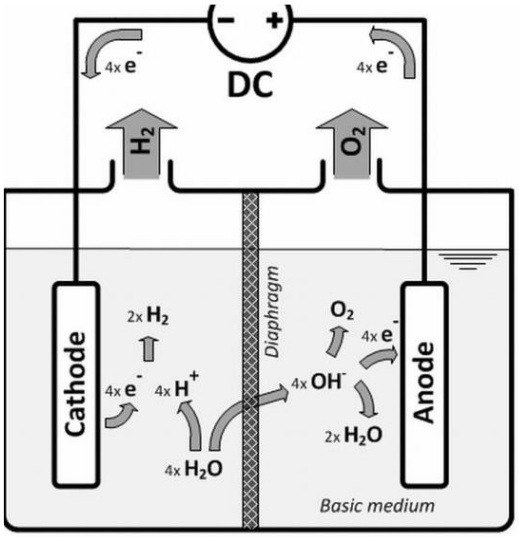

Figure 5: Simplified scheme for ALK electrolysis cell, reprinted from [17]

Several electrolyzers are currently studied, the alkaline (ALK), the proton exchange membrane (PEM), the anion exchange membrane (AEM) and the solid oxide (SOEL) electrolyzers. However, the most promising for low temperature applications in the next future are the ALK and PEM electrolyzers since they have a higher readiness which allows the creation of commercial applications at MW-scale.

The overall electrolysis reaction is reported in Eq. 3 and it is the same for PEM and ALK technologies, as well as the equilibrium potential difference equal to 1.23 V. However, these two options have several differences in terms of half-cell reactions, transported ions, electrolyte, membrane/diaphragm, adopted materials and balance of plant (BoP). This leads to different characteristics in terms of performances and costs, as it will be explained.

$$H_2O + electricity \leftrightarrow H_2 + \frac{1}{2}O_2 \qquad \text{Eq. 3}$$

Finally, it must be mentioned that some studies about direct electrochemical conversion of biomass are currently under investigation. The biomass is fed directly at the anode while at the cathode hydrogen is produced. The concept is similar to the one of traditional electrolyzers, but it is at a very early stage of research so it cannot be considered as a promising technology at the moment [9].

1.2. Focus on the most promising technologies

The two most promising technologies for the case study under consideration in this study are identified as biomass steam gasification and water electrolysis. They are chosen considering together two factors:

- The case study characteristics, hence, mainly the type of available biomasses and their amounts currently processed by the company
- The features of analyzed biomass-to-hydrogen processes.

Therefore, a detailed description of current state of art of these two processes is presented in this section.

1.2.1. Steam gasification

Steam gasification has been investigated with particular attention in the last decades for biomass to syngas with high H_2 content conversion in medium size plants because of the high gas and H_2 yields, and the better economic feasibility given by steam as gasifying agent.

Pure hydrogen is obtained after several successive steps. The outgoing flow from the gasification reactor must pass through a cleaning section and afterward syngas is treated in upgrading and purification sections. All the main components are described below.

Gasification reactor

Starting from the gasifier, it is useful to identify the possible reactor configurations, also according to the fact that the process is characterized by an indirect gasification, since the gasifying agent (steam) does not work as oxidant that partially oxidizes the biomass. Therefore, the heat required from the overall endothermic process has to be introduced in an external way. Firstly, it is useful to define the "cold gas efficiency" CGE (Eq. 4) since it shows the degree of effectiveness of the overall gasification process, taking into account also the fuel needed to produce the steam and the additional fuel that might be needed to control the temperature in the reactors. The CGE is a parameter defined as the ratio between the energy related to the syngas in output and the input energy related to the biomass and additional fuel:

$$CGE = \frac{m_{syngas} \cdot LHV_{syngas}}{m_{biomass} \cdot LHV_{biomass} + m_{add\_fuel} \cdot LHV_{fuel}} \qquad \text{Eq. 4}$$

Where m [kg/s] is the mass flow rate and LHV [MJ/kg] the lower heating value related to each input and output. The cold gas efficiency gives an idea of the process efficiency.

There are different types of reactors that can be applied to this project [18]–[21]:

Fixed bed reactor is the simplest option since the bed material does not move inside the reactor. In fact, it is present a proper matrix on which bed material and catalyst are placed. For this reason, it is also easy to split the reactor in zones where different processes occur at different temperatures. Drying, pyrolysis, reduction and combustion are the main zones that take place with an increasing temperature.

As shown in Figure 6 there are two main configurations of fixed bed reactor according to where the ingoing and outgoing streams are placed:

- "Updraft gasifier" is a counter-current layout where the feedstock is fed from the top, while the gasifying agent from the bottom and finally the syngas leaves the reactor in the top part.
- "Downdraft gasifier" is a co-current reactor, hence input streams are both fed in the top part, in particular the gasifying agent is introduced at reactor sides, while in the bottom part ashes are separated and the syngas goes out from the reactor.

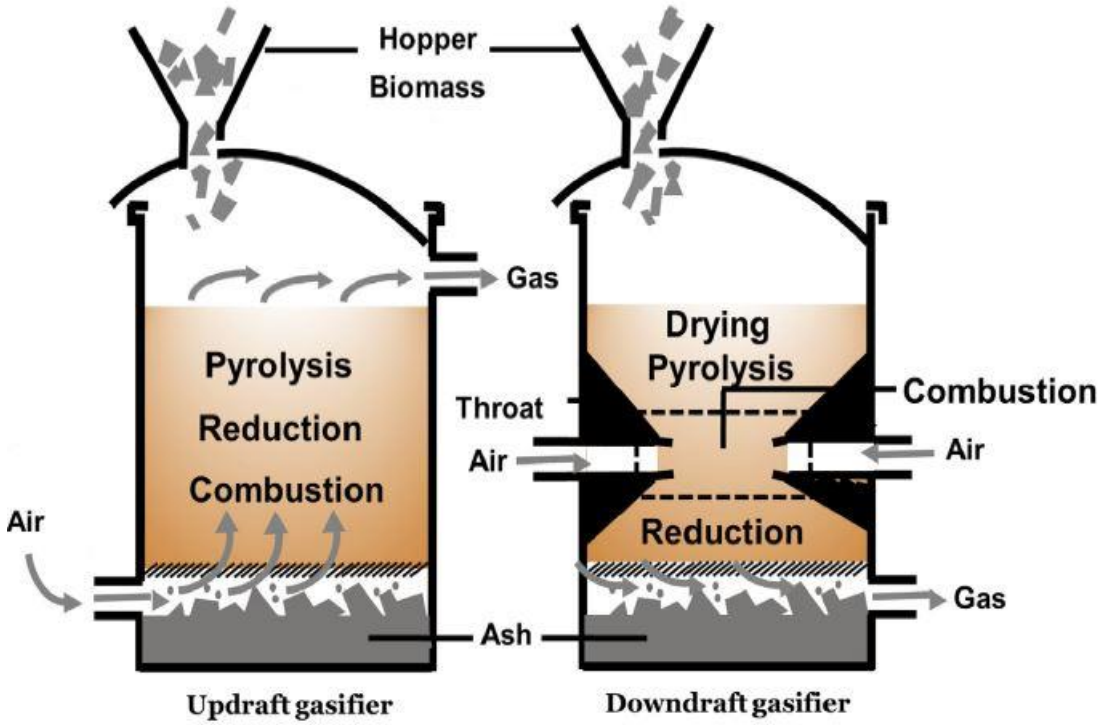

Figure 6: Simplified schemes of fixed bed reactors, reprinted from [21]

These different configurations give obviously different performances, from one hand the updraft gasifier is simpler, and it has a more efficient internal heat exchange, in fact the syngas outlet temperature is the lowest. On the other hand, the downdraft layout allows to have better tar cracking thanks to the different position of combustion zone and different syngas flow direction. The highest temperature in the reactor is achieved in the middle of the reactor where the gasifying agent is fed, and combustion occurs. Afterward, the syngas generated in the pyrolysis zone together with an important fraction of tar, goes through a hot section before leaving the reactor leading to a relevant tar content reduction.

Fixed bed reactors are typically used in direct gasification plants where air or pure oxygen or even a mixture of them are used. In this case it also represents the cheapest configuration since just a simple reactor is enough to also satisfy the heat demand. If pure steam is used as gasifying agent, the heat should be supplied by an external source. Hence, fixed bed reactor is not typically considered for steam gasification because it would be difficult to supply in a proper way all the required heat, even if hot tubes are placed inside the gasifier to provide heat.

Fluidized bed reactor is characterized by small particles as bed material, that are moving inside the reactor. In fact, the bed material and the feedstock particles, which are fed into the reactor typically at a middle height, are fluidized by the gasifying agent that is injected at the bottom of the reactor. It is possible to distinguish two categories of fluidized bed according to the gaseous stream velocity, as depicted in Figure 7. The particle terminal velocity represents the velocity such that gravitational force and drag force are equal and opposite, hence particle ideally does not move along the reactor height. The "bubbling fluidized bed" (BFB) reactor is characterized by a velocity of the gasification agent (1-3 m/s) lower than terminal velocity of solid particles in order to guarantee that solid materials (bed material, char and ash) move inside the reactor, but they do not leave it. While "circulating fluidized bed" (CFB) has a gasification agent velocity (5-10 m/s) that is higher than particles terminal velocity, hence solid particles are dragged from the gas flow outside the reactor and after they are separated from the gas stream by a cyclone.

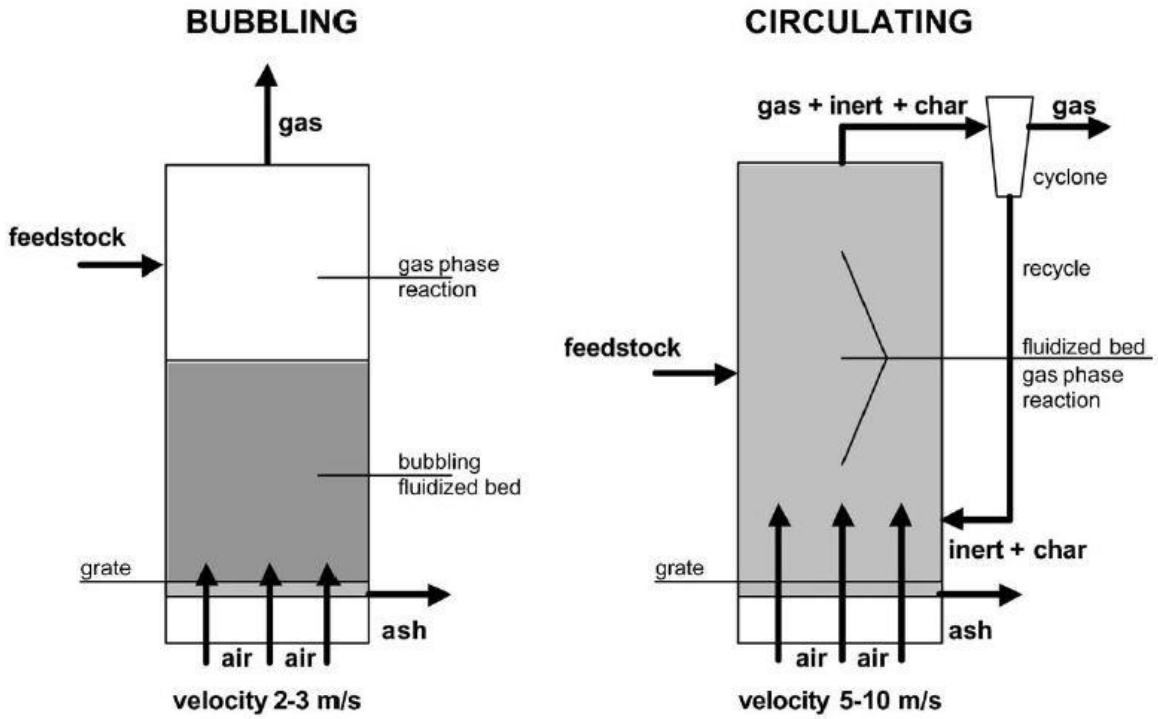

Figure 7: Simplified schemes of Bubbling (BFB) and Circulating Fluidized Bed (CFB) gasifiers, reprinted from [20]

Thanks to the fluidized regime, compared to fixed bed reactor, BFB and CFB reactors are more compact since the mixing and the heat transfer is enhanced leading to a greater

conversion rate. Moreover, the temperature profile along the gasifier height is more uniform since it is not properly possible to separate set of reactions in different zones. Finally, they are more suitable to scale up since typically fixed bed reactors have a maximum size of few MW.

Main drawbacks of fluidized bed reactors are due to the potential melting of ash, in fact the gasifier is commonly not operated above 900°C to avoid that phenomenon. Moreover, fluidized bed reactors require a better equipment for biomass preparation since particle size should typically be smaller than 10 mm.

Comparing the two types of fluidized reactors it is possible to notice that CFB has an improved gas-solid interaction thanks to a greater turbulence, but on the other side the residence time is typically smaller. Due to these characteristics, particles show lower tendency to agglomeration and segregation. Finally, CFB bed material should have better mechanical properties since it is subjected to a higher erosion due to the higher velocities.

A last possible option is the so called "**entrained bed reactor**" that is based on a direct gasification; a mixture of O_2 and steam is typically used.

The feedstock is fed together with the gasifying agent at a velocity higher than flame speed from the top via several burners, as shown in Figure 8. The entrained bed is characterized by very short residence time and a very high temperature, that is needed to achieve a proper conversion. For this reason, the oxygen consumption is typically higher than other direct gasification reactors. The high temperature leads to ash melting that is collected in the bottom part of the reactor where it can be removed after its solidification.

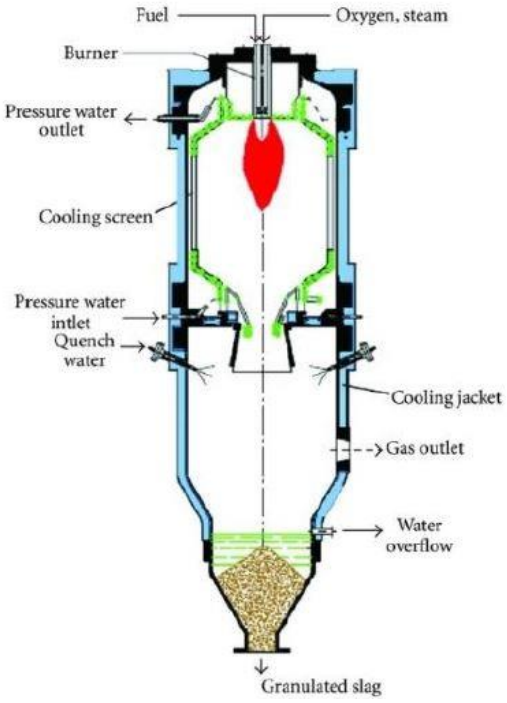

Figure 8: Entrained bed reactor scheme, reprinted from [19]

The main disadvantage of this reactor for biomass gasification is due to the strong requirement on feedstock particle size that must be extremely small in order to achieve good fluidization and reaction area.

The entrained bed reactor is suitable for large scale application of coal gasification since it is more compact thanks to his features, giving a reasonable magnitude of the reactor. Furthermore, it is coupled with an air separation unit to produce O_2 that results economically feasible only for large plant. It cannot be utilized for biomass gasification mostly due to different feedstock properties. In fact, biomass fibrous structure and tenacity make more difficult and expensive to grind biomass to the required size.

There are two main feasible options for indirect gasification [3],[4]:

1. Dual fluidized bed (interconnected fluidized bed reactors)
2. Indirectly heated fluidized bed reactor

Dual fluidized bed

The "dual fluidized bed" (DFB) configuration (interconnected fluidized bed reactors) is based on two fluidized beds, typically one BFB and one CFB, that are connected in order to exchange solid particles. The idea is to have the gasifier in which steam is fed together with

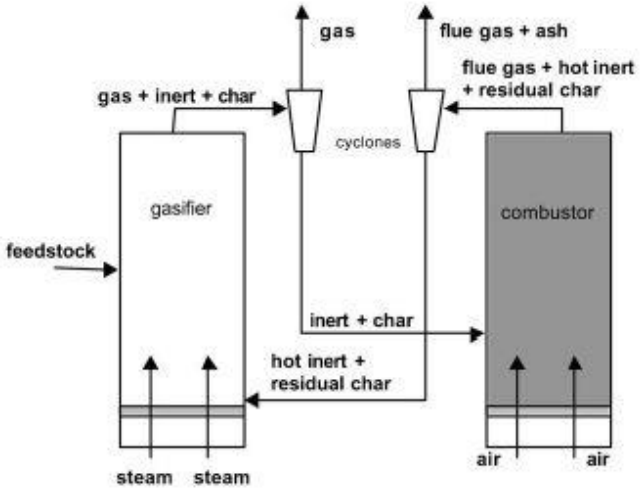

Figure 9: Simplified DFB scheme reprinted from [20]

biomass to produce syngas and secondary products as char. The latter is guided together with the bed material into the combustor reactor in which char is oxidized thanks to the feeding of an air stream, releasing heat that afterward is transported to the gasifier reactor via bed material, as shown in Figure 9. Therefore, the circulating bed material works as carrier of char from gasifier to combustion reactor and as heat carrier from the combustor to the gasifier. Moreover, it could be used as a catalyst to enhance certain reactions increasing gas yield and decreasing the amount of tar.

This technology is similar to that one adopted in fluid catalytic cracking (FCC) process for gasoline production in refinery industry, in fact, during the process carbon deposits (coke) deactivates the catalyst particles that are regenerated in the combustor producing also the heat to sustain the process. This note has the objective of explaining that, this type of configuration is well known since it is also used in an already developed sector. For this reason, the analyzed option is the easiest to scale up.

The advantage of this configuration is the ability to operate with two separated gas streams in the reactors. In the gasifier, steam is introduced, and syngas leaves the reactor as a nitrogen-free stream (<1%) [22], while in the combustor air is fed to oxides char, afterward the exhaust gases are sent to the energy recovery and post treatment systems, while the bed material is guided back into the gasifier providing heat. Hence, it is possible to obtain a N_2 free syngas using char as main fuel that provides heat to sustain the process, even if an extra fuel addiction could be present to regulate better the temperature in the gasifier. An advantage is represented by the gasification temperature that at least partially self-regulates since a decrease of gasifier temperature leads to higher char production which means more fuel for combustion, hence more heat is released during its combustion.

On the other side, typically indirect gasification requires greater investment and maintenance cost for reactors than direct gasification with air or oxygen.

The dual fluidized bed reactor represents the best working technology for biomass steam gasification since there are some successful commercial examples such as the Güssing plant in Austria that produces syngas from wood chips with a thermal input of 8 MW_{th} since 2001 [18]. Other examples can be found in [23].

In general, as for the Austrian plant, it is preferred to associate the gasifier with a bubbling fluidized bed (BFB) and the circulating fluidized bed (CFB) to the combustor, since it permits a higher residences time in the gasifier leading to a lower tar level and a higher hydrogen fraction.

Another famous example of DFB configuration is the "MILENA" gasifier, that is based on the same concepts, but the type of reactors is inverted, so the gasifier is operated as a fast fluidized bed (riser), while the combustion reactor is operated as BFB. Therefore, after the riser, bed material and char are separated from the syngas decreasing gas velocity thanks to a bigger section, afterward through a downcomer the solid particles reach the BFB combustor in which char is oxidized releasing heat that is transferred to the riser via bed material. A simplified scheme of "Milena" reactor is shown in Figure 10.

Compared to previous DFB configuration, Milena design leads to lower hydrogen yield and a greater amount of tar given the shorter residence time, but on the other side less steam is required as a gasifying medium, therefore a higher CGE is obtained. On the other side, there are no operating commercial plants from the literature, therefore the DFB option results more mature and ready to scale up.

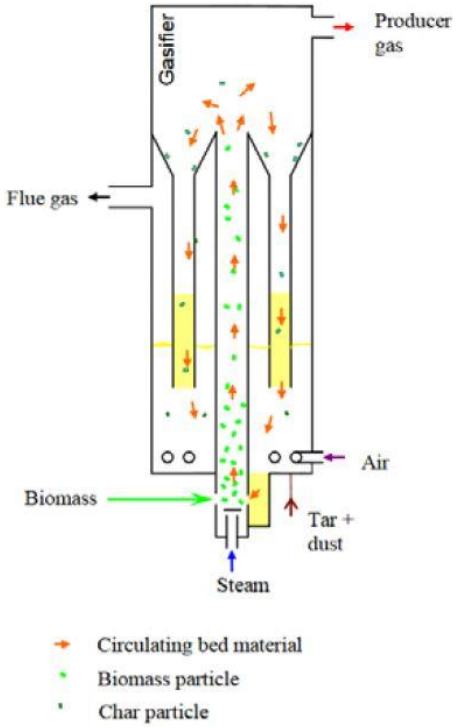

Figure 10: Simplified example of MILENA reactor, reprinted from [24]

Indirectly heated fluidized bed

The indirectly heated fluidized bed technology (Figure 11) is based on a different concept, in fact combustor and gasifier are completely separated, therefore it allows the usage of several fuels, and it is possible to operate the two reactors at different pressures. The bed material does not work anymore as heat carrier, but it remains inside the reactor (typically BFB reactor) with the main aim of catalyzing the reactions. Therefore, the heat needed for the process is provided in another way.

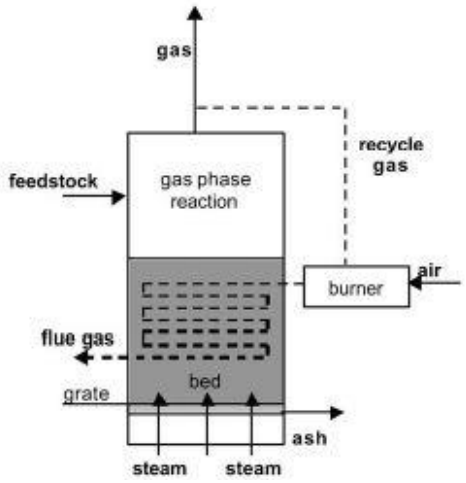

Figure 11: Indirectly heated fluidized bed, reprinted from [3]

An option was presented in 1993 (Figure 12) in which a fraction of syngas or another fuel is fed in the combustor and afterward the hot exhaust products pass through heat exchanger tubes inside the gasifier to release the heat needed. This configuration was not really performant due to the poor heat transfer given by the exhaust gases. Even though an impressive number of tubes were installed, it was not possible to reach the same operating temperature in the gasifier that is achieved in DFB configuration, therefore in this case was mandatory to implement a catalyst. In any case, the conversion is affected by the low temperature since the process equilibrium is thermodynamically favored at higher temperature because of its endothermic nature.

A more promising technology is the "heat pipe reformer" proposed in 2003 (Figure 13) that also has few examples of small-scale operating plants [18]. Instead of using heat exchanger tubes in which combustion products flow, the idea is to substitute them with heat pipes to transfer heat from the external fluidized combustor to the fluidized bed gasifier. This solution is based on closed tubes filled with liquid metals, for instance, sodium, which enhances the heat transfer from the combustion zone (in the bottom) and the gasification section in the top part. Hence, sodium vapor is generated in the combustion zone and after reaching the top part of the pipe that is inside the gasifier, it condenses releasing heat for the gasification process. This configuration significantly improves heat transfer performance thanks to the exploiting of condensation and evaporation that guarantee the highest heat transfer coefficient, in fact it also allows a reduction in the number of tubes [18].

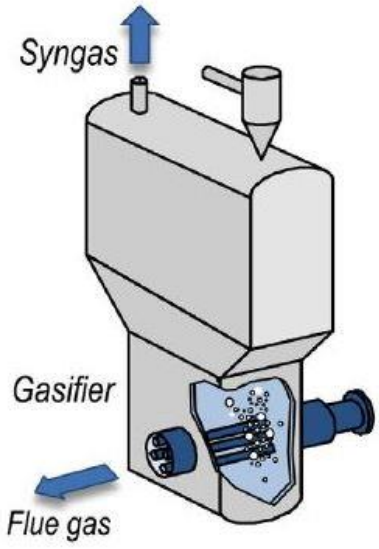

Figure 12: Pulse combustor 1993, reprinted from [18]

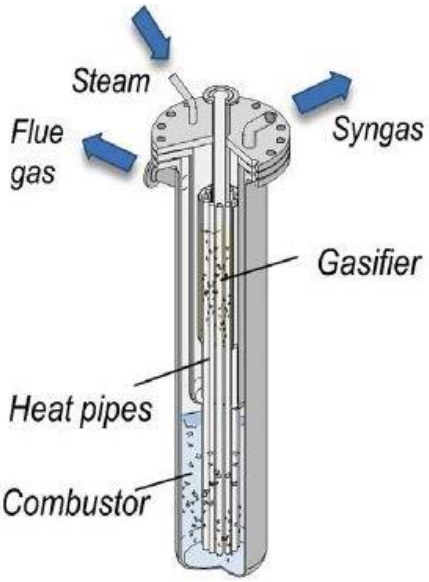

Figure 13: Heat pipe reformer 2003, reprinted from [18]

The main advantage of this configuration compared to the DFB technology is the great flexibility with a wide range of feedstocks and the absence of any risk for N_2 crossover. On the other side, despite the improvements in the heat transfer, the solution adopted in DFB plant with bed material that works as carrier, guarantees better performance, reliability, and the scale up is more feasible in the short period. In fact, there are just few small-scale plants of heat pipe reformer, and the technology has a lower readiness.

For what said until now the best reactor configuration is the DFB solution if the target is hydrogen production from biomass in a short term, since there are already commercial plants, and it is the easiest plant to scale up. For these reasons next paragraph on gasification theory and parameters is related to DFB technology. Despite that, most of the concepts are generally referred to steam gasification, therefore they can be adopted to further analyze more in detail even the mentioned above technologies.

Biomass gasification fundamentals and parameters

Via gasification biomass is converted into syngas that is mainly composed by H_2, CO, CO_2, H_2O, CH_4, light hydrocarbons (LHC), liquid hydrocarbon (tar), and nitrogen (NH_3, HCN) and sulfur (H_2S, COS) compounds depending on the biomass composition. The DFB gasifier typically works between 800°C and 900°C with a pressure close to the ambient one.

Biomass gasification can be divided ideally into two main steps, a first phase where the feedstock passes through a drying and pyrolysis process during which volatile compounds and char are formed, afterward a second phase where gasification and combustion reactions occur. In a fluidized bed, it is not possible to clearly separate temperature zones along the reactor as in a fixed bed reactor and this is also translated in a more uniform temperature inside the reactor.

The DFB reactor scheme in Figure 14 reports the inlet, outlet, and internal fluxes with their pathways. On the right the gasifier working as a BFB reactor where steam is fed from the bottom while biomass enters from a higher position as well as the regenerated hot bed material. Most of the reactions take place in the lower part where bed material and char are accumulated, while the syngas goes in the top part where some reactions still occur before it leaves the reactor. The solid particles collected on the bottom pass through a duct to reach the combustor that is developed as a riser (CFB) fed by air from the bottom, hence combustion of char (and any additional fuel) occurs. Afterward heated bed material is separated and guided back into the gasifier, while the exhaust gases leave the combustor from the top and they will further be utilized to exploit their high temperature, typically in this sequence: air preheating, steam generation, and fuel drying. The two fluidized reactors are connected by upper and lower seal loops that are fluidized with steam in order to avoid possible gas leakage between the two streams inside the gasifier and combustor.

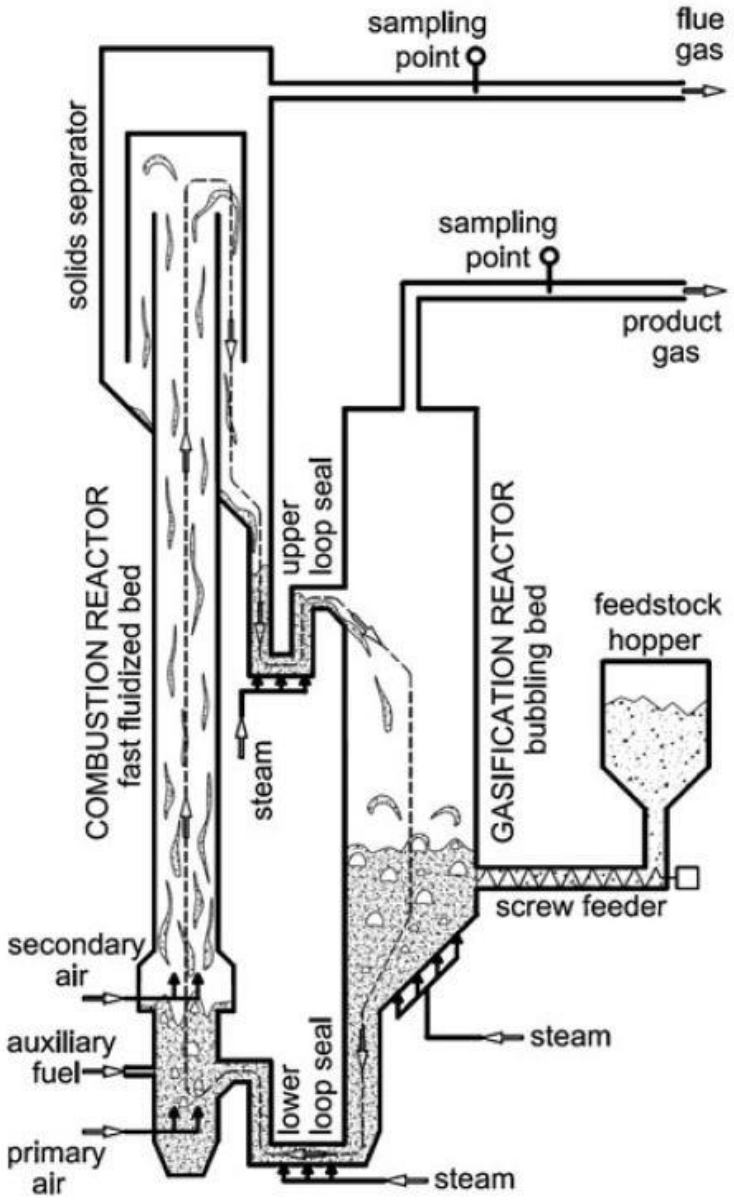

Figure 14: DFB detailed scheme for a pilot plant of 100 kW_{th}, reprinted from [22]

In the gasifier it is possible to distinguish two main groups of reactions, heterogeneous and homogeneous. In the following formulas representative reactions that take place inside the gasifier are presented [9], [21], [22], [24].

Heterogeneous reactions (solid-gas):

$$C + O_2 \leftrightarrow CO_2 \qquad \Delta H_{reac} = -394\ kJ/mol \qquad \text{Eq. 5}$$

$$C + 0.5O_2 \leftrightarrow CO \qquad \Delta H_{reac} = -111\ kJ/mol \qquad \text{Eq. 6}$$

$$C + H_2O \leftrightarrow CO + H_2 \qquad \Delta H_{reac} = +119\ kJ/mol \qquad \text{Eq. 7}$$

$$C + CO_2 \leftrightarrow 2CO \qquad \Delta H_{reac} = +160\ kJ/mol \qquad \text{Eq. 8}$$

$$C + 2H_2 \leftrightarrow CH_4 \qquad \Delta H_{reac} = -88\ kJ/mol \qquad \text{Eq. 9}$$

Homogeneous reactions (gas-gas):

$$CO + H_2O \leftrightarrow CO_2 + H_2 \qquad \Delta H_{reac} = -41\ kJ/mol \qquad \text{Eq. 10}$$

$$CH_4 + H_2O \leftrightarrow CO + 3H_2 \qquad \Delta H_{reac} = +203\ kJ/mol \qquad \text{Eq. 11}$$

$$CH_4 + 2H_2O \leftrightarrow CO_2 + 4H_2 \qquad \Delta H_{reac} = +162\ kJ/mol \qquad \text{Eq. 12}$$

$$CO + 0.5O_2 \leftrightarrow CO_2 \qquad \Delta H_{reac} = -283\ kJ/mol \qquad \text{Eq. 13}$$

$$H_2 + 0.5O_2 \leftrightarrow H_2O \qquad \Delta H_{reac} = -242\ kJ/mol \qquad \text{Eq. 14}$$

$$CH_4 + CO_2 \leftrightarrow 2CO + 2H_2 \qquad \Delta H_{reac} = +244\ kJ/mol \qquad \text{Eq. 15}$$

$$CO_2 + 2H_2O \leftrightarrow CH_4 + 2O_2 \qquad \Delta H_{reac} = +790\ kJ/mol \qquad \text{Eq. 16}$$

Since the pyrolysis reactions also lead to the formation of tar, if the objective is to do a detailed analysis of tar amount in the outgoing syngas, the reactions involved in its production and consumption must be considered. Tar cracking reactions, as well as tar reforming reactions, should be considered to describe its consumption (both reactions are endothermic). Moreover, it is possible to classify tar in primary, secondary and tertiary tars according to the temperature range in which it is formed, 400-700°C, 700-850°C and 850-1000°C respectively [22], since different compounds are present. Finally, it has to be considered that primary tar cracking produces also a part of secondary tar, as well as the secondary tar forms tertiary tar, even if for both processes the main products are gaseous compounds such as CO, CO_2, LHC, H_2.

Dry and steam reforming of methane, so Eq. 15 and Eq. 11 respectively, occur also for LHC and tar, but methane is usually taken as reference since it is the main component that undergoes through these reactions.

Typical range of syngas composition (dry-based) derived from steam gasification of wood chips at 800°C, using olivine as bed material, are reported in Table 2.

Table 2: Typical range of syngas composition, adapted from [24]

Components	Values
H_2 [vol%]	35-45
CO [vol%]	22-25
CO_2 [vol%]	20-25
CH_4 [vol%]	≈ 10
LHC (mainly C_2H_6) [vol%]	2-3
Tar [g/Nm³]	20-30

The gasification process strongly depends on operating conditions and type of biomass, hence in the following paragraphs the main parameters that influence steam gasification will be analyzed and a list is reported here:

- Biomass characteristics (composition and humidity)
- Biomass feed particle size
- Gasification temperature
- Gasification pressure
- Steam to biomass ratio
- Bed material
- Combustion process

Biomass characteristics influence

Biomass composition can differ widely according to the biomass type, and this affects importantly the produced syngas composition as well as the gas yield, hence the hydrogen production depends also on intrinsic characteristics of biomasses.

As presented by Pfeifer [22], keeping constant the other parameters, the variation of feedstock leads to relevant changes in syngas composition. In the literature most of the available data are referred to woody biomass, straws, bark and coal, underling important variation between results from woody biomass and coal. In particular, the latter gives the highest H_2 volumetric fraction in the syngas (58%) while woody biomass (pellets, chips, bark), sewage sludge and straws give more uniform results in the range of 37-44%, that is of the same magnitude given in the reference [24]. The results obtained in [22] are resumed in Table 3. While in Figure 15 other examples are reported from [25].

Table 3: steam gasification at 850°C, syngas composition as function of biomass type, reprinted from [22]

Fuel	Product gas composition (vol.%)			
	CO	CO_2	CH_4	H_2
Wood pellets	26.1	21.3	9.9	40.3
Wood chips	24.4	21.7	11.32	37.4
Bark	23.3	18.3	8.0	44.3
Wood chips (willow)	21.9	24.8	10.7	39.2
Wood/straw mixture 80:20 wt.%	20.3	24.3	9.9	40.4
Wood/straw mixture 60:40 wt.%	22.4	21.5	10.0	41.8
Sewage sludge	16.8	26.7	8.0	41.5
Lignite	23.0	17.2	5.3	54.5
Wood/coal mixture 50:50 energy%	7.7	23.85	17.7	45.8
Coal	11.5	18.0	7.9	57.9

It also must be underlined that for each type of biomass there are different optimal parameters values that should be adopted in order to optimize performances of the plant according to the feeding.

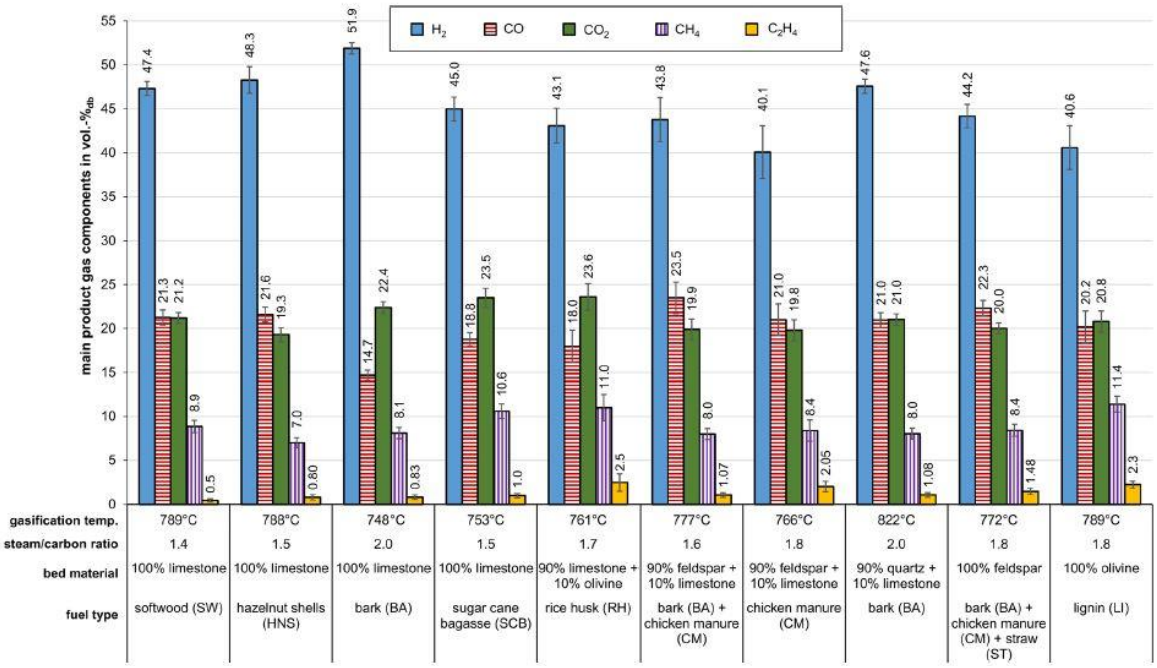

Figure 15: syngas composition as function of feedstock types, reprinted from [25]

In addition, cellulose and lignin content in the biomass also influence the process. It is demonstrated that a higher cellulose and lignin content increases syngas yield, and as a consequence a greater H_2 production is achieved. Moreover, biomasses with high cellulose fraction are easier to be gasified, hence they can be processed with a shorter residence time [9], [10].

Syngas content of nitrogen and sulfur compounds such as NH_3 and H_2S strongly depend on the elementary composition of biomass. High percentages of N and S in the biomass are translated into higher fractions of those undesired compounds in the syngas. Therefore, if several biomasses are processed in the same plant, it is extremely important to consider this aspect to design the upgrading section in order to satisfy requirements for sellable hydrogen.

Syngas tar content also changes according to the biomass composition. Some experimental results are presented in Figure 16.

Diagrams similar to those reported in Figure 15 and Figure 16 for some other biomasses can be found in [26].

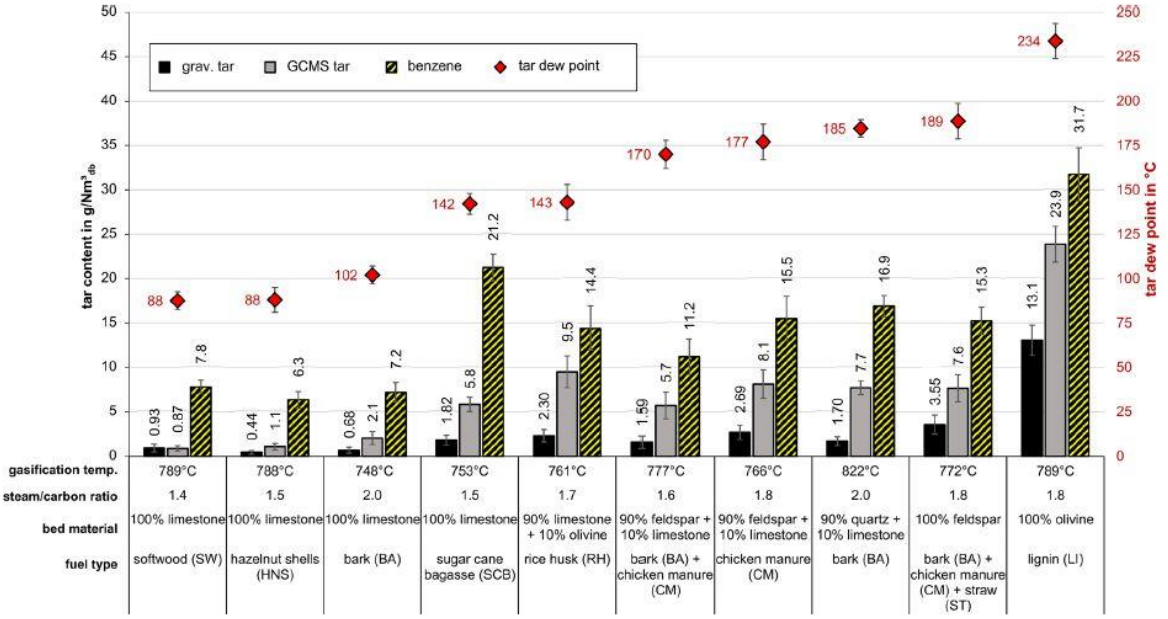

Figure 16: Tar content and dew point as a function of biomass type, reprinted from [25]

Another important parameter is the biomass humidity. The greater the fuel humidity the higher the heat required for gasification since a higher amount of water has to evaporate. Therefore, gasification temperature decreases unless an additional fuel is used to cover the higher humidity effect. On the other side, the overall steam to biomass ratio increases leading to a higher H_2 and CO_2 fractions and a lower CO content in the syngas. Also tar content is affected by fuel moisture, very dry biomasses (<6 wt%) lead to high tar content, while a minimum is achieved for humidity of about 20 wt%; moreover, for higher humidity content, tar production increases again, as shown in [22]. But, as it will be explained later, it must be specified that it is more common to reason on the effect of the overall steam to biomass ratio.

The last factor to consider is the ash content that is relevant since it can cause several problems also due to its low melting point that oblige to operate the gasifier typically under 900°C. A possible issue is related to agglomeration which leads to plugging and fouling of components. Moreover, ash content increase determines a greater heat demand for heating up at gasification temperature more inert material. More details about the role of ash and other mineral particles on gasifier reliability can be found in [27]. After several years of tests, it was determined that biomasses with an ash deformation temperature higher than 1100°C is suitable for gasification in DFB configuration [25]. The ash deformation temperature is defined as the temperature where the first rounding of a cubic sample edges occurs [25].

Biomass particle size influence

The effect of biomass particle size on gas and H_2 yields is significant since smaller particles provide a greater surface area per mass unit, hence the total available biomass surface increases for a given feed stream. This enhances the heat and mass transfer, that is translated in a higher effectiveness of heterogenous reactions and as consequence the overall process results to be more efficient: the syngas yield and hydrogen fraction are greater and the amount of tar and char decrease. However, a trade-off is present, even though from a theoretical point of view particles should be as small as possible to improve the process, on the other side the biomass pretreatment and grinding costs becomes higher if lower particle size is required. Furthermore, too small biomass particles could lead to undesired phenomena such as their sintering. Typical values of particle size are between several millimeters to less than one millimeter [10], [22], [27], [28].

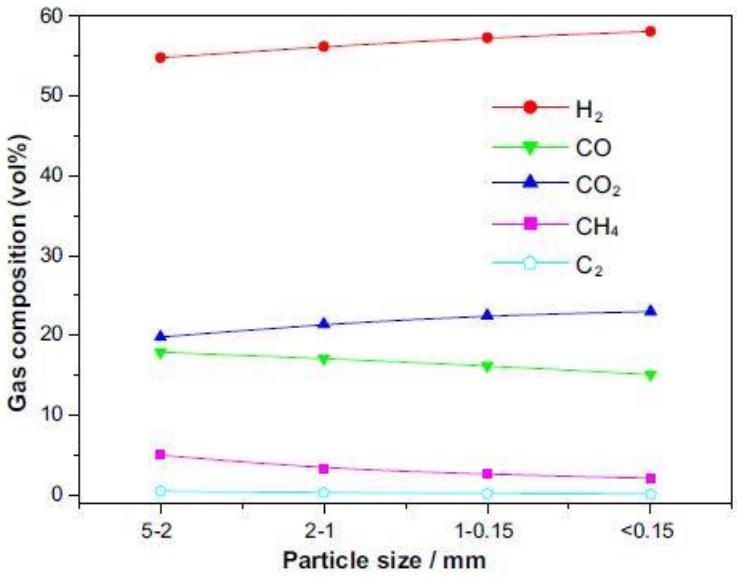

Figure 17: syngas composition vs particle size, reprinted from [28]

Gasification temperature

It is common to reason on an average bed temperature since fluidized bed leads to a more uniform temperature than fixed bed reactors. Despite that, it is possible to identify some local hot and cold spots along the reactor. The profile along the gasifier height is reported in Figure 18, a hot region is identified where the regenerated hot bed material is re-immitted in the gasifier, while a colder region is present where steam is injected due to its typical lower temperature. However maximum temperature difference along the reactor is less than 100°C.

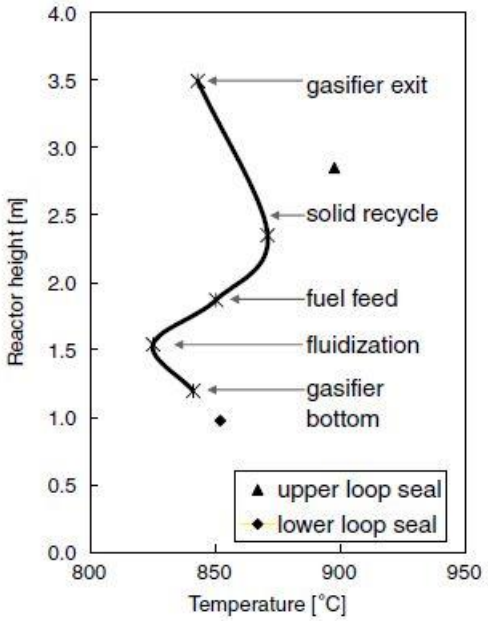

Figure 18: Temperature along reactor height, reprinted from [22]

Gasification temperature is one of the most important parameters on which syngas composition and yield depend, since it influences thermodynamic equilibrium and kinetic of the reactions. The gasification process is overall endothermic therefore the higher the temperature the more the equilibrium is shifted towards the products. Under the kinetics point of view, the reaction rate always increases with the temperature, hence there is not a compromise between kinetics and equilibrium since both are enhanced when the gasification temperature increases.

An increase of the gasification temperature not only improves the syngas yield, but it results in a different syngas composition. In fact, hydrogen content becomes greater as well as the carbon dioxide content, while methane and carbon monoxide fractions decrease. The detailed description of what happens is complex due to the several reactions that occur and their changes in reaction kinetics and equilibriums, but intuitively a bed temperature increase enhances the endothermic reactions of methane and LHC reforming, Eq. 11 and Eq. 12 are representative of these reactions. On the other side, for exothermic reactions, such as WGS (Eq. 10) and CO oxidation (Eq. 13), it is more difficult to do a priori reasonings, since temperature increase affects positively reaction rates but equilibrium is shifted towards reactants, and finally reactants amount is modified by the changes in the other reactions. Several studies [10], [22], [29] have demonstrated these trends that are also reported in the following Figure 19.

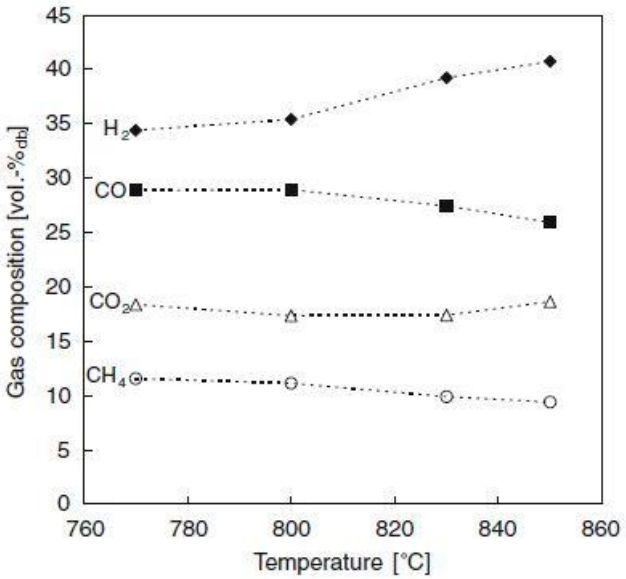

Figure 19: Syngas composition as a function of temperature, reprinted from [22]

The change in syngas composition is also translated into a variation of its LHV, in fact the higher H_2 content leads to a higher LHV by mass, but lower by volume due to the low hydrogen density.

Also tar content strongly depends on gasification temperature, in fact, the higher it is, the lower the tar generated since its reforming and cracking are enhanced. This aspect is particularly relevant because tar content and its removal are one of the main weak points of producing hydrogen via biomass gasification, [10], [22], [29].

The syngas yield and composition quality increase as tar content decreases for higher gasification temperatures, but also the cold gas efficiency (Eq. 4) is affected by that increase. The numerator increases thanks to a better gas yield and a higher LHV [MJ/kg], but the denominator increases too because to sustain reactions at higher temperature more energy (additional fuel) is needed to superheat more the steam and to compensate for the higher heat losses.

To conclude, besides gasified biomass characteristics and technology and materials developments, there is an optimal temperature that leads to the minimum syngas cost. It has to be found a compromise between syngas quality requirements and process efficiency that typically decreases when temperature goes up. Common values of gasification temperature are in the range of 800-850°C, but it is typically preferred to operate around 850°C in order to have a lower tar content [9], [10], [22], [24], [29].

Gasification pressure

Considering the overall effect of the chemical reactions, the equilibrium indicates that gasification is favored at low pressure. This is one of the reasons that guides to operate the reactors close to ambient pressure [10].

Steam-to-biomass ratio

The ratio between the steam and the fuel fed to the gasifier is a relevant parameter that leads to changes under several points of view. It can be useful to define the Steam to Biomass ratio "SB" taking into account also the water content of the biomass:

$$SB = \frac{m_{steam} + m_{H2O\_fuel}}{m_{fuel\_dry}} \qquad \text{Eq. 17}$$

Where m_{steam}, m_{H2O_fuel} and m_{fuel_dry} are respectively the mass flow rate [kg/h] of fed steam, water contained in the biomass and dry biomass.

A higher SB ratio has three main consequences on the process:

- Higher gas and hydrogen yields
- Lower tar content
- Lower cold gas efficiency (CGE)

Introducing more steam with the same amount of fuel, gas yield increases because more reactants are present, hence Eq. 7 is shifted towards the products as well as Eq. 10, Eq. 11 and Eq. 12 that determine greater hydrogen yield and CO_2 content. On the other side, CO and CH_4 content in products are lower. This leads to have a syngas of better quality (on dry basis) that is attractive since the objective is to produce hydrogen. In Figure 20 results from steam gasification of wood pellets at 850°C are presented, while Figure 21 reports the gas yield and LHV as a function of steam to biomass ratio.

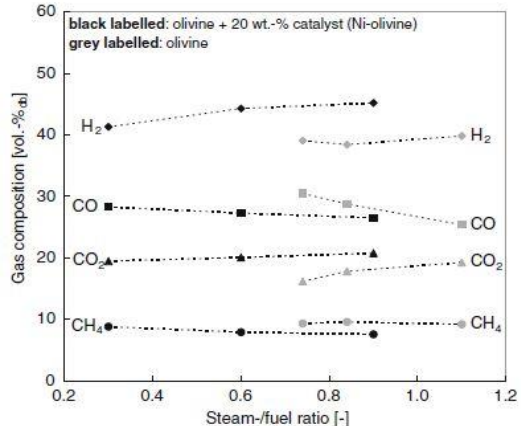

Figure 20: Gas composition as a function of SB, reprinted from [6]

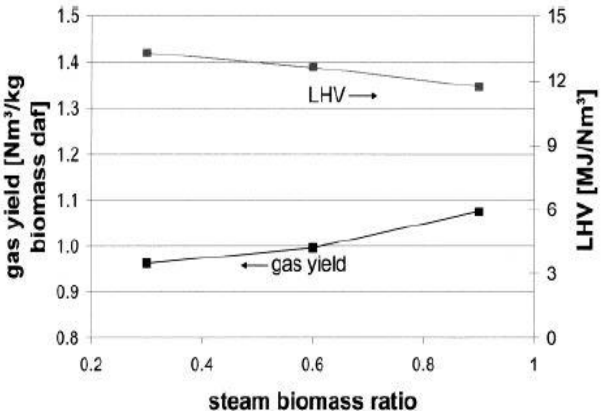

Figure 21: Gas yield and quality as a function of SB, reprinted from [8]

Reforming reactions of tar are promoted too by the presence of steam, therefore tar content decreases when SB is increased, keeping constant bed temperature [18], [22], [23].

The higher amount of fed steam as reactant is translated in some advantages and in a higher water conversion, as shown in Figure 23, since the reactions mentioned above are enhanced. Obviously, another factor that is predominant on water conversion is the gasification temperature since it influences equilibrium and kinetic of reactions. In Figure 22 the trend of water conversion as a function of temperature can be observed. It is proven by several studies [18], [22], [23] that water conversion is very low, typically 6-10% depending on the temperature and the SB, therefore in any case around 90% of the inlet steam leaves the gasifier unreacted. This represents an important energy loss, since water needs a lot of heat to become superheated steam and after most of that is not exploited. Therefore, the outgoing flow with unreacted steam must be cooled, in order to limit the reduction of process efficiency and recover heat from the syngas stream (Figure 29).

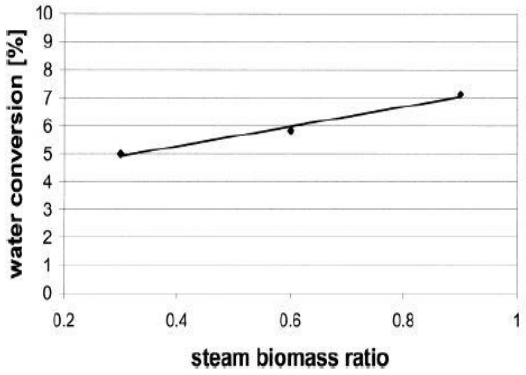

Figure 23: water conversion as a function of SB, reprinted from [8]

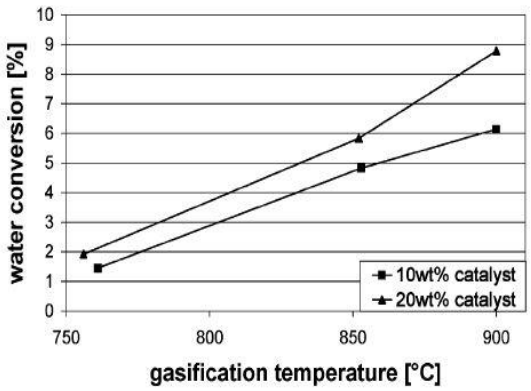

Figure 22: water conversion as a function of gasification temperature, reprinted from [8]

Although an increase in SB is translated into a greater water conversion, the CGE gets lower due to the greater heat demand and higher amount of unreacted steam.

A steam excess is also recommended by manufacturers to avoid relevant carbon formation on catalyst material if present. Typical values of SB are in the range of 0.3-1.1 kg of steam to kg of dry fuel [18], [22].

To summarize, steam to biomass ratio must be optimized together with process temperature as a compromise between syngas quality (gas yield, composition, tar content) and overall process efficiency.

Bed material

The type of bed material relevantly influences results in terms of syngas quality as well as costs and process efficiency. Bed material is chosen according to the following criteria: attrition resistance, heat transfer properties, catalytic activity, and chemical stability. In general, in fluidized bed reactors silica sand is used, but for steam gasification application is not common since it does not have any catalytic activity [22].

The main reason to introduce a catalyst is to enhance tar reforming reactions in order to reduce its level in the outgoing flow. Consequently, also other reforming reactions are enhanced, hence syngas composition and water conversion improve as shown in Figure 20 and Figure 22.

Several bed materials have been tested and compared with the main objective of tar level reduction. Some of the investigated options are natural minerals such as olivine, dolomite, and limestone, as well as synthetic materials like Ni-supported olivine, Fe-supported olivine, feldspar, and alkaline metal-based materials [22]. The most used material for steam gasification is olivine that with respect to silica sand has similar attrition resistance, but higher catalytic activity that leads to the improvements in tar level and syngas quality. Its catalytic activity derives from the formation of calcium-rich layer on the particles surface during long-term operation, which is responsible for the increased kinetics for reforming and tar cracking reactions [25], [30]. Olivine is also the bed material adopted for the first most successful project about steam gasification, in Güssing Austria [24]. Finally, it must be mentioned that even the biomass ash composition can affect the catalytic activity [31].

Further advantages are given by a bed material that has a greater catalytic activity, in fact to reach same tar level and syngas composition of a non-catalyst material, fixed the temperature, it is possible to reduce the steam to biomass ratio, thus increasing the cold gas efficiency. Same reasoning can be done varying gasification temperature keeping constant the SB and always achieving an increase in the CGE.

Nickel enriched olivine has been tested successfully since it shows same attrition properties of olivine, but a higher activity [22]. Considering a mixture of pure olivine and catalytic material (Ni-supported olivine) and varying its compositions between 0% and 43% [29], it is demonstrated that increasing the catalytic fraction a lower tar content and a greater hydrogen yield are obtained, keeping constant all the other parameters. In particular, a tar reduction of 75% can be achieved using the catalyst as 43% of the bed material.

The trends given by variations in SB or gasification temperature are not changed, but they are just intensified as shown in Figure 24.

Moreover, it is possible to notice how catalytic activity depends on the temperature, in fact catalysts show an increased action at higher temperature, in particular temperature range to exploit properly the catalytic material is between 800°C and 900°C.

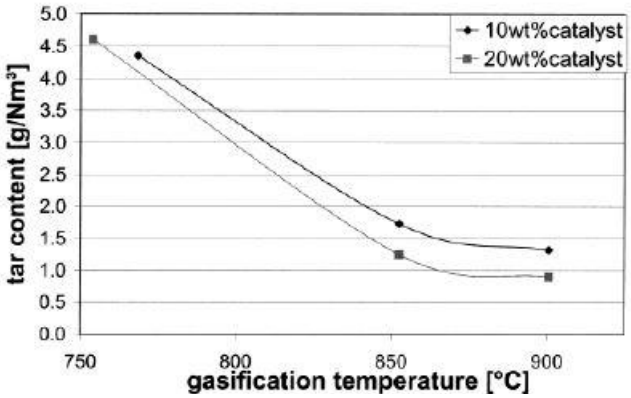

Figure 24: Tar content vs gasification temperature, reprinted from [29]

The main causes of deactivation of metal catalysts are coke deposition and sulfur deactivation, but they are typically removed in the combustion reactor where coke is combusted together with char and possible additional fuel.

An example of how the syngas composition changes according to the bed material is reported in Figure 25.

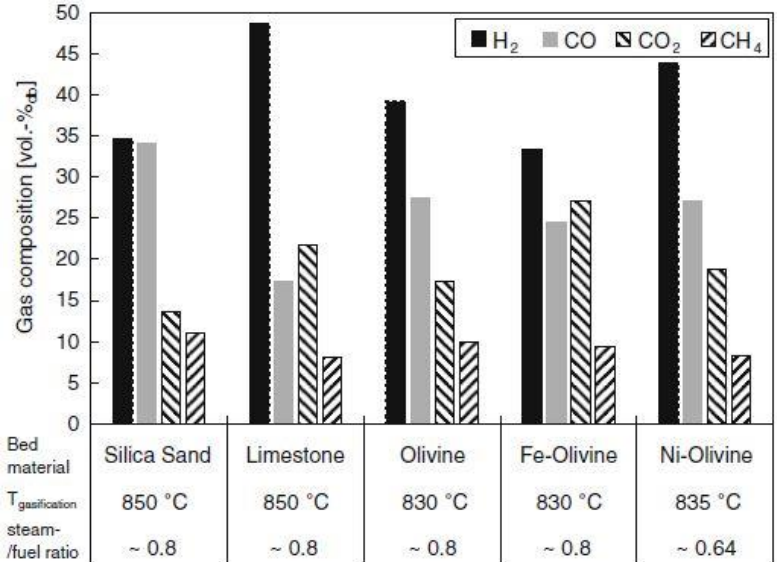

Figure 25: Syngas composition as a function of bed material, reprinted from [22]

Attrition resistance is a fundamental parameter to evaluate catalyst lifetime and consequently it affects also the cost related to the addition of fresh bed materials. As said, Ni-supported olivine shows same characteristic of pure olivine, therefore it is a suitable substitute that can improve the overall process, while dolomite has the main problem of mechanical stability and attrition resistance that are worse if compared with olivine, hence it is not commonly used in commercial plants [18].

Finally, a note about limestone as bed material must be done. It can be used as classical bed material increasing performances thanks to the great catalytic activity, as shown in Figure 25 and Figure 27, or to perform carbon dioxide separation inside the gasifier, as in Figure

26. A lot of research is being carried out on steam gasification coupled with CO_2 capture since it is a very promising technology that could improve performance of steam gasification based on DFB [18], [22], [24].

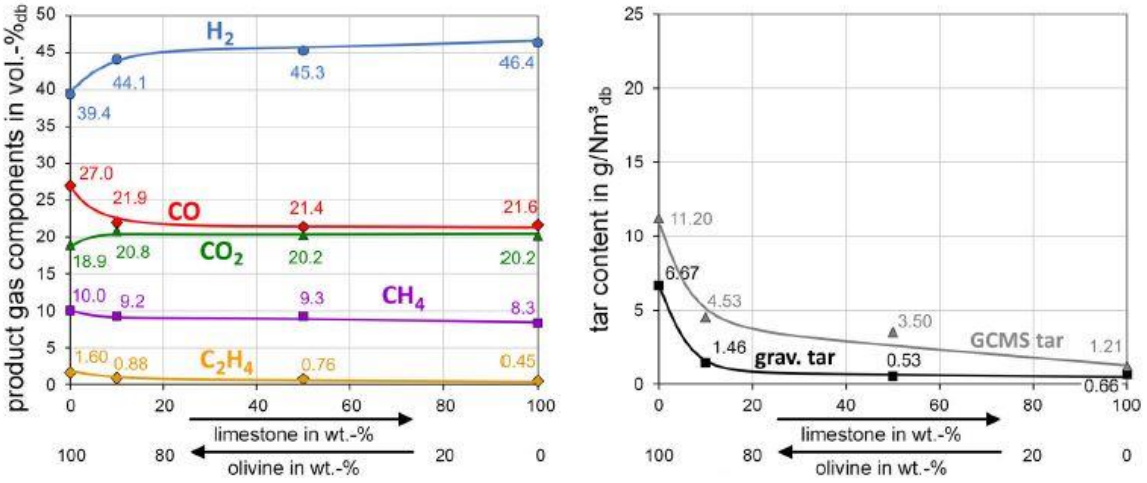

Figure 27: Syngas composition and tar content vs bed material, reprinted from [25]

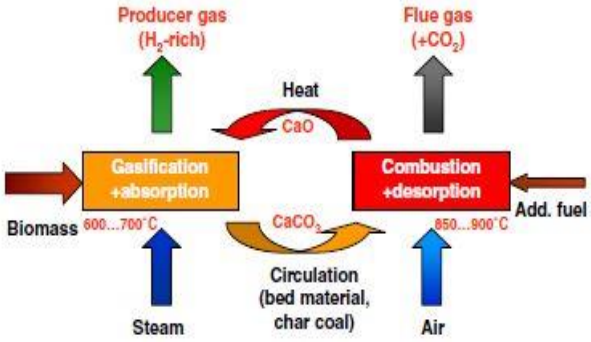

Figure 26: Simplified scheme of SER configuration, reprinted from [22]

This technology is typically called in two main ways: Sorption Enhanced Reforming (SER) or Absorption Enhanced Reforming (AER) [18]. The simplified scheme is shown in Figure 26, the bed material, limestone ($CaO/CaCO_3$), works always as heat carrier, but it has the additional function of adsorbing CO_2 selectively in the gasifier and releasing it into the combustor reactor producing syngas with low CO_2 content and flue gases rich in carbon dioxide. Carbon dioxide separation is based on the following reaction Eq. 18 that permits by a circulating bed material to separate an important part of CO2 directly into the gasification section.

$$CaO + CO_2 \leftrightarrow CaCO_3 \qquad \Delta H_{reac} = -178\ kJ/mol \qquad \text{Eq. 18}$$

In the gasifier the direct reaction, carbonation, occurs hence bed material is transformed into $CaCO_3$ that, afterward, is transported into the combustor where at higher temperature is regenerated via the reverse reaction, calcination. As shown in Figure 28, the driving forces of this process are the difference between the partial pressure of CO_2 inside the two

reactors and the equilibrium change due to the different temperatures in the gasifier and combustor [19], [25], [30]. In particular, to make this process feasible it is necessary to operate at lower gasification temperature with respect to a classical steam gasification, in fact typical temperature for carbonation is between 600°C ad 700°C, while reverse reaction, that is so endothermic, happens at 850-950°C.

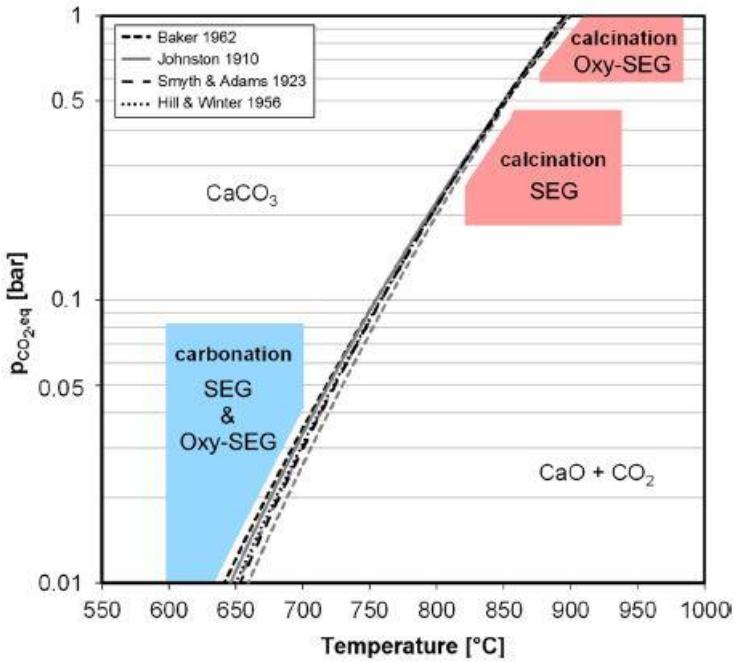

Figure 28: Representation of driving forces of SEG process, reprinted from [25]

SER technology presents several interesting advantages [18], [22], [24], [25], [30]:

- Higher catalytic activity of limestone (with respect to olivine) enhances reaction kinetics.

- Carbonation reaction releases additional heat inside the gasifier, since exothermic, that covers part of total heat required for gasification. On the other side, in the combustor additional heat is required for the reverse reaction.

- Lower gasification temperature increases cold gas efficiency since steam is superheated less and heat losses are lower, moreover WGS and carbonation equilibriums are influenced positively since they are exothermic reactions.

- Lower tar level in the outgoing syngas thanks to the catalytic activity of limestone that promotes tar reforming and thanks to the lower operating temperature that avoids tertiary tar formation that is also the most difficult to remove due to the high presence of stable aromatic ring compounds. Therefore, tar content is lower compared to standard steam gasification processes, despite the lower gasification temperature.

- CO_2 removal and lower gasification temperature influence also WGS equilibrium, in fact a product is subtracted and moreover equilibrium goes towards products with a lower temperature since WGS is an exothermic reaction. Therefore, hydrogen content in dry syngas can achieve values up to 75%. This is a relevant point if final objective is to produce pure H_2, in fact it permits to have a smaller upgrading section. Since WGS is enhanced inside the gasifier, WGS reactors can be avoided as well as CO_2 separation by absorption, hence the complexity and costs of upgrading section are lower.

- Higher CO_2 concentration in the outgoing exhaust gas from the combustor can facilitate the sequestration of carbon dioxide. A further technical improvement could be achieved by "OXY-SEG" process where the oxidant fed to the combustor is pure oxygen instead of air, leading to a CO_2 dry basis fraction in flue gas up to 90%.

The SER process is still under development and no demonstration plant is yet available. Only experiments on pilot plants have been carried out with successful results. The main key challenge related to this technology is the bed material lifetime, since limestone shows a significantly lower attrition resistance than olivine, which is translated into relevant material losses. Furthermore, particle sintering can occur mainly during sorbent heating, leading to a reduction in the area available for reaction. Finally, competitive chemical reactions with impurities may occur, for instance with sulfur. In Table 4 an achievable syngas composition via SER steam gasification is presented.

Table 4: Syngas composition by SER configuration [15]

Components	Values
H_2 [vol%]	73
CO [vol%]	8
CO_2 [vol%]	6
CH_4 [vol%]	11
LHC (mainly C_2H_6) [vol%]	2
Tar [g/Nm^3]	10

Combustion process

Combustion process has the aim to burn char, regenerate bed material from possible coke deposition and supply heat. Unless the combustor is not able to guarantee bed material regeneration and operating temperature in the gasifier, the combustion process has not directly influence on gasification. Anyway, it is relevant to make the combustion process as efficient as possible, adopting air preheating, low air excess and heat recovery from exhaust gases in order to have a greater cold gas efficiency.

Gasification plant configuration

An example of heat recovery strategy in gasification plant is presented in Figure 29. To enhance performance of the plant is necessary to recover the huge amount of energy related to the outgoing streams to avoid low process efficiency, since syngas typically leaves the gasifier around 800-850°C while the flue gas at 900-950°C.

A possible strategy for energy recovery is represented in Figure 29, in this case flue gases are firstly utilized for air preheating, afterwards to cover a minor part of steam generation and finally to dry the biomass. While heat recovery from syngas is focused only on steam generation because it is an energy consuming process. This process configuration allows to achieve good efficiency that otherwise could not be obtained, moreover it permits to have possible synergy like the fuel drying or other low temperature applications.

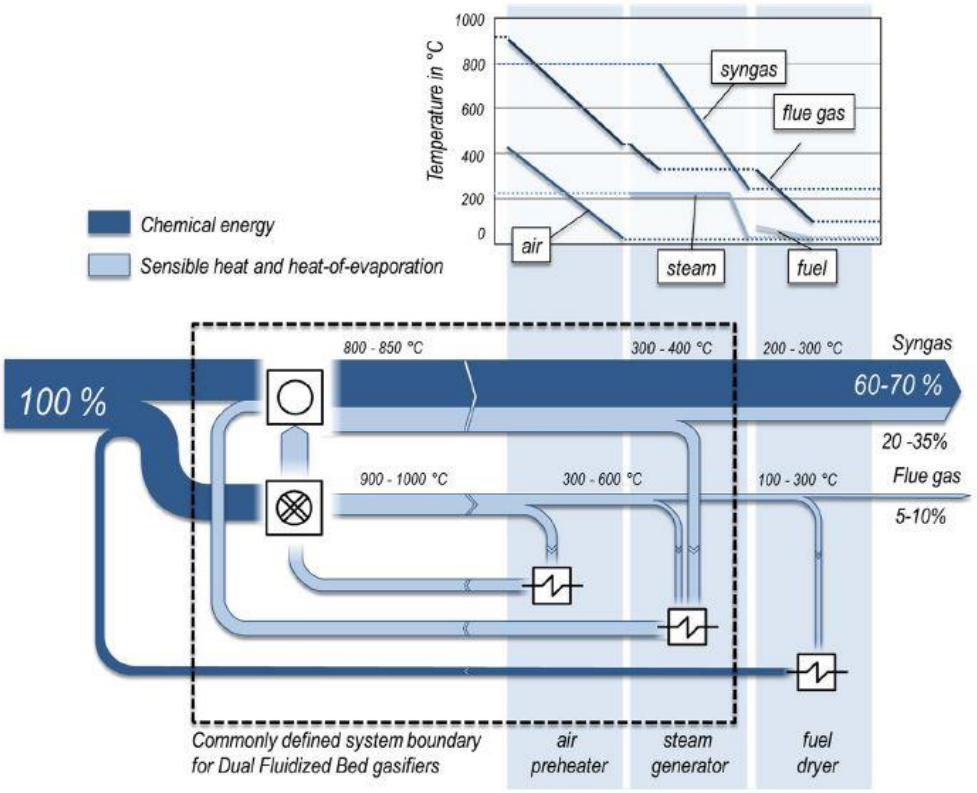

Figure 29: Energy fluxes diagram and T-Q diagram for heat recovery, reprinted from [18]

Syngas upgrading and purification

The outgoing syngas from the gasification section is firstly filtered in a cyclone due to the high temperatures and, after a high temperature heat recovery, it is filtered again in bag house filters in order to avoid even the carryover of smaller solid particles and dust in the upgrading section. Another option currently exploited is the usage of electrostatic precipitator filters. Besides the important removal of these solid components, the syngas goes through additional operational units that have the aim of increasing the hydrogen content and/or separate undesired compounds (WGS reactor, RME scrubber, amine scrubber, PSA unit).

WGS reactor

This unit has the objective of converting the CO contained in the syngas, leading to an increase of H_2 content. As shown in WGS reaction (Eq. 10), carbon monoxide and water vapor react to produce hydrogen and carbon dioxide. Since it is an exothermic reaction there is a compromise between equilibrium and kinetics. The first is shifted towards the products if temperature decreases, vice versa kinetics improves with a temperature increase. Moreover, a catalytic bed material is required to achieve a proper conversion of CO.

Pressure does not affect equilibrium composition due to the moles' conservation, therefore operating pressure is typically set according to the entire process. It can influence slightly the kinetics but not relevantly since it is mainly dominated by temperature level.

This process is well established in commercial plants because it is already used to set CO-to-H_2 ratio of synthesis gas in several chemical processes. WGS reaction is carry out in a fixed bed reactor and it is possible to distinguish two main types of reactors according to the bed material. The high-temperature (HT) reactor has a Fe-Cr based catalyst that typically operates with a syngas inlet temperature in the range of 350-500°C in adiabatic conditions. This catalyst results to be robust against poisoning given by possible sulfur compounds from gasification process [24].The low-temperature (LT) reactor works with a Co-Mo or Cu-Zn catalyst that allows to operate with a syngas inlet temperature in the range of 180-280°C, hence it makes it possible to reach higher CO conversion. Co-Mo catalyst is activated by the presence of H_2S therefore it can resist to sulfur compounds, but this solution cannot be used in biomass-to-H_2 plants because of the too low hydrogen sulfide content in the syngas that does not permit a proper activation of the catalyst [24]. Cu-Zn catalyst is sensitive to sulfur poisoning and deactivation, hence it is not possible to utilize this solution without a sulfur removal section. Due to this reason is not possible to achieve extremely high CO conversion, since it would be necessary at least a two steps solution, where after a HT reactor the syngas is cooled and fed to a LT reactor. To conclude, syngas upgrading by WGS is typically performed by a single HT reactor operated at about 350°C.

Moreover, utilizing a HT reactor, the WGS unit can be placed before tar removal since it operates at temperatures above tar condensation level.

Another parameter that plays a key role is the steam-to-dry syngas molar ratio. Keeping constant syngas inlet temperature, increasing the amount of fed steam the reaction shifts towards the products since more reactants are fed. Furthermore, steam fed to the reactor must be enough in order to avoid coking and carbon deposition on the catalyst surface that reduce available area for reactions. Depending on the syngas inlet composition and temperature, typical steam-to-dry syngas molar ratio is between 0.6 and 2.2 [24] and it could be suggested form the manufacturer according to inlet conditions.

Tar removal section

As already mentioned, tar removal is crucial for every gasification plant since it causes issues in downstream equipment, and furthermore it reduces the process efficiency. Therefore, it is necessary to remove tar before operational units that operate at temperatures below tar dew point, hence around 350°C.

It is possible to distinguish primary methods, which remove tar directly in the gasifier, and secondary methods that are applied downstream. Primary methods have been discussed previously and they mainly consist in optimizing operating conditions (temperature and SB, in particular), and bed material (utilizing materials with greater catalytic activity). However, these methods are not able to provide a tar reduction such that downstream equipment is not damaged, therefore secondary methods are needed to have a reliable process[19], [32].The latter methods can be divided in two main categories, the ones performed at high temperature like thermal and catalytic cracking, and the ones operated at low temperatures such as tar scrubbers.

Thermal cracking decomposes tar compounds at temperature around 1200°C without any catalytic material, while catalytic cracking occurs at lower temperatures, around 750-900°C thanks to a catalytic bed. Both processes can occur directly after gasification section and they require additional heat to be performed, hence the overall process efficiency decreases, despite tar decomposition can produce useful species. For these reasons and considering possible additional issues like soot formation, these processes are usually not utilized at commercial scale.

Nowadays, cold tar removal processes are the ones adopted at industrial scale. They are based on physical absorption process, which is performed by wet scrubbing. Water is not used as solvent since the wastewater treatment would require energy consuming process in order to be compliant with environmental requirements. Therefore, oil scrubbing is adopted, rapeseed oil methyl ester (RME) is used since it permits to avoid wastewater treatment and furthermore it allows to achieve a higher tar reduction (until 99%) compared to water [19].

Oil scrubber has two possible configurations, a classical one where there are an absorption column and a stripper column that exchange RME in order to regenerate the solvent [24], and OLGA tar absorption system developed in ECN, that is operated in a different way adding a third column called collector, as shown in Figure 30 [19], [33].

Columns are typically filled with structured packings or trays in order to enhance contact between gaseous and liquid phases. Streams flow in a counter-current configuration, hence the fresh solvent enters from the top and the tar-rich gas from the bottom. Tar-poor syngas leaves the column from the top while tar-rich solvent from the bottom. Vice versa, it happens the opposite in the stripping column.

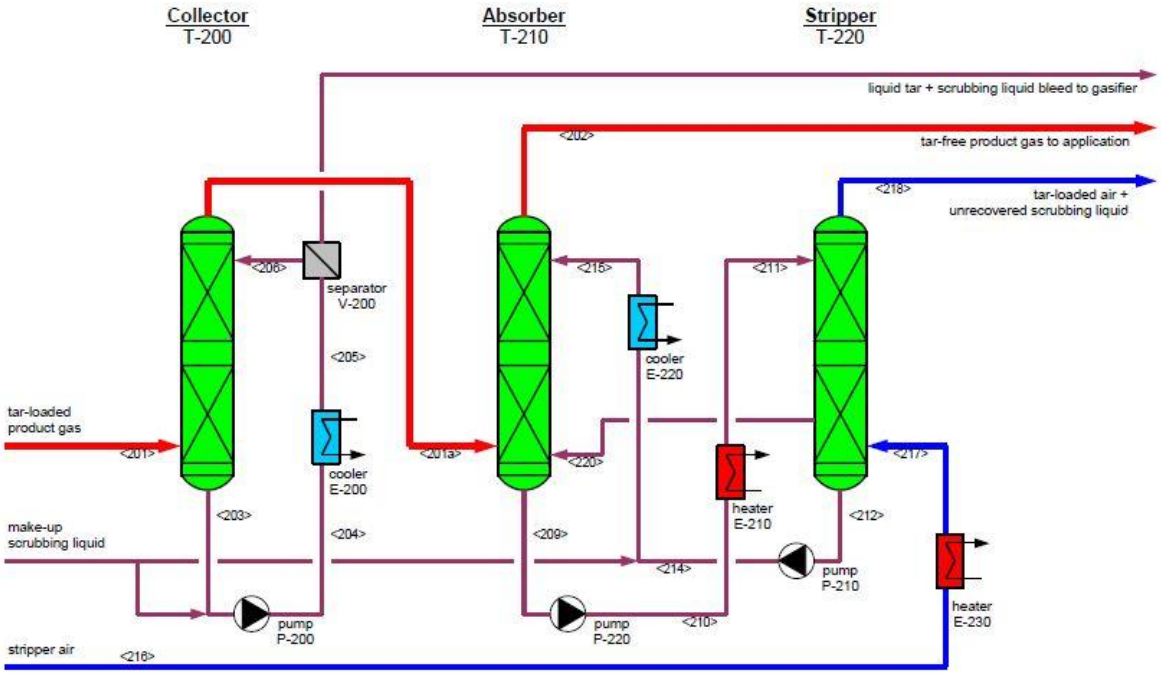

Figure 30: OLGA process flow diagram, reprinted from [33]

In the OLGA system, syngas enters at temperature above tar dew point (350°C) and it is cooled thanks to the contact with colder RME in the collector. Lowering the temperature heavy tar compounds starts to condense and they are collected with the solvent in the liquid phase. Pre-treated syngas passes through the absorber where light gaseous tars are absorbed by the RME, finally tar-free syngas leaves the absorber from the top, while tar-rich RME is sent to stripper columns where regeneration occurs. Both air and steam can be used as stripping mediums.

Condensed tar and lost RME after the first column separator, as well as the rich-tar air and lost RME in the outgoing stripping medium, do not need treatments since they are sent to the combustor where they are burned providing heat to the process.

In OLGA system, water does not condense since it is operated above water boiling temperature, therefore it is separated by a successive section of water removal.

Classical RME scrubber is operated in a different way. First, inlet syngas temperature (150°C) is lower than tar dew point, therefore some tar compounds can condense in

upstream equipment (heat exchanger). In the same column condensation of heavy tar and absorption of light tar occur. Finally, in the same section also water is condensed since syngas reaches an outlet temperature around 50°C.

Condensate separation is achieved in the scrubber basin thanks to density difference between water and RME. The water is then typically sent back to the steam generation unit and afterward it is fed to the gasifier, while remaining condensate is separated in a second step, and heavier condensate, which are not separable, are sent to the combustion reactor together with RME as additional fuel to the process. Therefore, no waste streams are present in the OLGA solution.

Acid gas removal

Biomass gasification produces mainly CO_2 as acid gas, with traces of H_2S and COS according to gasified biomass. Acid gases are removed by absorption that is favored at low temperature and high pressure. Adsorption columns is coupled with a stripper column with the aim of regenerate solvent. Vice versa, desorption process is favored at higher temperature and low pressure.

A first distinction must be done between physical and chemical absorption. The first option exploits solvent that remains chemically unchanged, hence acid gas molecules just dissolves in the solvent. While chemical absorption adopts solvent with a reactant that is sensitive to acid molecules, hence it reacts leading to the creation of new soluble species. Cited characteristics lead to have different peculiarities, as also depicted in Figure 31:

- Physical absorption can treat streams with very high CO_2 partial pressure since it is not limited by reactant content in the solvent. It does not require relevant energy consumption to regenerate the solvent because there is no chemical bond between carbon dioxide and solvent, hence regeneration typically occurs by a pressure decrease (flashing).

- Chemical absorption can treat effectively streams with low CO_2 partial pressure, but the solvent absorption capacity is strictly link to the fraction of reactants in the solvent, therefore after a certain CO_2 partial pressure physical absorption could be advantageous. Furthermore, solvent regeneration requires more energy due to chemical bond between CO_2 and solvent reactant, in fact it is typically carried out by increasing the temperature (reboiling).

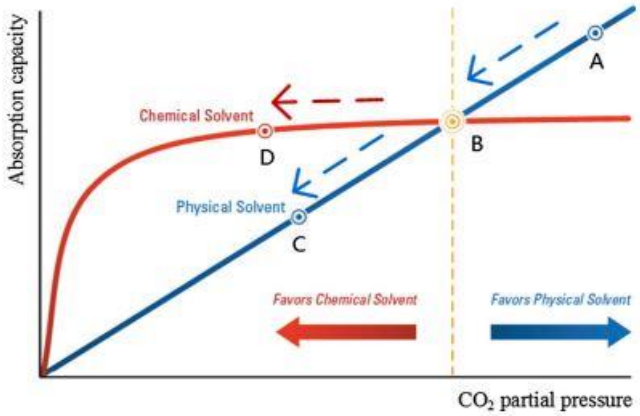

Figure 31: chemical and physical absorption comparison, reprinted from [65]

An example of commercial physical absorption is "Rectisol process" [19], [32] that utilize methanol as solvent to capture acid gases. It is preferred for high acid gas concentration, but it can achieve very good capture efficiency since it operates at high pressure (28-70 bar) and low temperatures (-30°C to -70°C). This process is very effective, and it can also give the opportunity to selectively separate H_2S and CO_2. Despite the solvent regeneration is achieved by a simple expansion, the process is very energy demanding due to costly refrigeration since absorber is operated below 0°C.

Chemical absorption uses solvents based on aqueous amine solution. It is possible to distinguish primary, secondary, and tertiary amines, respectively mono-ethanolamine (MEA), diethanolamine (DEA), methyl-diethanolamine (MDEA). These three possible alkanolamines have a great affinity to acid gas therefore it is possible to operate the process at low pressure, with an absorber temperature between 40 and 70°C. In general, these solvent gives the following CO_2 removal efficiency: MDEA < DEA < MEA [19], [24], [34]. Primary amine looks the solvent with highest reaction rate, however heat duty for regeneration is higher. Furthermore, they are more corrosive. Nowadays the most common solvent is a mixture of MDEA and piperazine (PZ), also called activated MDEA (aMDEA) since piperazine works as catalyst. In fact, aMDEA gives same reaction rate of MEA, but at the same time it requires less heat for regeneration and furthermore it results less corrosive.

In Figure 32 chemical absorption process is shown, rich-CO_2 syngas enters from the bottom of the absorber while fresh solvent is fed from the top. After absorption process, CO_2 lean syngas leaves the absorption column from the top while rich solvent goes to the stripper where is regenerated increasing the temperature thank to a boiler. A heat exchange for heat recovery is placed between the two columns, since absorber works at temperature around 40-70°C while stripper at 100-160°C [19], [24], [34]. Steam is used as stripping medium, hence with temperature increase, acid gas is desorbed, and it goes in the gaseous phase. Finally, in the top part of the stripper a condenser is placed in order to separate acid gases and to recycle back the condensed water. Hence, stripper is operated like a distillation column.

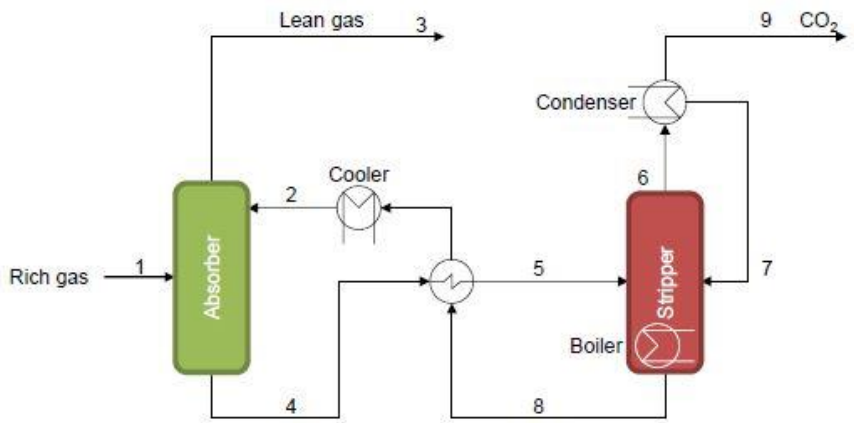

Figure 32: simplified scheme of acid gas removal section, reprinted from [24]

According to several authors this kind of system can reach CO_2 removal efficiency beyond 99% for a typical syngas CO_2 content [24], [34] . Moreover, it must be underlined that if relevant amount of hydrogen sulfide has to be captured the stripper must work at higher temperature due to the greater affinity of solvent to that compound, therefore typically a 10% extra energy consumption is needed [34].

Hydrogen purification section

After CO_2 removal section hydrogen content is typically above 70% on a volume basis, therefore it is ready to be purified at requirements level. To reach high purity (>99%) adsorption process is the only economically feasible option.

This process is based on selective adsorption of gaseous species on solid material. Physical adsorption based on van der Waals forces is adopted since it is easily reversible compared to chemical adsorption that results less reversible and with higher activation energy.

Commercial adsorbent has typically microporous structure in order to achieve high adsorption capacity and it must be chosen according to the application. For hydrogen purification activated carbon is used as bed material since it has the following qualitative order of adsorption forces presented in Eq. 19 [8].

$$Water > H_2S > NH_3 > LCH > CO_2 > CH_4 > CO > N_2 > O_2 > H_2 \qquad \text{Eq. 19}$$

Therefore, some molecules have a greater affinity with adsorbent. Hydrogen has the lowest adsorption force allowing its purification. However, the process depends on several aspects, but mainly on species partial pressure (hence syngas composition and pressure), adsorbent type and temperature, because they influence kinetics and equilibrium. Furthermore, mass transport to solid surface and afterward inside porous structure is one of the others limiting factors.

Adsorption is an exothermic process therefore is favored at low temperature, furthermore it is enhanced by high pressure as shown in Figure 33. On the other side, bed regeneration is favored at low pressure and high temperature.

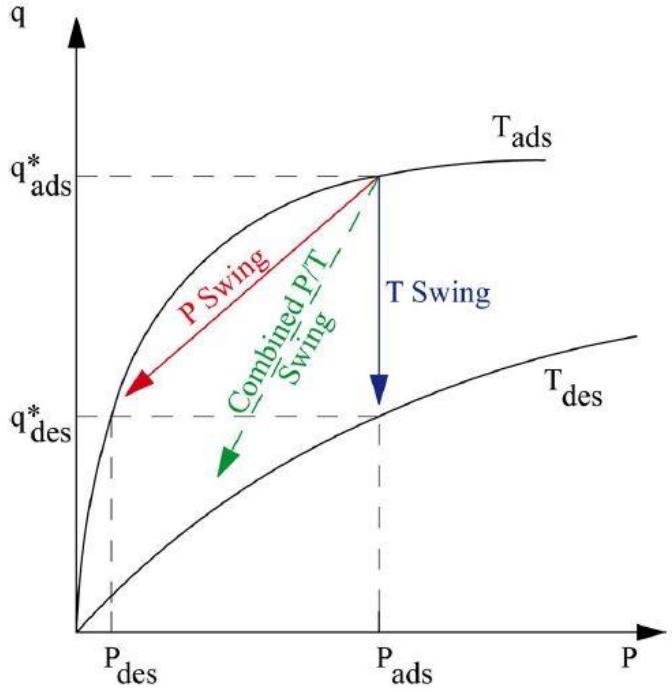

Figure 33: PSA vs TSA regeneration method, reprinted from [8]

One of disadvantages of adsorption process is due to operation in transient conditions. Several fixed bed reactors are performed in parallel, hence the saturated beds undergo through regeneration while fresh beds operate to purify H_2. This implies a complex valves and tubes system in order to manage the different operation phases of each bed, as shown in Figure 34.

Desorption phase, during which saturated beds are regenerated, can occur preferably by a pressure reduction since it requires less energy. Adsorption process with this configuration is called "pressure swing adsorption" (PSA) and it is typically used for H_2 purification application. The other option is "temperature swing adsorption" (TSA) that regenerates saturated beds by a temperature increase. This method is generally preferred for strongly adsorbed components, in fact a small temperature increase leads to relatively large change in equilibrium constant. A further advantage of PSA compared to TSA is because pressure can be changed more rapidly than temperature, allowing to operate PSA process with faster cycles.

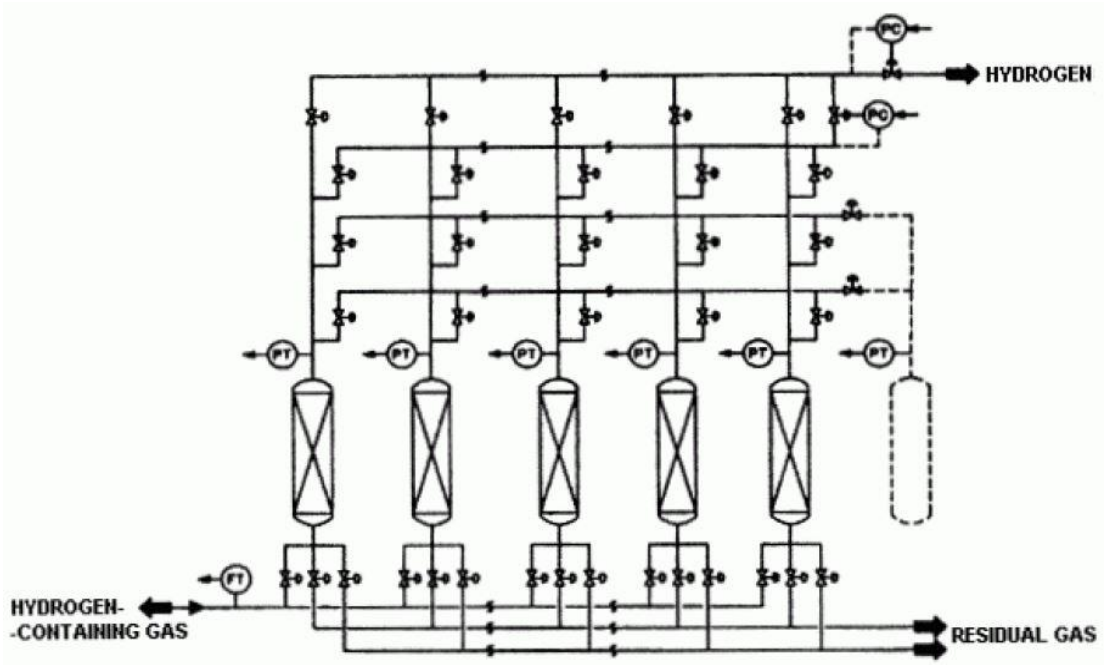

Figure 34: PSA adsorption scheme for hydrogen purification, reprinted from [8]

A regenerated bed, that undergoes through adsorption process, has a mass transfer zone (MTZ) that represents the bed portion in which adsorption occurs, hence where gaseous species are adsorbed in the solid phase. During operation MTZ moves progressively from bed inlet towards the outlet, until it reaches the breakthrough point that represents point after which raffinate (H_2) does not fulfill requirements anymore, as shown in Figure 35.

Therefore, it is relevant to understand the presence of a trade-off between hydrogen recovery and its purity. In fact, a shorter adsorption period leads to greater hydrogen purity, but lower hydrogen recovery.

It is demonstrated that hydrogen recovery can reach 90% if CO_2 is previously removed from syngas [24], [34]. Moreover, according to 2030 objectives the goal is to reach an H_2 recovery of 95% with a purity equal or higher than 99.995% [35].

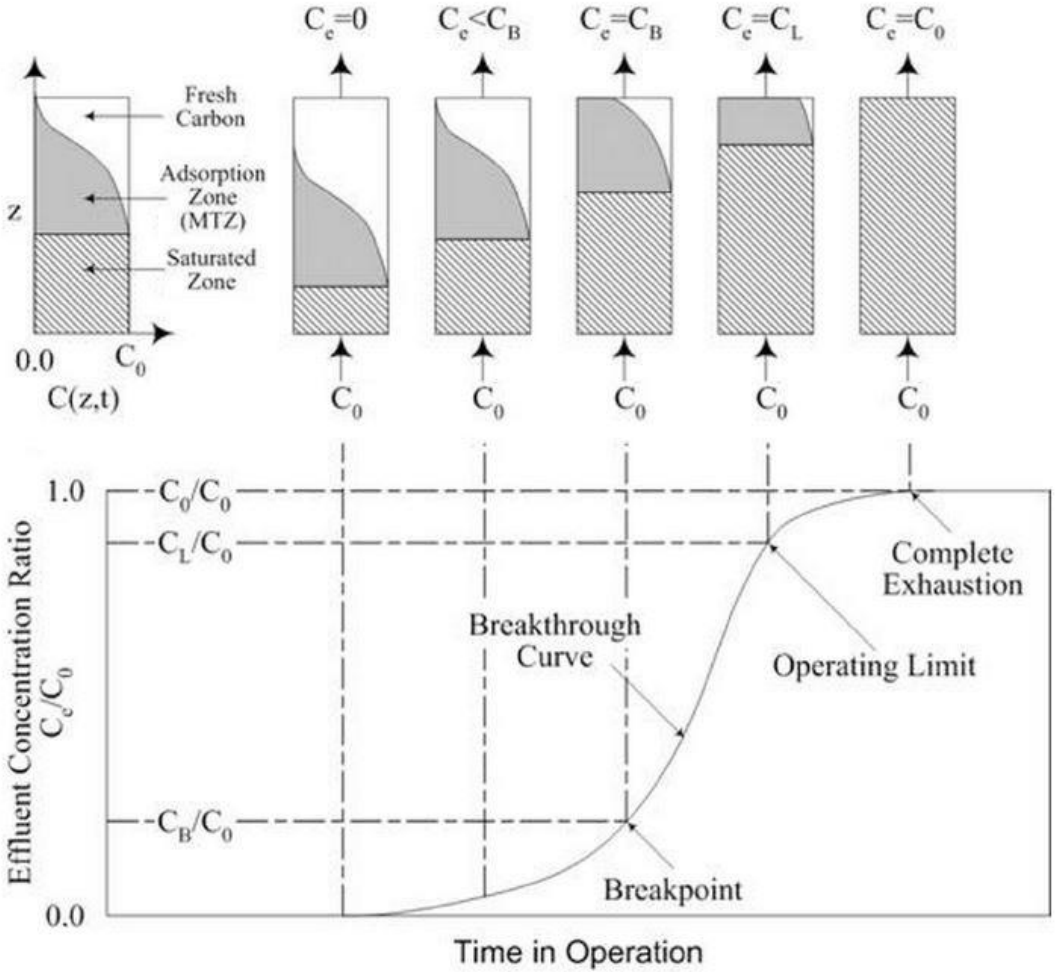

Figure 35: MTZ and breakthrough point, reprinted from [8]

1.2.2. Electrolysis

This paragraph has the objective of explaining more in detail electrolysis technology and its features, underling differences between ALK and PEM electrolyzers.

Firstly, an electrolyzer can be described at three different levels:

1. **Cell level** that is the element at the base of the technology, in which reactions and cell structure can be studied.
2. **Stack level** that represents the connection of several cells in series to reach the desired power. More stacks are connected in parallel for large scale application.
3. **System level** that even comprises all the balance of plant necessary to run properly an electrolyzer.

The two analyzed technologies differ firstly at cell level, consequently, balance of plant components and so all the system is different.

ALK electrolyzer

The alkaline electrolyzer is the technology with the highest readiness because it has been adopted since the beginning of 20th century. It utilizes a liquid electrolyte, typically a 20-40% acqueos potassium hydroxide (KOH) solution, that allows OH^- ions transport from cathode to anode. Electrodes are separated in half-cells by a porous diaphgram that reduce as much as possible product gases crossover [17], [36].

The reactions that occur at cathode and anode are reported in Eq. 20 and Eq. 21, while in Figure 36 is reported a representation of a ALK electrolyzer cell.

Cathode (-): $$2H_2O + 2e^- \rightarrow H_2 + 2OH^-$$ Eq. 20

Anode (+): $$2OH^- \rightarrow \frac{1}{2}O_2 + H_2O + 2e^-$$ Eq. 21

Typical operating conditions of alkaline electrolyzer are in the range of 60-90°C and 1-30 bar, and nowadays it can reach efficiency of 50 kWh/kg [4], [35]–[37].

As shown in Figure 36, the electrods are placed as close as possible to the separator in order to achieve two important advantages. Firstly, the ionic resistance decreses reducing the distance between electrods. Secondly, reaction are achieved mainly on the free surface of the electrodes, hence losses due to overpotential are reduced.

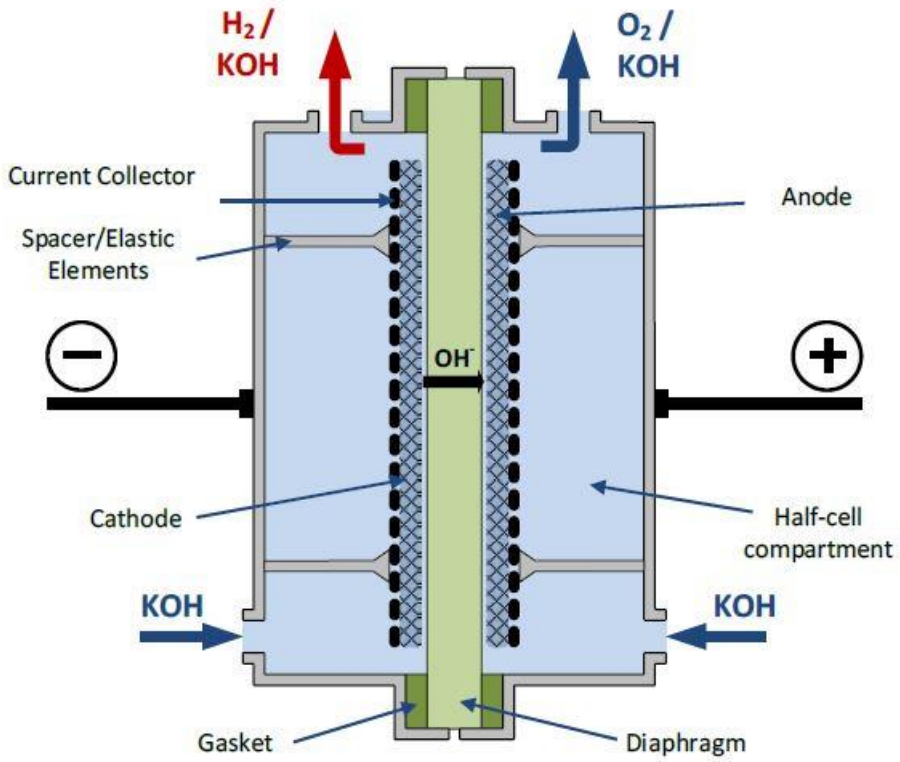

Figure 36: Simplified scheme of ALK cell, reprinted from [17]

This sandwich-like configuration is typically achieved by pressing the components together and regulating that pressure by elastic spacer.

Typical electrodes are composed by a substrate with catalyst coating in order to ehnance kinetic of the half cell reactions. The substrate can be metal sheets with porous surface as well as woven metal meshes, accoridng to the manufacturing company.

Due to high Ph value given by liquid alkaline solution, materials must be resistant to corrosion and at the same time they have to provide good catalytic activity and electrical conductivity. For this reason nickel is commonly adopted as coating of stainless steel or it is even used as pure specie [17]. The utilization of nickel is an advantages of alkaline electrolyzer since it is not a noble and scarce raw material.

Due to the use of a liquid electrolyte and a simple porous separator that even allows liquid and gas transport, the pressure must be the same on both side in order to avoid relevant gas crossover. This aspect is extremely important to manage since, beyond limits on the purity of H_2 and O_2, it is crucial to stay quite away from flammability limits between oxygen and hydrogen. This peculiarty of ALK electrolyzer provides some consequences:

- Thicker separator to limit gas crossorver, that is translated in higher ionic resistance. Current state of art separator thickness is about 460 μm [4].

- It is not feasible to pressurize just cathode half-cell since a pressure gradient would lead to a great increase in gas crossover. Therefore, both side has to be pressurized if the aim is to operate the cell at higher pressure. Furthermore, a trade-off is

present, despite a pressure increase leads to compression power saving, on the other side, it increases the activeties of gaseous products, consequently electric power required for the process increases.

- Partial load operation are typically limited to 20-30% of maximum load, since the crossover becomes too relevant below those load values [4], [36].

In addicition, bubble formation limit current density (J) typically around 0.5-0.8 A/cm^2 since increasing J, gas production and so bubbling increases as well, hence water molecules are not able to reach catalytic surface as for lower current densities. Chosen a nominal power, this is translated in a larger footprint compared to PEM electrolyzer [4], [17], [36].

Beyond limited load range, ALK electrolyzer is less flexible compared to PEM electrolyzer, in fact it has typically longer transient time for start-up, shut-down and load change, therefore the direct coupling with intermittant renewables is not totally feasible nowadays.

The state of art for ALK electrolyzer stack construction is based on bipolar plate configuration. Bipolar plates allows to avoid electric connection between cathode and anode of single cell, in fact, electrons are exchanged between neighboring cells thanks to the fact that the back side of the cathode of one cell is the anode of previous cell. Therefore, electric contact must be created only between end plates, as depicted in Figure 37 [17].

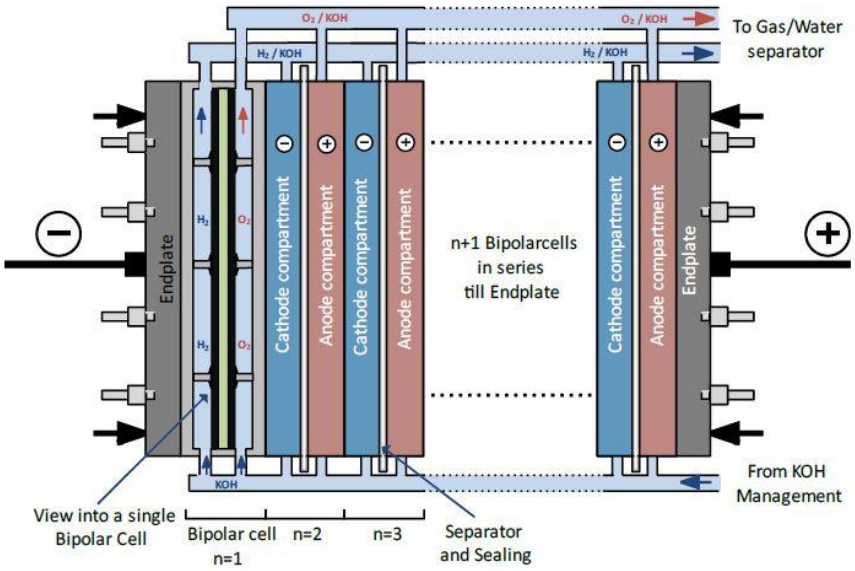

Figure 37: Scheme of ALK electrolyzer stack design, reprinted from [17]

The whole system, including balance of plant, is shown in Figure 38. Alkaline solution is recircultaed to remove gaseous products and heat. The circulation can be forced via pumps or by natural convection, exploiting the temperature gradient. The outgoing flows from cathode (KOH solution + H_2) and from anode (KOH solution + O_2) pass through two different gas-liquid separators, leading to the recovery of liquid electrolyte and a separated purification of hydrogen and oxygen.

Separated gases pass through filters (demister) in order to separate carry-over of electrolyte droplets. Furthermore, at least hydrogen stream goes through a gas scrubber in which remaing KOH solution is washed out. Afterward, hydrogen is purified at requirments level removing entrained oxygen in the deoxidizer reactor and finally it undergoes through a deep drying in PSA or TSA unit before its delivery. Typical hydrogen purity level is in the range of 99.5-99.9%, while it is 99.0-99.8% for oxygen [4], [17], [36], [38].

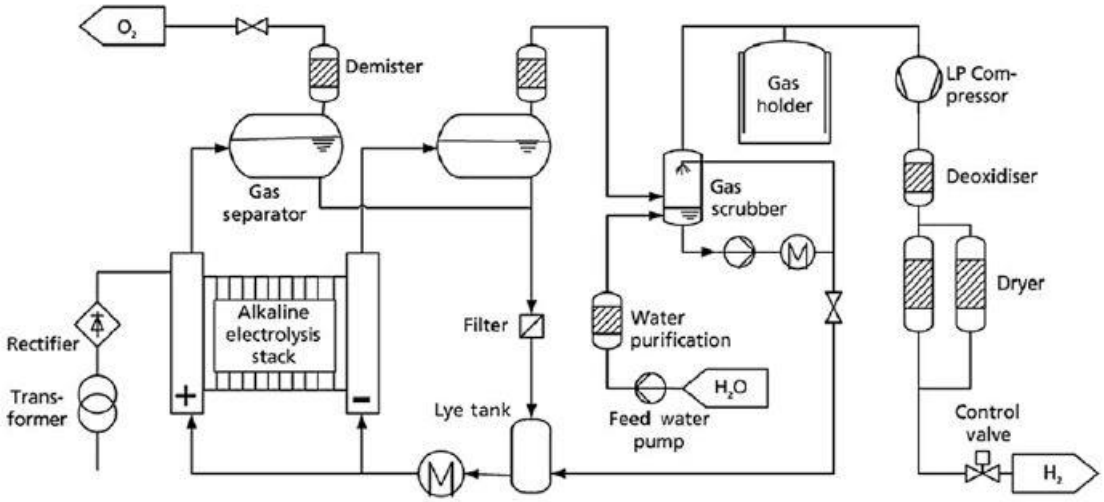

Figure 38: simplified ALK electrolyzer system, reprinted from [17]

As underlined in Eq. 20 and Eq. 21, water is consumed at cathode side while it is produced at anode side, therefore, after electrolyte separation it is necessary to mix in a dedicated collector (Lye tank) the electrolyte streams coming from the two half-cells, in order to maintain a constant KOH concentration of the solution fed to the stack. Make-up water is also needed to achieve this goal since in the total process is consumed.

Electrolyte streams mixed in the Lye tank contain dissolved gases, O_2 from anode gas-lquid separator and H_2 from the stream recycled by cathode gas-liquid separator. This electrolyte contamination is typically less relevant than gas crossover, but it has to be considered at partial load as another limiting factor. This phenomena becomes more relevant with higher operative pressure and slower KOH solution circulation .

Every electrolyzer cost is affected by economies of scale as well as the creation of well establish market that allows higher electrolyzer production. For these reasons, the capital cost is expected to decreases significantly in the next future, as happened for photovoltaic panel and wind turbine.

In Figure 39 cost breakdown structure is shown for a 1 MW_e ALK electrolyzer. First of all, it must be noticed that stack accounts just for 45% of total Capex, while 55% is relative to BoP. In absolute terms, nowadays total investment cost for an alkaline electrolyzer is about 600 €/kW for a reference power of 100 MW_e [35].

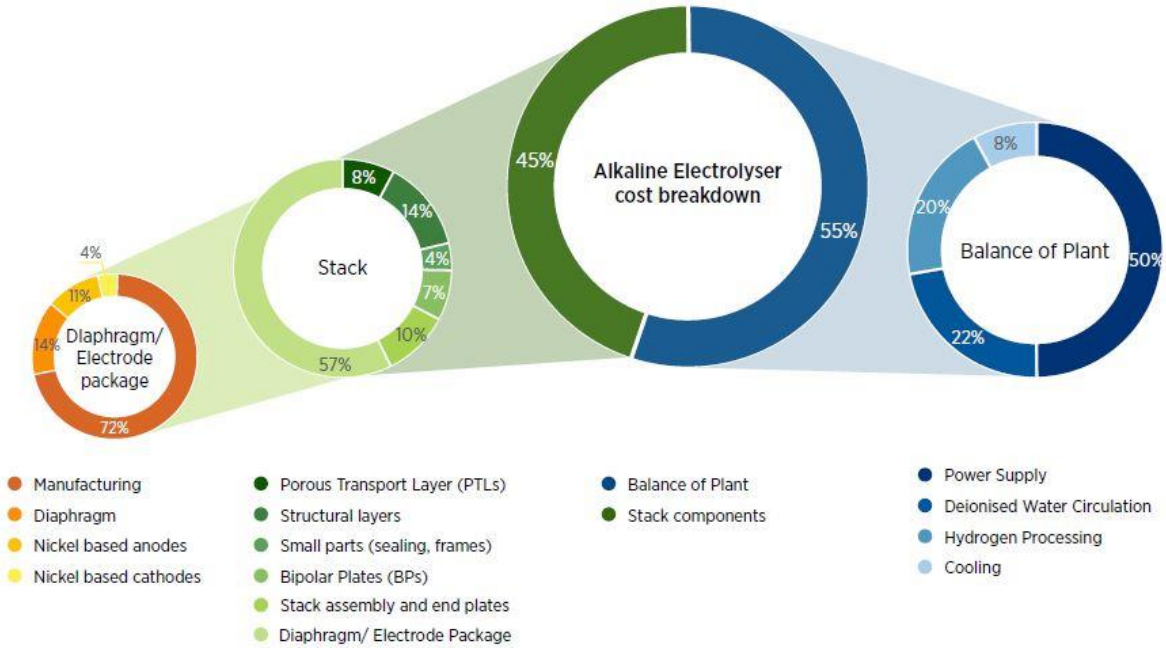

Figure 39: 1 MW_e ALK electrolyzer cost breakdown structure, reprinted from [4]

For alkaline technology, the main rooms for improvements are related to power supply that accounts for more than 25% of total Capex and manufacturing of electrodes and diaphragm, while costs associated with bipolar plates and materials are low thanks to simple design and relatively cheap material such as nickel and stainless steel.

The objective for 2030 are a cost reduction until 400 €/kW for a nominal power of 100 MW_e and efficiency increase up to 48 kWh/kg [35], [39]. At the same time, the R&D for alkaline technology focus mainly on: increase maximum current density in order to achieve a higher power density, and extend exploitable load range as well as improve dynamics, in order to be able to have a direct coupling of ALK electrolyzer with intermittent renewables. To reach these objectives, the key themes are the followings [4]:

- Develop diaphragms in order to reduce their thickeness
- Increase operating temperature
- Re-design catalyst compositions
- Develop new electrodes concepts, increasing the area and introducing novel PTL concepts.

Plant lifetime is extremely important for economic performance of electrolyzer. First of all it is necessary to distinghish stack and balance of plant components. In fact, BoP lifetime of alkaline electrolyzer is 20 years and with a proper maintanance it could be extended up to 30-50 years [36]. While stack has a typical lifetime in the range of 60,000-100,000 operative hours [4], [36]–[38], hence operative years can vary widely according to the electrolyzer usage.

PEM electrolyzer

PEM technology is more recent, commercial application started 20 years ago, despite it is studied since the 1960s [17]. It is based on different membrane which material is the perflourinated sulfonic acid (PSFA), that allows proton (H^+) conductivity. The reactions that occur at cathode and anode side are reported in Eq. 22 and Eq. 23.

Cathode (-): $$2H^+ + 2e^- \rightarrow H_2$$ Eq. 22

Anode (+): $$H_2O \rightarrow 2H^+ + \frac{1}{2}O_2 + 2e^-$$ Eq. 23

Nowadays, typical operating conditions of PEM electrolyzer are in the range of 50-80°C and 1-60 bar, and it can reach efficiency of 55 kWh/kg [4], [35]–[37].

In Figure 40 the scheme of a PEM cell is reported. Electrodes are directly placed onto the membrane like a coating, creating a unique component, the so-called MEA (membrane electrode assembly). The electrodes in PEM technology are made by different material in the two half-cells. At the cathode side, since the potential is close to zero, the electrode substrate is carbon on which platinum nanoparticles are dispersed as catalyst of reduction reaction. On the other side, anode electrode substrate must be made by titanium due to high potential that would lead to corrosion of other materials. While iridium is used to catalyze oxidation reaction at the anode. Bipolar plates are made by titanium as well, with golden coating at the cathode and platinum coating at the anode, in order to prevent titanium passivation [4].

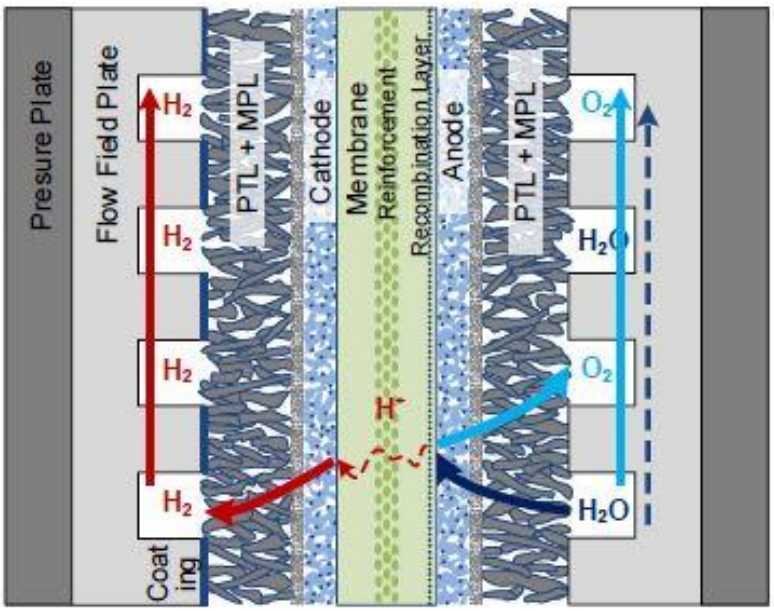

Figure 40: PEM electrolyzer cell, reprinted from [17]

Compared to ALK technology, PEM electrolyzer adopts noble metals as catalysts, therefore they are more expensive. Furthermore, titanium is quite expensive, and it could have

mechanical and chemical instability. For instance, titanium oxide can be produced on the surface when it is in contact with oxygen, creating a passivation layer that increase cell resistance. One of main research aim on PEM electrolysis technology is to reduced catalyst loading by decreasing nanoparticles' size and improving catalyst utilization, in order to decrease costs and dependance from critical raw material. In particular, iridium could be a scarce resource for a future large scale electrolyzer production [17].

The PFSA membranes are a more complex system respect to porous diaphragms in ALK electrolysis technology, in fact it works as electrolyte giving great proton conductivity and half-cell separator to prevent gas crossover. PEM electrolyzer membrane conducticity is strongly affected by water content in the membrane, in fact a higher water content turns into a higher proton conductivity. During operation membrane absorbs water that leads to a swelling behavior. This phenomenon could lead to mechanical damages, mostly for pressurized operation and large surface cell [36].

PSFA membrane is able to limit much more the gas crossover, hence it is possible to have a thinner membrane. A typical thickness for commercial application is about 100-200 μm, however studies are going on for membrane thickness reduction until 20 μm [4]. This characteristic allows to operate the half-cells with pressure difference, hence only cathode is operated at higher pressure, with the advatage of having hydrogen already partially compressed without performing all the system at higher pressure. Consequently, costs and efficiency penalization are lower. However, if the cell is operated with great pressure difference, typically a thicker membrane is used in order to prevent the increase of gas crossover. Moreover, pressurized operation increases investment cost and finally, it could increase degradation. Therefore, commercial PEM electrolyzer are typically performed at a pressure equal or lower than 50 bar, even though theoretically it is possible to achieve much higher hydrogen pressure at cathode [36].

The flow field of the bipolar plates is connected to MEA through a porous layer, that has the objective of ensuring a uniform distribution of gas and electric current between bipolar plates and electrode surface [17]. This layer is called GDL (gas diffusio layer) as well as PTL (porous transport layer). In addition, a microporous layer (MPL) with higher hydrophobicity is usually adopted between GDL and electrode surface in order to a have a better water management inside the cell.

Thanks to cell structure and the solid electrolyte, the maximum current density is not limeted by bubble formation on electrodes surface as for ALK electrolyzer. Therefore, maximum current density is higher, typically 2.0-2.2 A/cm^2 for commercial system, and it is limited from mass transport losses that lead to rapid end relevant efficiency decrease for current density beyond that level. Hence, PEM electrolyzers are characterized by higher power density, so they are more compact if compared to ALK ones [4], [35]–[38].

Thanks to cell configuration and metioned features, PEM electrolyzers are even more flexible. Firstly, the load range is wider, current state of the art is about 10%-160% [37]. Futhermore, some manufacturers do not give technical minimum load. Finally, it is possibile to operate beyond nominal power, but the upper limit actually depends on the definition of nominal load by supply company. Secondly, the transients during dynamic

operations are shorter, hence it can directly use electricity from aleatory renewables. However, PEM as well as ALK electrolyzer are typically held in stand-by mode, keeping constant the temperature for flexible operation. This procedure is needed to provide quicker load change, since cold start-up implies longer time for heating up the system and lower performances during this period [36]. Currently warm start-up takes less than 10 seconds for PEM electrolyzer, while between 1 and 5 minutes for ALK one. On the other hand, typical cold start-up takes respectively less than 20 minutes for PEM electrolyzer and less than 50 minuts for ALK one [4], [37], [39].

An example of stack is depicted in Figure 41. It is based on several cells connected in series by the usage of bipolar plates that provide electrical connection between neighboring cells, similarly to ALK electrolyzer stack. Peculiarities of PEM electrolyzer stack design are: the flow feeding occurs in parallel in order to reduce pressure drops and to have a better and more uniform performances in the single cells. Futhermore, the stack is characterized by two end plates that pressurize the stack in order to avoid gas leakeges since the typical higher operative pressure compared to alkaline stack.

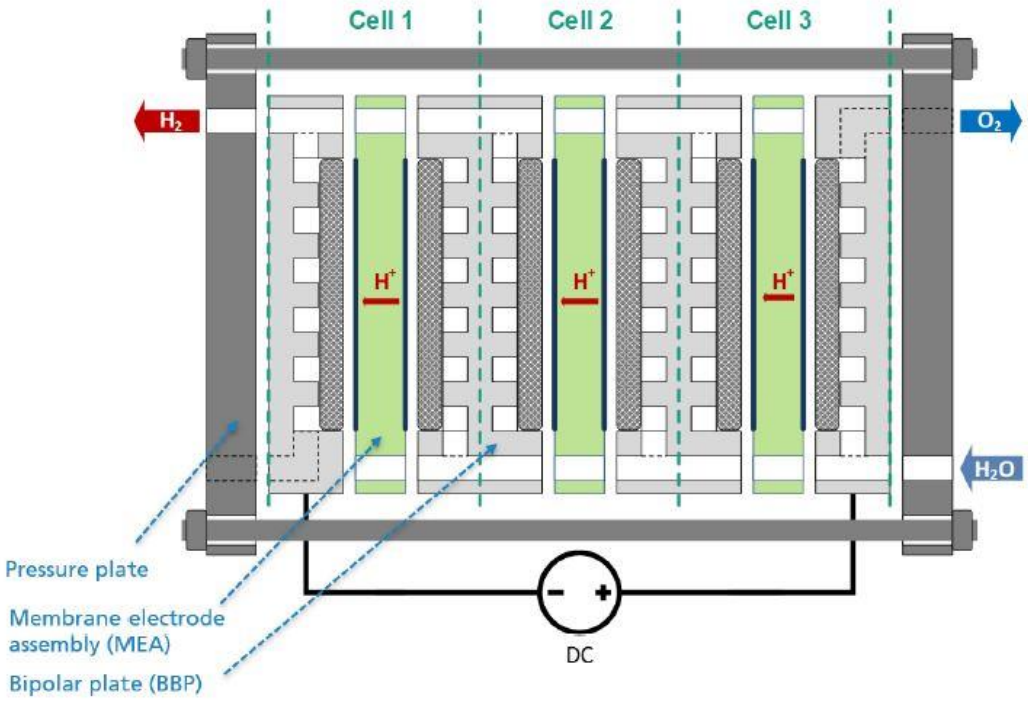

Figure 41: simplified scheme of PEM electrolyzer, reprinted from [17]

The plant layout is smaller if compared with ALK electrolyzer, because there is not a liquid electrolyte that required to be separated, mixed and re-injected in the stack. However, the other components of the BoP are similar as it possible to notice comparing Figure 38 and Figure 42.

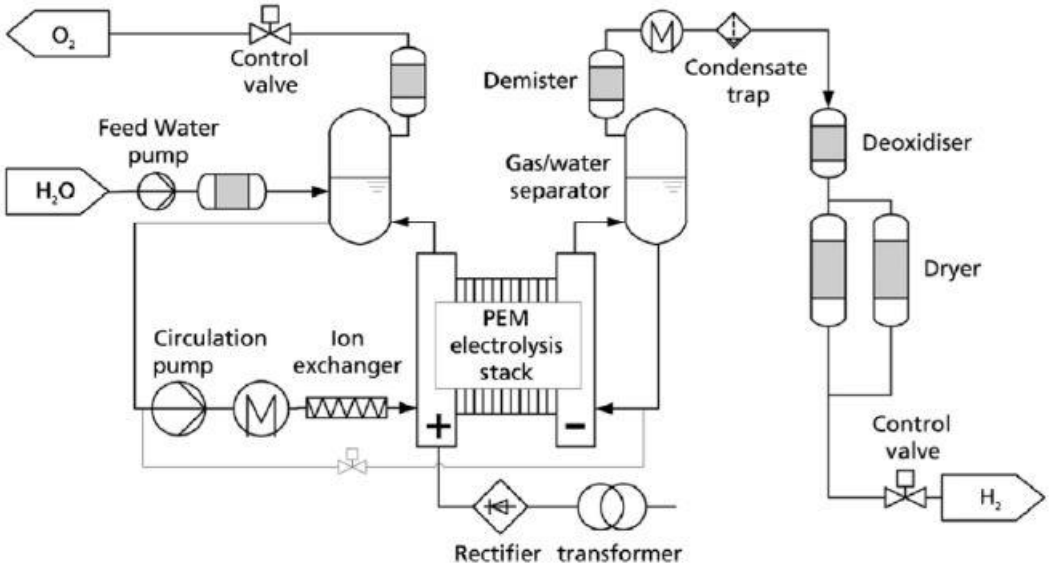

Figure 42: PEM electrolyzer plant layout, reprinted from [17]

Current investment cost for a PEM electrolyzer is around 900 €/kW for a reference size of 100 MW, while cost breakdown is presented in Figure 43. First of all, it is possible to notice how BoP and stack account respectively for 55% and 45%, as for the ALK electrolyzer. However, if the cost related to balance of plant have same distribution, the stack cost breakdown is completely different. The most relevant cost for PEM electrolyzer stack is the bipolar plates (24% of total capex) since titanium coated with gold and platinum is needed to prevent their corrosion.

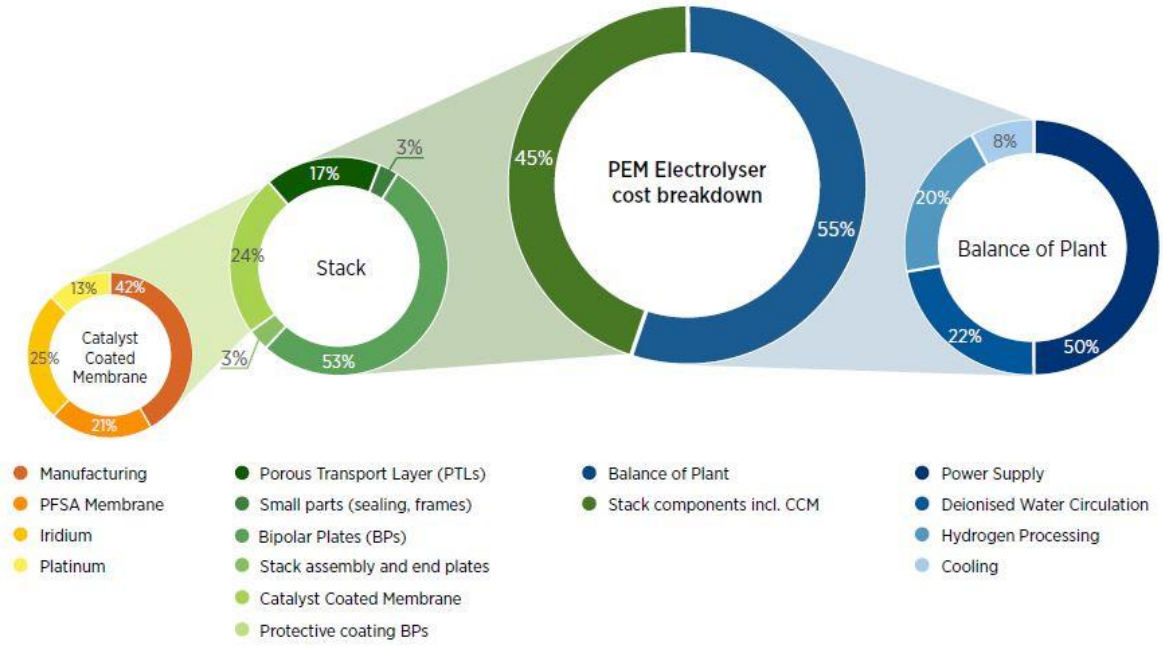

Figure 43: Cost breakdown for 1 MW_e PEM electrolyzer, reprinted from [4]

Afterward, the membrane assembly is quite expensive, mostly due the usage of noble material as catalyst and a more advance membrane respect to a diaphragm. While manufacturing cost is low because the process directly provides the MEA, hence the membrane and the electrodes with catalyst are a singular piece. While ALK electrolyzer manufacturing require the separated construction of electrodes and diaphragm that afterward are placed together. Finally, PTL also represents a significant fraction of stack cost.

To reduce stack cost and improves efficiency of PEM electrolysis, the focus is on the following key aspects [4]:

- Use thinner membrane
- Reengineering electrodes concepts, enhancing catalyst utilization and reducing catalyst loading
- Remove or substitute expensive coating on PTL
- Development of novel concept for recombination catalysts

While, for balance of plant cost reduction the focus is related to the power supply as mentioned for alkaline technology that it will mainly achieved by economies of scale and standardized designs [4]. The objective in 2030 is to reduce the cost down to 500 €/kW for a size of 100 MW_e and to increase efficiency up to 50 kWh/kg [35].

BoP lifetime of PEM electrolyzer is about 20 years [36]. While nowadays stack has a typical lifetime in the range of 50,000-80,000 operative hours [4], [37], [38], hence currently PEM electrolyzer lifetime is typically lower than alkaline one. However, in the long run PEM electrolyzer could have an equal or higher lifetime [4], [37], [38]. In general, it can be noticed that for PEM electrolysis greater improvments are expected, since it is a less mature technology. In Table 5 the state of art features for electrolysis are summarized. Furthermore, in Table 6 2030 objectives are reported. Finally, a comparison between current ALK and PEM electrolysis technologies is done in Table 7.

Table 5: SoA summary for electrolyzer [4], [17], [35]–[40]

Technology	ALK	PEM
Electrolyte	Liquid KOH solution	Acidic polymer membrane
Transported ion	OH^-	H^+
Bipolar plates	(+) nickel coated stainless steel (-) nickel coated stainless steel	(+) Platinum coated titanium (-) Gold coated titanium
Catalyst materials	(+) Nickel (-) Nickel	(+) Iridium (-) Platinum

Temperature	60-90°C	50-80°C
Pressure	1-30 bar	1-60 bar
Current density	0.2-0.8 A/cm^2	1.0-2.2 A/cm^2
Efficiency	50 kWh/kg	55 kWh/kg
Stack lifetime	60,000-100,000 hours	50,000-80,000 hours
Minimum load	15-40%	0-10%
Warm start-up	1-5 min	< 10 s
Maximum stack size	6 MW	2 MW
Capex (referred to 100MW size)	600 €/kW	900 €/kW
Footprint	70 m^2/MW	45 m^2/MW
Use of critical raw materials	0.6 mg/W	2.7 mg/W

Table 6: 2030 objectives for electrolysis system [4], [35], [37]

Technology	**ALK**	**PEM**
Temperature	>90°C	60-80°C
Pressure	30-50 bar	30-80 bar
Current density	1.0 A/cm^2	3.5 A/cm^2
Efficiency	48 kWh/kg	50 kWh/kg
Stack lifetime	80,000-100,000 hours	90,000-110,000 hours
Minimum load	10-15%	0-10%
Warm start-up	10 s	1 s

Capex (referred to 100MW size)	400 €/kW	500 €/kW
Footprint	40 m^2/MW	25 m^2/MW
Use of critical raw materials	0.0 mg/W	0.3 mg/W

Table 7: Comparison of current ALK and PEM electrolysis [4], [17], [37], [39], [40]

Technology	**ALK**	**PEM**
Advantages	Mature and robust Use of relatively cheap and non-critical materials Today's cheapest electrolyzer Multi-MW system already available	High power density → lower footprint Wide load range Fast start-up time and load change Allow high pressure operation even in differential mode Simpler BoP
Disadvantages	Low power density → higher footprint Limited load range Slow start-up and load change No pressure difference between half-cells More complex BoP to manage liquid electrolyte and achieve H_2 requirements	Use of expensive materials as titanium, iridium, platinum, and gold Higher capex Lower lifetime Reliability and lifetime of MW PEM stack still must be validated

To conclude, each technology has its own peculiarity, with pros and cons, but there is no a best electrolyzer since the several possible applications and the strong research and development in this industry.

2 Case study

This thesis develops a techno-economic feasibility study regarding the installation of a hydrogen production process within an industrial facility. This chapter aims at introducing the case study, i.e., describing the existing industrial site and its characteristics. After an explanation about current processes and energy management inside the company, the purpose of this study and the constraints imposed by the company are underlined.

2.1. Industrial site and energy analysis

The industrial site is owned by the Tampieri Financial Group S.p.A. that is the parent company of nine separate firms in which it holds the majority of the shares. The main firm produces vegetable oil, and it is one of the European leaders for sunflower, corn germ and grape seed processing. Afterward, there is a company whose purpose is to manage and supply energy demands, a company whose business is related to wastewater purification, and other companies that handle other activities with low-energy demands.

Vegetable oil production, which is the core activity of the company, requires several processes, such as drying, preparation, extraction, and refining. All these steps have a relevant demands of low pressure (LP) vapor and electricity. Furthermore, the oil refining process requires high pressure (HP) vapor. Therefore, it is possible to notice how just the oil production implies a complex system to manage, where three different energy flows are needed. In addition, all the other firms and activities in the industrial area have electricity demands that must be satisfied. In Figure 44 the total daily electricity demand for a representative year is reported.

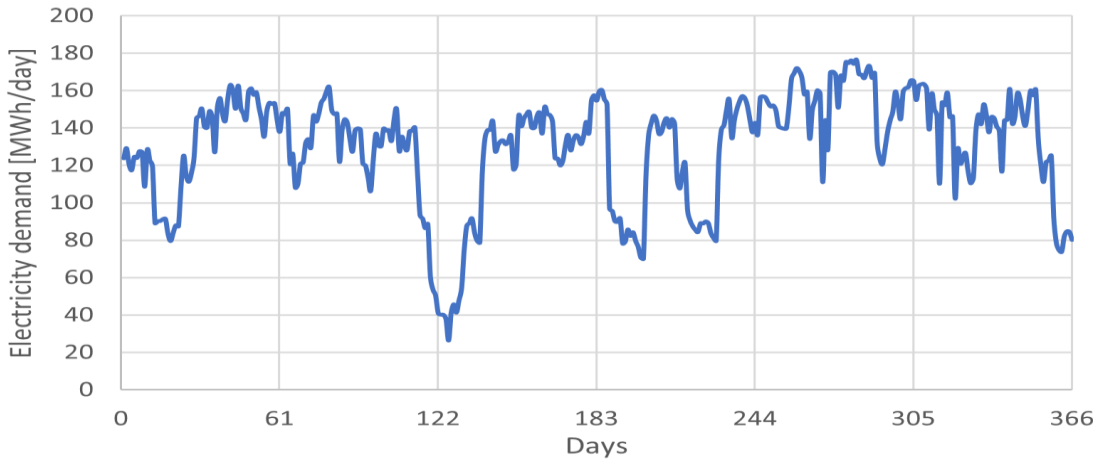

Figure 44: Total daily electricity demand 2021

The average electric demand of the whole industrial site over the past four years (between 2018 and 2021) was equal to 5.46 MW_e, where the consumption from oil production company accounts for the 84%, while all auxiliary systems for energy streams generation are equal to 8%. Finally, 4% of total consumption is related to the wastewater treatment section and the remaining 4% is the sum of all low electricity demand firms.

Instead, the total daily LP and HP vapor demands are reported respectively in Figure 45 and Figure 46.

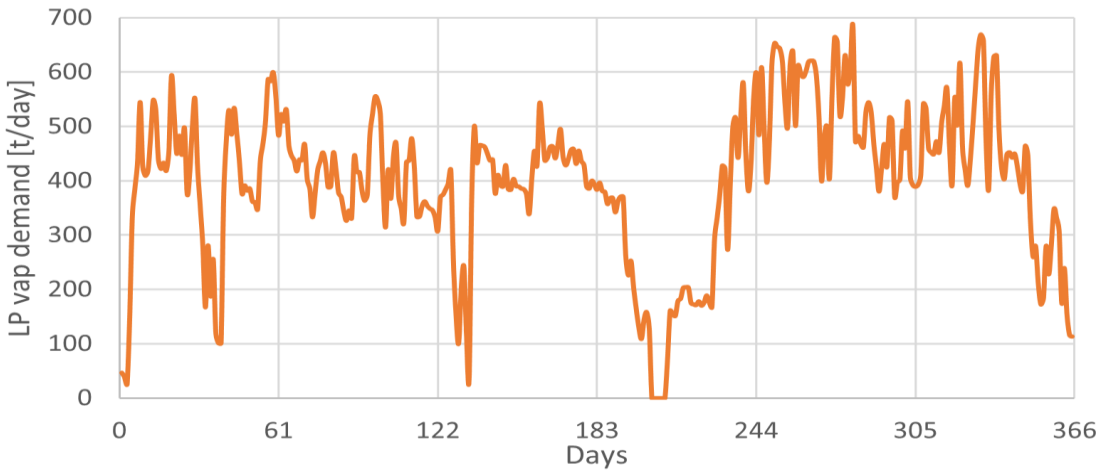

Figure 45: Total daily LP vapor demand 2021

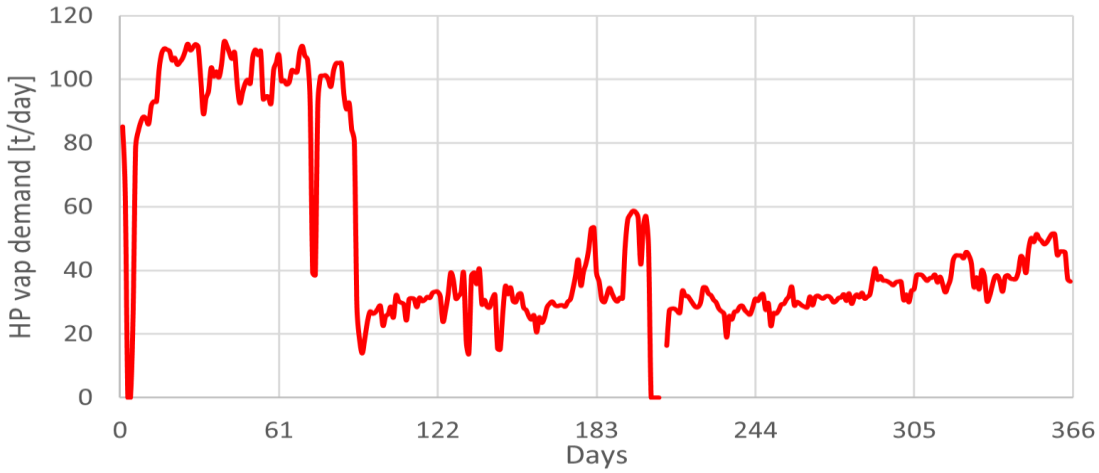

Figure 46: Total daily HP vapor demand 2021

During May of each year typically the processes in the industrial site are interrupted for a week to perform the regular maintenance. According to company knowledge, the energy demand at hourly level is quite steady with some differences between day and night. Therefore, most of the data provided are daily based and they are assumed as a good representation of real behaviors. The extra electricity profile is the only one received hourly based in order to have a better approximation since it is the exploitable electric power.

As reported in Figure 46, the high-pressure vapor demand shows to have a strong decrease after the first months of the year. The current HP vapor request must be considered as in the second part of 2021 according to further company indications, considering the first part of the year as exceptional.

To satisfy these demands the company is currently adopting a combined heat and power (CHP) system, composed of three steam generation units using biomasses as fuel, two steam turbines, and a number of connection elements. This type of plants typically has a high LCOE, from 100 to more than 200 €/MWh [41]–[43]. The average values for the CHP plants of the case study ranged between 130 and 168 €/MWh in years 2018-2021. The levelized cost of electricity of this kind of plants depends mainly on the mix of treated biomass types and their costs, but it is also affected by the plant efficiency and the yearly electricity generated. Despite the positive aspects such as CO_2 emission reduction, source diversification, and limited dependency from energy imports, in general the investment on CHP plants fed by biomass is not profitable if the electricity is sold on the electricity market, since the average price of electricity in Italian market before 2020 was below 80 €/MWh. Currently, biomass CHP plants have access to incentives in order to make them competitive. In fact, in the case study, the electricity excess of the industrial area that is currently injected into the national electric grid is receiving green certificates incentives for 20 years since the commissioning.

A simplified representative scheme of the industrial site with CHP plants is reported in Figure 47, depicting the overall plant configuration and the main energy flows.

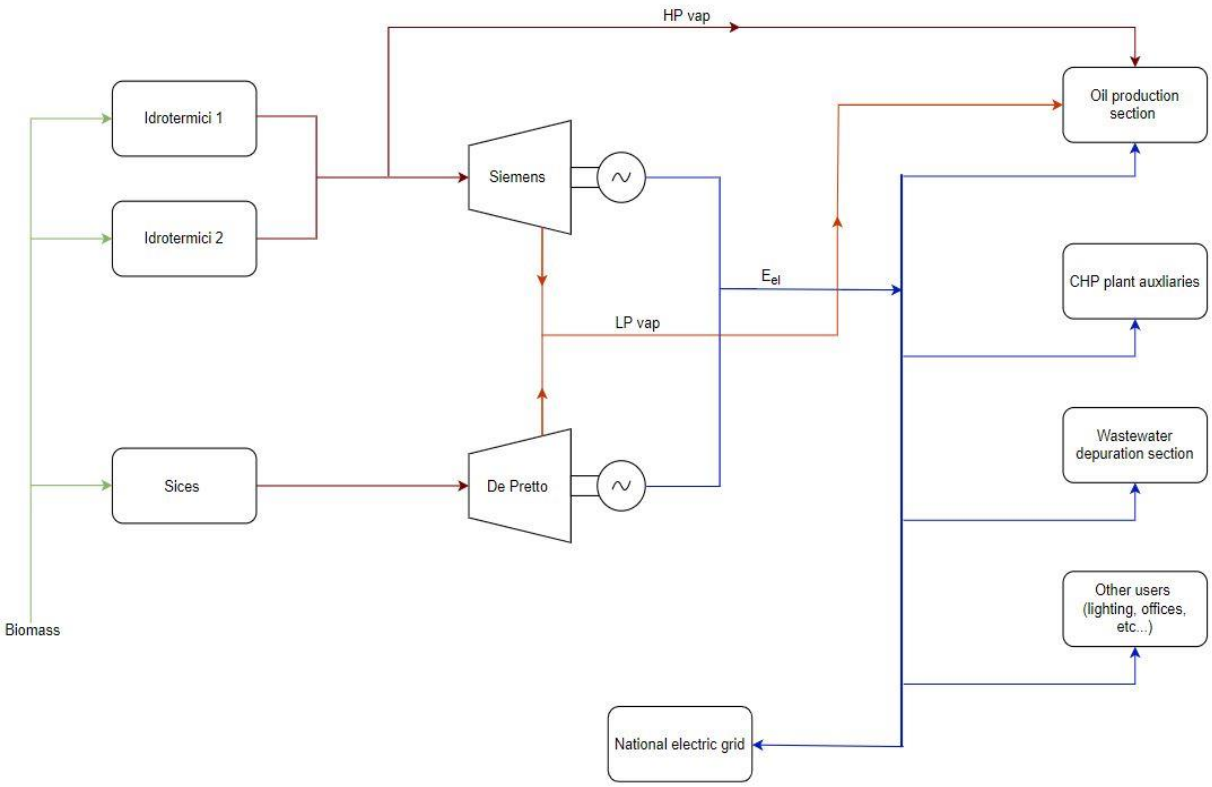

Figure 47: Simplified scheme of industrial site energy systems with main energy streams

Given the incentives, the company designed the CHP plants in order to produce a large amount of surplus electricity to sell on the electricity market. In fact, the nominal electric power was oversized as it can be noticed in Table 9 or comparing it (Table 8) with the electricity demand reported in Figure 44. The industrial site has two CHP groups. One composed by Sices boiler of 49.5 MW_{th}, coupled with De Pretto steam turbine with a nominal electric power output of 20.1 MW_e, that started to operate in 2007. The second group is older (2003), and it has two boilers, Idrotermici 1 and 2 of power 31.5 and 18 MW_{th}, respectively. These boilers serve the Siemens turbine that has a nominal electric power of 14.8 MW_e. Steam bleeding before last stages to provide LP vapor is possible in both turbines. Furthermore, the available data include the maps for turbines performance that give relations between the HP vapor flow rate fed to the turbine, the LP vapor bleed and the electrical power generated. Table 8 summarizes relevant data regarding the CHP plants.

Table 8: CHP plants data and average parameters (2018-2021).

CHP group	Sices + De Pretto	Idrotermici + Siemens
Construction year	2007	2003
Year of incentive end	2026	2022
Boiler size [MW_{th}]	49.5	31.5 + 18.0
Nominal electric power [MW_e]	20.1	14.8
Boiler efficiency [-]	0.84	0.83
Electric efficiency [-]	0.23	0.22
Operative hours [h/y]	8520	8380

The control strategy of these power plants is totally based on the demands of oil production processes, looking at HP and LP vapor demands, while electricity demand is satisfied consequently given the oversized plant. Typically, high pressure vapor is provided by Idrotermici boiler, taking it before the turbine inlet, while low pressure vapor is bled from De Pretto turbine, therefore Siemens turbine expand all the inlet high pressure vapor without any bleeding. Furthermore, Sices boiler works steadily at nominal power for most of the year while Idrotermici boiler operating point varies day by day and it never reaches nominal power. In addition, the Idrotermici boilers are not designed to receive biomasses classified as waste, hence all those streams are burned in the Sices boiler.

Table 9 reports the average values over the last four years (2018-2021) of net electricity generation and extra electricity that is sent to the national grid.

Table 9: Average electric power quantities in years 2018-2021

Siemens turbine	De Pretto turbine	Power generation	Power to the grid
5.11 MW_e	8.79 MW_e	13.90 MW_e	8.44 MW_e

In Figure 48 the load duration curve of the surplus electricity injected into the electric grid is presented, hence it corresponds to the electricity that could be possibly used for a new industrial application. It can be noticed the initial steep decrease, therefore a reasonable available power is significantly lower than the 12.5 MW_e peak, in fact electric power is higher than 6 MW_e only for 1448 hours per year. This can affect the size of a possible hydrogen production section.

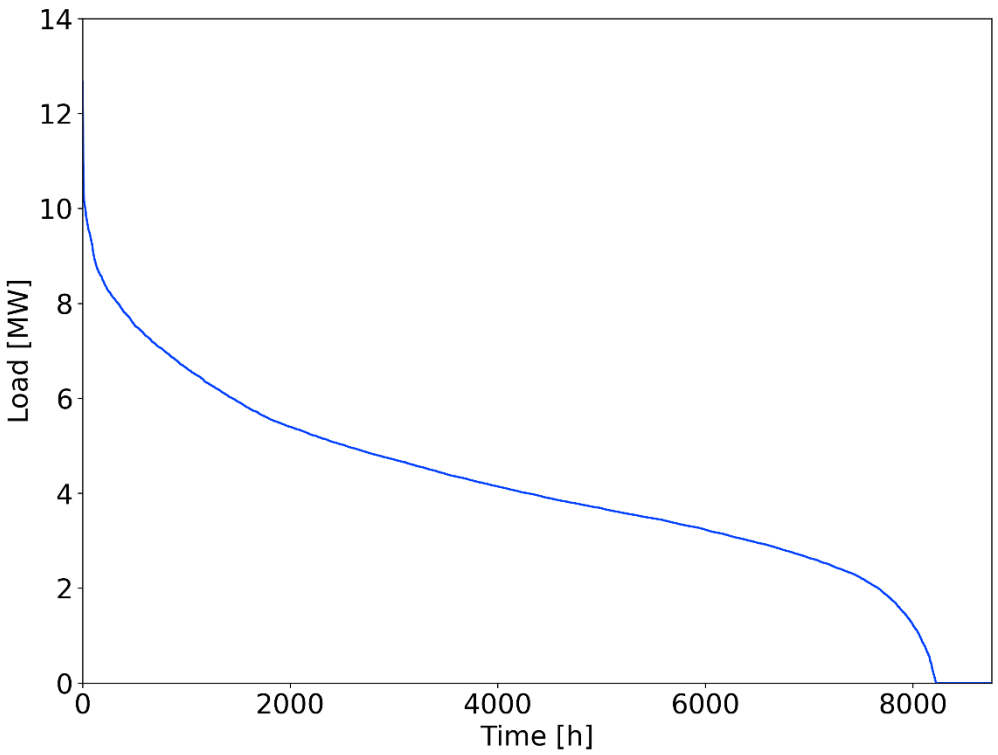

Figure 48: Load duration curve of surplus electricity.

The biomass fed to the CHP plants to satisfy electricity and heat demands derives partially from by-products of vegetable oil production processes. This represents about 42% of total annual amount of fed biomasses. The remaining part is bought on the market, and it mostly derives from agri-food value chain.

The following list summarizes the main biomass types currently used by the company:

- Meat and bone meal
- Dried and not-dried grape skin
- Grape pomace
- Residual wood
- Residual vegetable waste
- Sewage sludge

The mix of biomasses can change over the year due to market reasons; hence, new biomass types may enter the mix, and some may not be processed anymore, given the input flexibility of the power plants. The change in the biomass mix is one of the factors that, together with the price of each biomass type, impacts the average price of the CHP fuel.

In Figure 49 the current (2021) mix of biomasses is presented. The correspondent total annual amount is 169,215 t.

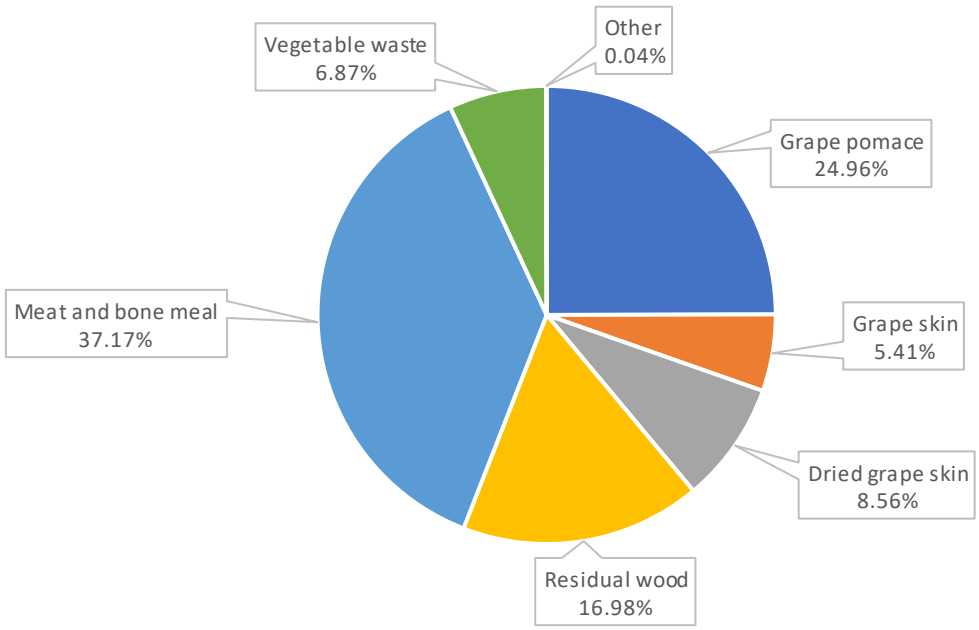

Figure 49: 2021 biomass mix.

Natural gas is also utilized in the industrial site in two different ways, for a total amount of 7,232,189 Sm^3 in 2021, which corresponds to 69,429 MWh_{LHV}. The 54%of the gas is used in the drying process of the oil production chain, since some of the driers work with natural gas, while other with low-pressure steam. The remaining 46% is fed to the boilers, both Sices and Idrotermici, mainly during start-up process and possibly for superheating the vapor. In any case, the amount of natural gas fed to the CHP plants must be equal or lower than 5% of the total energy input to be compliant with regulation to get access to green certificates incentives.

The firms inside the industrial site do not have to pay all the costs related to electricity as a regular consumer does. According to the Italian regulation the electricity consumed in the industrial area is not charged for transmission and distribution costs, as well as for social and environmental obligations and other indirect costs (grid fees and levies); hence, this represents a great advantage. The electric grid in the industrial district is managed privately, and for the case study, the associated cost is close to zero according to discussion developed with the company, hence negligible. Therefore, the different sections consume electricity generated from the CHP plants in the industrial area, and they pay it according to hourly price generated from the resolution of day ahead market (DAM).

2.2. Aim of the study and set constraints

The objective of the company is to evaluate new ways to valorize their biomass residues and to find new solutions for their businesses, since the incentives on electricity generated by the CHP plant will end in the next years (see Table 8). Therefore, this study has the aim of proposing and assessing possible solutions to valorize the biomass by producing hydrogen instead of electricity. Hence, a techno-economic assessment of the proposed configuration is carried out in order to understand if and when it could be technically and economically feasible to make an investment on green hydrogen production. The time horizon on which the study is based is from 2027-2030 onwards, in line with the time when all incentives from green certificates will end.

Some limits are imposed on this study by the company; in fact, the new configuration of the energy system cannot affect the firms in the industrial area nor the reliability and availability of energy streams supply to vegetable oil production processes.

Moreover, the company that manages the power production has already taken an important choice: one of the CHP groups (the Idrotermici boilers and the Siemens turbine) will stop operation from 2023. This is due to a combination of factors, such as the end of incentives on that power plant, the uncertainty of biomass prices, and the difficulties in procuring them. Since the other CHP group is still incentivized until 2026 and it can satisfy all the energy demands, there are no reasons to continue operation in the next year, even because an extra maintenance would be required. One of the two Idrotermici boilers will be converted to a natural gas fired boiler and it will be used as a back-up unit to generate steam and guarantee the continuity of processes during ordinary or extra maintenance of the Sices boiler. The new control strategy to supply energy streams from 2023 is still under discussion, therefore possible further modifications would be needed. The most conservative case is considered, where the biomass CHP plant satisfies all the energy needs of the industrial site and the excess of electricity is the lowest.

For this reason, the available surplus electricity will be lower than the discussed historical values in section “Industrial site and energy analysis”, since the Siemens turbine will not generate electricity and the Sices boiler has to provide the high-pressure vapor previously

supplied by the Idrotermici boiler. This will reduce to 58,310 MWh_{LHV}/y the amount of natural gas consumed, if the new consumption of back-up NG-fired boiler is excluded. In addition, other modifications have already occurred in the last months of 2021 and at the beginning of 2022. In fact, the electric consumption of the wastewater purification firm has slightly increased, 100 kW on average, due to an additional new unit. Finally, high-pressure steam demand decreased and stabilized around a mean value of 1.40 t/h, compared to a previous average value of 3.37 t/h. All these mentioned modifications are taken into account for the assessment, by modifying the surplus electricity profile available accordingly. The load duration curve presented in the previous section (Figure 48) shows the updated profile that is also taken as the baseline for the next years.

3 Configurations modeling

Two configurations are analyzed to implement hydrogen production systems into the industrial area. In this chapter the chosen configurations are presented, and their tecno-economic modeling is explained.

The first proposed configuration is based on steam gasification. This choice derives from what has been mentioned in section 1.1. In fact, steam gasification is the most promising technology for direct hydrogen production from biomasses. Moreover, since the company currently processes a large amount of biomasses, gasification is the only direct-conversion technology that can process these flow rates. Moreover, it is the easiest technology to scale-up in the next future, as already explained in the previous chapters. Instead, biological processes are not considered due to the specific biomass required that does not match with case study biomasses, the too large amount of processed biomasses and finally, except for anerobic digestion, the lower technology readiness.

The second configuration is based on electrolysis, which is chosen because of its higher readiness level and its compactness, and because it can exploit the power plant that is already operating in the industrial site.

Both models firstly evaluate technical performances taking into account year-long operation. Afterward, an economic assessment is performed assuming a 20 years perspective. The models repeat the evaluation for several sizes and for the last four years (2018-2021) prices of electricity, natural gas, and biomass.

All assumptions and input values are based on achievable target values in 2030, since it is the most likely year for the investment to start. However, values from the current state-of-the-art are used for parameters with challenging goals, or whenever 2030 objectives are not available.

3.1. Gasification model

General features and modeling logic

Gasification plants as well as CHP plants are characterized by high thermal inertia, hence long transient times are required for start-up, shutdown, and load change. Due to this feature, it is not possible to adopt an hourly control strategy that continuously chooses to produce either hydrogen via gasification or electricity to sell on the electricity market, according to electricity cost and hydrogen price. Therefore, it is assumed that the plant will work at nominal thermal power input, for a target number of hours per year, equal to 8,000 h/y [24], [34], [44]. Due to these assumptions the hydrogen production results constant during the year, and average yearly prices of electricity, natural gas and mix of biomasses are used. The modeling is not based on the current amount and mix of processed biomasses since there is a lot of uncertainty on their prices as well as their availability in the next years, according to company view. It is assumed that all the components have a lifetime equal or higher than the investment evaluation horizon (20 years) [35].

The main inputs of the model are:

- Processed mix of biomasses and characteristics of each biomass (LHV, ash and water contents)
- Experimental data from similar gasification systems for each biomass fraction
- Cost functions for each unit operation, in order to evaluate Capex and Opex

The process is designed according to other literature examples such as [24], [34], [44]. In Figure 50 the process flow diagram is presented and in Figure 51 the gasification section components are made explicit.

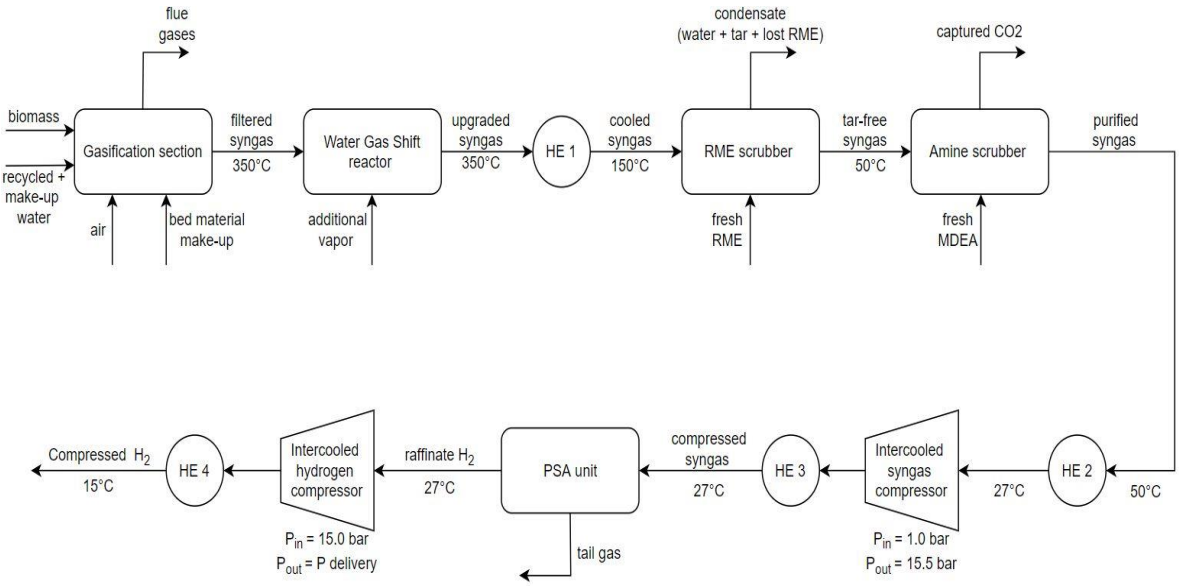

Figure 50: Simplified process flow diagram of gasification based H_2 production

Starting from the gasification section, syngas is produced, and heat is recovered for steam generation and air pre-heating, both from the hot syngas and from the flue gases stream. In the WGS reactor the CO content is strongly reduced, increasing H_2 and CO_2 content according to Eq. 10. Afterward, the upgraded syngas is cooled down at the inlet temperature of the RME scrubber, in which tar compounds are separated from the syngas stream and unreacted water is recovered by condensation. In the amine scrubber carbon dioxide capture is performed via absorption. Finally, high hydrogen content syngas is compressed and sent to an adsorption bed to be purified according to the requirements. The high-purity hydrogen is then compressed to the desired delivery pressure.

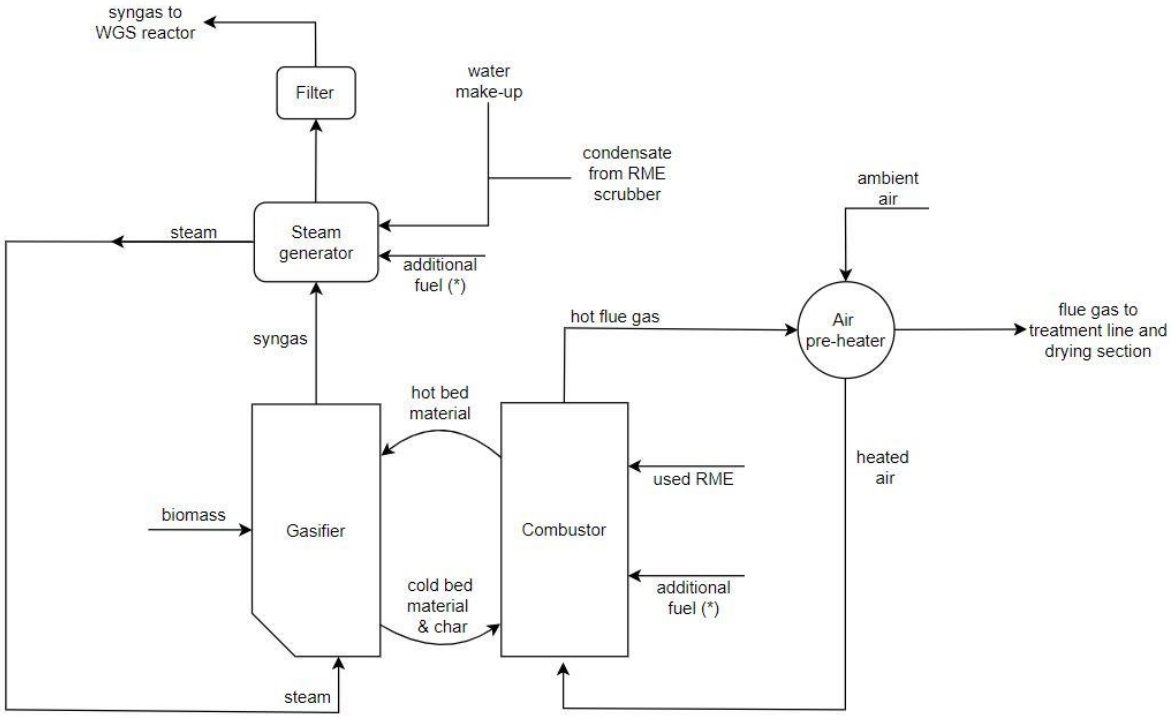

Figure 51: Simplified gasification section scheme

Given that biomass composition may vary widely according to the type, and given the several heterogenous reactions that occur, the most critical process to model is the gasification. A detailed approach like the one implemented in "FLEDGED project" in Horizon 2020 [45] could be applied via Aspen Hysys software. For the present thesis work it is decided to use a simplified approach and to develop the entire model in Python environment utilizing experimental data available from literature for each of the operational units presented in Figure 50. This approach is considered sufficiently reliable in order to assess the techno-economic feasibility of producing hydrogen via gasification technology, nevertheless, a further detailed simulation is required during the design phase, to assess properly technical aspects.

Gasification modeling is based on available results from a pilot plant of 100 kW of thermal fuel input [25], [26]. First, the CHNOS composition of the company biomasses are taken from Phyllis biomass database [46] since they were not provided by the company. Afterward, according to the CHNOS composition, each biomass is coupled with one from

literature for which gasification results and parameters are available. Ash content is taken from biomass database as well, while relative humidity (RH) and LHV are provided by the company. By a comparison of the latter values with RH and LHV from the database, it was even possible to verify the reliability of CHNOS database data. Therefore, selected the amount and the type of biomass input, it is possible to estimate the amount of syngas produced and its composition.

In this study only the main biomasses processed by the company are considered, hence meat and bone meal (M&B meal), residual wood, grape skin, and grape pomace, as shown previously in Figure 49. These biomasses are coupled in a proper way with data in [25], [26], except for M&B meal. In fact, for M&B meal there is no similar biomass in the literature used for gasification purposes, hence it is associated with chicken manure, which is the most similar given the high content of nitrogen. The company and literature biomasses characteristics are presented respectively in Table 10 and Table 11. It can be noticed that grape pomace, grape skin, and residual wood are well coupled with lignin, sugarcane bagasse, and softwood, respectively. Coupled biomasses do not need to have the same composition for two reasons: biomass characteristics slightly change from purchase to purchase; the CHNOS analysis has an accuracy that must be accounted for.

Table 10: Characteristics of the available biomass

Biomass	Grape pomace	Dried grape skin	Residual wood	M&B meal
Water content [$\%_{wt}$]	12.54	7.18	26.84	12.27
Ash content [$\%_{wt}$]	6.51	6.41	5.56	19.46
Carbon [$\%wt_{daf}$]	57.68	49.41	50.93	57.39
Hydrogen [$\%wt_{daf}$]	6.29	6.11	6.14	8.32
Nitrogen [$\%wt_{daf}$]	2.11	2.20	0.51	12.08
Oxygen [$\%wt_{daf}$]	33.77	42.29	42.35	20.85
Sulphur [$\%wt_{daf}$]	0.13	0.00	0.06	0.86
LHV** [MJ/kg]	16.27	16.66	9.87	17.14

*CHNOS composition is dry and ash free based (daf)

**LHV is for as received biomass

Table 11: Reference biomasses from literature

Biomass	Lignin	Sugarcane bagasse	Softwood	Chicken manure
Carbon [%wt$_{daf}$]	57.20	48.90	50.80	50.10
Hydrogen [%wt$_{daf}$]	6.10	5.90	5.90	6.50
Nitrogen [%wt$_{daf}$]	1.86	0.41	0.20	5.51
Oxygen [%wt$_{daf}$]	34.70	44.70	43.10	36.80
Sulphur [%wt$_{daf}$]	0.15	0.05	0.01	0.66

Once biomasses are coupled, the gasification section is modeled at technical level with the experimental data reported in Table 12. For each biomass gasification operating conditions (bed material, temperature, SB) are reported, as well as the cold gas efficiency and the dry syngas composition.

Table 12: Gasification parameters and experimental conversion data [25]

Biomass	Lignin - Grape pomace	Sugarcane bagasse - Grape skin	Softwood - Residual wood	Chicken manure - M&B meal
bed material	100% olivine	100% limestone	100% limestone	90% feldspar + 10% limestone
T gasification [°C]	789	753	789	766
Steam to Biomass [kg/kg]	1.0	0.7	0.7	0.9
CGE [%]	73	67	73	71
%vol$_{dry}$ H2	40.60	45.00	47.40	40.10
%vol$_{dry}$ CO	20.20	18.80	21.30	21.00
%vol$_{dry}$ CO2	20.80	23.50	21.20	19.80
%vol$_{dry}$ CH4	11.40	10.60	8.90	8.40
%vol$_{dry}$ LHCs	7.00	2.10	1.20	3.34
%vol$_{dry}$ other	0.00	0.00	0.00	7.36

Light hydrocarbons (LHCs) are modeled as C_2H_4, while the voice "other" comprises NH_3, H_2S, COS, HCl, HCN species; however, the amount is typically negligible. Relevant quantity of ammonia is produced only for high-nitrogen content biomasses as for chicken manure or M&B meal. Hence, in that case the voice "other" is modeled as ammonia.

Known the logic behind the modeling, in the next paragraphs it will be explained how each unit of the process is modeled, underling inputs, assumptions, and outputs.

Gasification section

Giving as input the biomass mix, selected a gasifier size and 8,000 yearly operating hours, the used amount of each biomass over the year is computed as well as the hourly flow rate to feed to the plant. To evaluate syngas production, hence H_2 production, it is assumed to gasify singularly each biomass for which experimental data is available. Therefore, the yearly hydrogen production is given by the sum of the singular biomasses production over the year and depends on the adopted biomasses mix. If in the real plant biomasses are fed as mix of biomasses different from the ones modeled in the present study the actual performance of the gasifier could vary; in fact, if the composition of input biomass changes, gasification parameters such as temperature and steam-to-biomass ratio should be adjusted accordingly in order to optimize the process, and the syngas and H_2 yields might be affected.

Syngas production is computed thanks to the CGE, the biomass flow rate, its LHV and the syngas LHV. This approach is equivalent to saying that the gasification section is thermal independent, since if additional fuel is required to sustain the gasification process, it is assumed to be supplied by a fraction of the produced syngas. This is a precautionary assumption, but it is in accordance with green hydrogen production since the additional fuel must be green as well. Finally, it is not a strong assumption because most of the heat is provided by residual solid carbon generated in the gasifier, while, in MW-scale reactor, additional fuel is typically used to regulate in a better way the temperature.

The outgoing syngas composition and LHV derive from experimental data according to the processed biomass. Moreover, the steam flow rate is evaluated from SB value and finally the vapor stream after the gasification section is computed knowing the water conversion from experimental data. Hence, the outgoing syngas is totally defined. It is assumed that the syngas leaves the gasification section at 350°C, after a first heat recovery for steam generation [18].

At economical level, capital cost function for gasification section is based on one of the most recent gasification plants, the GoBiGas project [47]. It represents the reference case at which an exponential factor (scaling factor n) is applied to adjust the value according to the selected size as shown in Eq. 24.

$$Capex = Capex_{ref} \cdot \left(\frac{Size}{Size_{ref}}\right)^{n} \quad \text{Eq. 24}$$

The reference Capex is 26.69 M€ for a size of 32 MW_{th} of biomass input [34], while the chosen exponential factor is 0.65, which is a value in the literature range (0.6-0.72) [34], [48], [49]. Gasification section Capex comprises a quite high uncertainty, typically about $\pm$ 30%.

Variable costs are divided in the following voices:

- Electricity consumption, that is assumed equal to 3.5% of biomass thermal power input [24], [34], [44]
- Bed material consumption, which is equal to 37.53 kg/MWh_{th} for limestone and 2.13 kg/MWh_{th} for olivine [44], at which correspond a price respectively of 0.150 €/kg and 0.156 €/kg [24], [34]
- Solid disposal cost associated to ashes disposal, with a specific cost of 0.9 €/kg [24], [34], [44]
- Water consumption cost, assumed equal to 0.0025 €/kg

A further note must be done for the cost of the bed material. As presented in Table 12, available experimental data are not with the same bed material, that implies different technical and economic performance compared to a situation with the same bed material. It is not realistic to change bed material according to the gasified biomass, especially if it changes continuously. Therefore, the technical performances of singular biomasses should be meant also according to the bed material adopted in the experimental tests. At an economic level it is assumed that bed material consumption and its cost are those of limestone for all the biomasses; it is a precaution given the higher cost associated to the usage of this material. With the sensitivity analysis a comparison with the usage of a bed material mixture 20% limestone - 80% olivine will be carried out to understand how much the bed material choice affects the economical assessment, assuming that conversions and compositions do not change relevantly as already explained in the state-of-the-art chapter with Figure 27.

Water-gas-shift reactor

The WGS reactor is modeled as one high temperature stage operated isothermally at 350°C. The achievable CO conversion is assumed to be 85% according to literature range (81-91%), while the molar steam-to-dry syngas ratio is taken equal to 1.4, hence in the middle of literature range (0.6-2.2) [24], [44].

The isothermal reactor assumption is made for simplicity and to be conservative in the estimation of recoverable heat after the WGS, since if the reactor is adiabatic the temperature will increase due to the exothermic reactions involved.

In this operational unit, the following calculations are executed:

1. Additional vapor needed to reach steam-to-dry syngas ratio equal to 1.4 as well as heat required to generate that amount of steam at 350°C
2. Outlet dry syngas composition and amount of unreacted water leaving WGS reactor.

The WGS reactor Capex function is given similarly to that of the gasification section. The reference values are 141.3 k€ for a daily H_2 production of 1500 kg. While the scaling factor is assumed equal to 0.7 according to literature [50], [51].

Heat exchangers

The heat exchanger sections are modeled in order to compute just the heat recoverable from the process. In fact, they are not sized, hence they are not accounted in the economic assessment since the Capex as well as the variable costs should not be relevant compared to other components. Furthermore, all heat exchangers are included in the sections of intercooled compressors, except for "HE 1" (Figure 50). The latter is the only one that recovers exploitable heat, since it cools down the syngas from 350°C to 150°C, while other heat exchangers cool down the compressed flow typically from 150-180°C to 27°C, hence these heats have less value. For this reason, they are not considered as recoverable in the process. However, an evaluation of low temperature application (drying or water pre-heating) can be evaluated at least for a first part of cooling.

Data input for calculations are the specific heats at constant pressure (C_P) for each compound. The average C_P between 400 and 600 K used for the "HE 1" is reported in Table 13, and the syngas C_P is evaluated knowing the mass fractions of the components in the stream.

Table 13: Average species' C_P between 400 K and 600 K

Species	H_2	CO	CO_2	CH_4	C_2H_4	H_2O (v)
C_P [kJ/kg K]	14.515	1.068	1.007	2.891	2.205	1.958

Tar removal section

The RME scrubber is not taken into account as process, since tar is not model in the gasification section. Therefore, this block is needed just for the economic evaluation. The specific Capex function is reported in Eq. 25 as a function of inlet volumetric flow rate [33].

$$Capex\left[\frac{€}{\frac{Nm^3}{h}}\right] = 35{,}291 \cdot V_{syn}\left[\frac{Nm^3}{h}\right] \qquad \text{Eq. 25}$$

This cost function will be also used to evaluate the Capex of the amine scrubber since for syngas flow rate above 1500 Nm^3/h the specific investment results similar [52].

A variable cost for the tar scrubber is the solvent consumption. RME consumption is set to 2 kg/MWh$_{th}$ with a price of 1.1 €/kg according to literature [24], [34], [44].

Amine scrubber

The amine scrubber is modeled with following assumption according to values range from literature [24], [34], [44]. CO_2 absorption is assumed equal to 90%, while thermal and electric consumption are given as function of the absorbed carbon dioxide, and they are respectively taken equal to 2.4 MJ/kg$_{CO2}$ and 0.4 MJ/kg$_{CO2}$. The solvent (MDEA) consumption is neglected since the cost related to its consumption is not available in literature and furthermore some experts say that it is not a relevant variable cost [34].

Therefore, the following steps are made in the amine scrubber block:

1. Calculate CO_2 separated from syngas stream
2. Calculate new composition of outgoing syngas
3. Compute electrical and thermal consumption as well as the related costs

Finally, it is assumed that captured CO_2 is vented into the atmosphere, but techno-economic evaluation for storage or alternative application can be included in future studies.

Compressors

Syngas and hydrogen compressors are modeled in the same way. An ideal power consumption is evaluated and after divided for a total efficiency. Both compressors are intercooled in order to limit maximum temperature of hydrogen and syngas at stage outlet, and to reduce the overall energy consumption for compression. The number of intercooling stages is chosen according to the total required pressure difference. Typically, an intercooling stage is added when stage pressure ratio is more than 3, since the temperature goes above 180°C.

The formula used to compute the power in kW is reported Eq. 26 [53], [54].

$$P = \dot{m}\frac{ZT_{in}R}{\eta_{cmp}\eta_{el}MW}\frac{N\gamma}{\gamma-1}\left[\left(\frac{p_{out}}{p_{in}}\right)^{\frac{\gamma-1}{N\gamma}} - 1\right] \qquad \text{Eq. 26}$$

Where:

- $\dot{m}$ [kg/s] the mass flow rate
- Z the compressibility factor
- R [J/mol K] the universal gas constant 8.314 J/mol K
- T_{in} [K] the inlet temperature set to 300 K
- η_{cmp} and η_{el} the compressor and electrical motor efficiencies set to 0.7 and 0.95
- MW [kg/kmol] the molecular weight of the flow
- N the number of stages
- γ the specific heat ratio
- p_{in} and p_{out} [Pa] the inlet and outlet pressure of the compressor

The differences between syngas and hydrogen compression are the compressibility factor, molecular weight, specific heat ratio, as well as the mass flow rate and the number of stages according to inlet and outlet pressure. In Table 14 input values are reported. MW, γ and Z for syngas stream depend on its composition which in turn depends on gasified biomass. However, Z and γ are set to average values that derive from typical composition of syngas at compressor inlet, while the molecular weight is computed according to real syngas composition.

Table 14: syngas vs hydrogen compressor parameters

Compressed gas	Syngas	Hydrogen
P_{in} [bar]	1.0	15
P_{out} [bar]	15.5	115-200-350-550-700
MW [kg/kmol]	According to syngas composition	2.016
γ	1.371	1.400
Z	1.027	1.03198
N	3	2-3-3-4-4

Thanks to Eq. 26 it is possible to size the compressors according to the maximum flow rate and afterward to evaluate the Capex, and to compute the specific electricity consumption (in kWh/kg) to compress the flow at the desired pressure. Afterward, it is verified through a comparison with point values in literature [39].

Capex cost functions are distinguished according to the number of intercooling stages as reported in Eq. 27, Eq. 28, and Eq. 29 [55]. The cost functions are adjusted according to most recent point values [39] since [55] has 2008 data and relevant developments are supposed to be achieved after 15-20 years. A cost reduction of 30% is assumed. Capex cost functions for hydrogen and syngas compressors are assumed to be the same since the syngas has typically a high hydrogen content (>70 %vol).

$$Capex_{N=2}[€] = 11{,}691 \cdot P[kW]^{0.6089} \quad \text{2 stages} \quad \text{Eq. 27}$$

$$Capex_{N=3}[€] = 14{,}029 \cdot P[kW]^{0.6089} \quad \text{3 stages} \quad \text{Eq. 28}$$

$$Capex_{N=4}[€] = 17{,}536 \cdot P[kW]^{0.6089} \quad \text{4 stages} \quad \text{Eq. 29}$$

A final note about hydrogen compressor must be done. There is not a best and confirmed technology, in fact several compressor technologies are studied and each of them has its own characteristics. Therefore, compressor data are difficult to find in literature and the available values have associated a relevant uncertainty.

Pressure swing adsorption

The PSA unit is assumed to work at 15.5 bar of flow inlet pressure, with an associated pressure drop of 0.5 bar, hence the outgoing purified hydrogen will have a pressure of 15 bar. It is assumed a hydrogen recovery equal to 90% with a purity level higher that 99.997% according to literature range [24], [34], [35], [44].

When adsorption beds are regenerated a valuable tail gas is produced, since it is composed mainly by methane, light hydrocarbons, 10% of hydrogen adsorbed in the bed, and small fractions of CO and CO_2. Therefore, it is crucial to exploit that stream to increase process efficiency. Tail gas is utilized firstly to satisfy additional heat requirements from hydrogen production plant that cannot be supplied by heat recovery in "HE 1", and afterward it may be utilized in several possible ways, for instance:

1. Sending it to a steam reforming reactor to produce more H_2 and recycle the stream back to the WGS reactor inlet.
2. Utilize it to substitute natural gas in industrial processes
3. District heating

In the case study it is assumed to valorized tail gas as a substitute of natural gas currently used in the industrial site. As further assumption, the tail gas economic value is set to zero when all the NG currently used is substituted. Extra tail gas could be further exploited in the boiler substituting part of fed biomasses.

The specific Capex cost function for the PSA unit is given in Eq. 25 and it is equal to the one adopted for RME and amine scrubbers, since for capacities higher than 1500 Nm^3/h the values collapse on one line according to [52].

Therefore, in PSA section the following steps are carried out:

1. Calculate the amount of purified hydrogen and the yearly H_2 production
2. Calculate the amount of tail gas, its composition and LHV, hence the available heat to substitute NG
3. Evaluate Capex of PSA unit

Final notes

Variable costs related to maintenance of all unit operations, assurance, labor cost, auxiliary consumption and plant overhead are considered as 9% of total Capex. However, a wide range of values is present in literature, from 5% to 14% of Capex [24], [34], [44], [56].

An installation factor of 1.1 of the Capex is accounted for each section, except for the compressor for which is advised an IF of 2.0 according to [55].

The model is verified through a comparison with previous results of studies or articles on similar topics. Furthermore, a check on electricity consumption is done in order to guarantee that the excess from the CHP plant is enough to cover the additional demand from the hydrogen production section [24], [34].

The hydrogen production via gasification is divided in three main sub-cases:

1. Techno-performance analysis varying reference year and size from 5 to 50 MW_{th} of biomass input, for a set mix of biomasses
2. Techno-economic analysis of each biomass, for a set size
3. Sensitivity analysis for most relevant parameters:
    - Total Capex due to high uncertainty on the estimated value
    - Biomass cost since it varies widely according to biomass type; furthermore, markets for each biomass are unpredictable for the next years
    - Electricity and natural gas prices due to high variability and difficult forecast about these markets
    - Operating hours, since 8,000 h/y is a target for a new plant, but currently operating plants are more likely working for a bit less hours per year
    - Bed material since the use of limestone for conventional DFB gasification is not applied at commercial scale, because it is not economical. A blend of 20% limestone – 80% limestone is evaluated because it gives similar conversions at lower cost [25]
    - "other Opex" voice since it represents a relevant cost for which a wide range of values is given in literature.

Through sensitivity analysis, it is possible to assess how an assigned variation on one parameter affects the techno-economic KPIs, such as the LCOH and the profitability index (PI). When the sensitivity is concurrently performed on electricity and natural gas prices, a matrix is built in order to include all possible scenarios, varying the average prices between 50 and 400 €/MWh for electricity and from 10 to 200 €/MWh for natural gas.

3.2. Electrolysis model

General features and modeling logic

Electrolyzers have a fast dynamic compared to gasifier and boilers, moreover electricity generation does not have significant variations hour by hour. Finally, CHP plants are dispatchable, hence the exact electricity generation for each hour is known. Thanks to these features with both type of electrolysis technology, ALK and PEM, it is possible to adopt a control strategy that allows to optimize the investment. An hourly choice is done to decide if produce hydrogen or sell extra electricity on the market, according to hourly price of electricity and daily price of natural gas at which is liked the hydrogen price nowadays. The calculation for the latter will be explained in the next paragraph (section 3.3). Known hydrogen price, it is possible to evaluate the willingness-to-pay (WTP) which associates a value to the electricity used to produce H_2. Hence, this value is compared to electricity price on the DAM. The formula to evaluate WTP [€/MWh], reported in Eq. 30, considers only marginal cost since production choices are taken on the moment, just taking into account variable costs [57].

$$WTP\ [€/\text{MWh}] = \frac{P_{H_2} + C_{inc} - C_{H_2O} - C_{tr}}{e_{electrolyzer} + e_{compressors}} \qquad \text{Eq. 30}$$

Where:

- P_{H_2} the hydrogen price [$€/kg_{H_2}$]
- C_{inc} the incentives on hydrogen selling [$€/kg_{H_2}$]
- C_{H_2O} the cost related to water consumption [$€/kg_{H_2}$]
- C_{tr} the cost related to hydrogen transport [$€/kg_{H_2}$]
- $e_{electrolyzer}$ the electrolyzer efficiency [MWh/kg_{H_2}]
- $e_{compressors}$ the compressor efficiency [MWh/kg_{H_2}]

It is assumed that in the industrial site hydrogen is just produced and compressed at the delivery pressure. Therefore, transport cost is set to zero since it is assumed to be performed by a third part or the hydrogen buyer. Furthermore, if the end application is "transportation", the cost for transport to a hydrogen refueling station will be negligible since the industrial site is close to one of main highways in Italy.

Hour by hour, WTP is compared with electricity price on DAM, therefore, if WTP is equal or higher than electricity price on DAM, hydrogen is produced in that hour, otherwise electricity is sold to the grid since more profitable.

Hence, using NG and electricity prices, and their trends in last years, it is possible to estimate for which hours the electrolyzer works during the year. Despite this approach consider hourly trend of electricity price, it assumes that it will not change in the future. In fact, it is not possible to have reliable forecasts for next 20-30 years. Therefore, if for electricity price a sensitivity analysis can be performed, variations on electricity price trends are not considered. Even though, due to production mix change, higher renewable

penetration, and net zero 2050 objective, significant change in electricity trend might occur, as happened through the last 15 years.

This approach respect to the modeling of gasification implies that hydrogen production depends on its price and electricity price. Therefore, it is needed to run more simulations according to the end use, since hydrogen value changes as explained in the section 3.3.

The input parameters of electrolysis configuration are the following:

- Hourly electricity profile available for electrolysis equivalent to load duration curve in Figure 48
- Hourly electricity prices on DAM from Italian market administrator website [58]
- Parameters to model electrolyzer and compressor at technical and economic levels

A representative scheme of electrolysis configuration is presented in Figure 52. As mentioned in section 2.1, power plant is managed in order to satisfy first LP and HP vapor demands, and afterward the electricity demand. If electrolyzer works, excess of electricity is used to produce hydrogen and to compress the latter at delivery pressure. Therefore, electrolyzer is sized taking into account that part of the available electricity is consumed by the compressor.

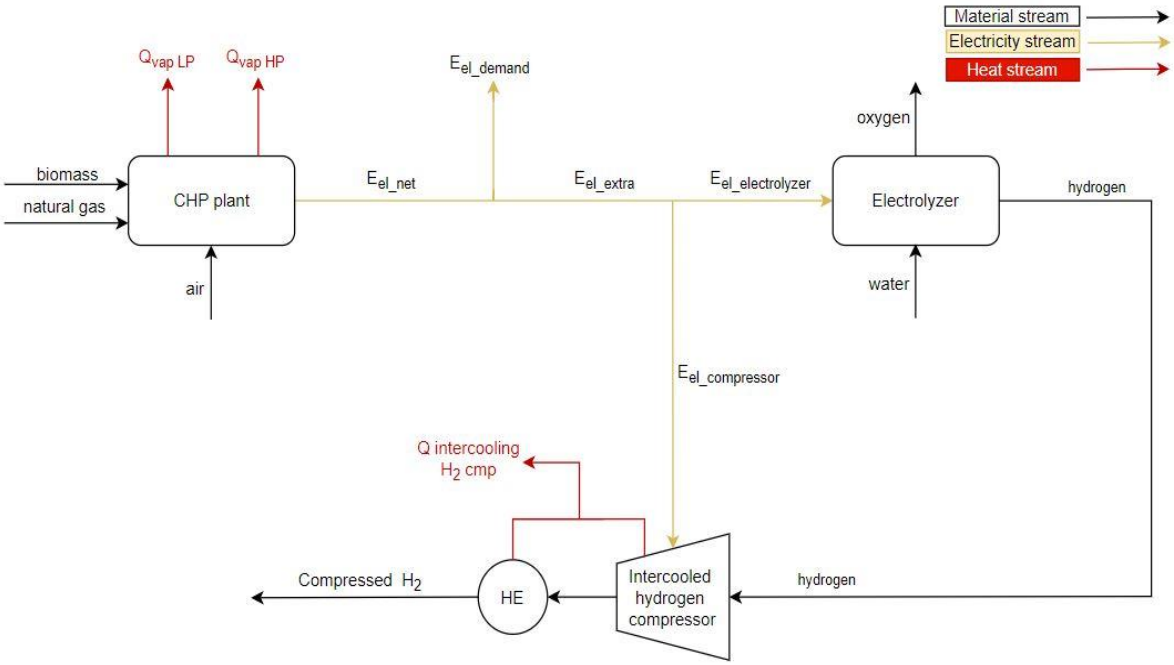

Figure 52: Electrolysis configuration flow diagram

Known the control logic and knowing the cited input data is possible to discuss in detail how the electrolyzer is characterized. While hydrogen compressor is modeled exactly as done for the previous configuration of above paragraph.

Electrolyzer

The model gives the possibility to simulate different type of electrolyzers just varying parameters' values on which it is characterized. In Table 15 input data for the electrolyzer are reported according to literature [4], [35], [37]–[39], [53], [54].

Table 15: Electrolyzer parameters

Technology	ALK	PEM
Efficiency [kWh/kg]	48	50
Minimum load [%]	30	10
Operating pressure [bar]	15	30
Opex	3% of Capex_tot	3% of Capex_tot
Stack lifetime [hours]	75,000	60,000
Stack Capex	45% of Capex_tot	45% of Capex_tot

The efficiency is assumed constant with the load and over the years for simplicity. However, it is a good approximation because the higher efficiency during part load operation and the decrease in efficiency over the years due to degradation somehow balance. Efficiencies for both technologies are chosen according to 2030 targets.

Instead, a more conservative minimum load value is assumed. In fact, both values derive from current state of the art, despite a lot of work is going on to increase ALK electrolyzer flexibility.

Operating pressure of the electrolyzer depends on the design philosophy and objective, therefore values in SoA ranges are taken, also according to other parameters values.

Variable costs, except for electricity and water costs, are united under the voice Opex that is assumed in the middle of range given from literature.

Lifetime of balance of plant components is assumed at least equal to 20 years as well as for hydrogen compressor, while the stacks lifetime is given according to the operating hours. Values reported in Table 15 for stack lifetime are assumed around the middle value of wide ranges currently given in the SoA literature. Stack costs are taken from literature as well, from Figure 39 and Figure 43 that are referred to 1 MW_e electrolyzers. Hence, it is a good approximation since the sensitivity analysis on the size goes from 0.5 MW_e to the maximum input power available for electrolysis that is equal to 12.5 MW_e.

Finally, Capex cost functions consider economies of scales as well as a cost reduction in the next years. In fact, the trend is shaped according to 2020 curves [59] and afterward they are re-scaled following European 2030 objectives, which aim to reach 400 €/kW and 500 €/kW

for a 100 MW_e scale, respectively for ALK and PEM electrolysis technologies [35]. The specific capex cost functions are shown in Figure 53.

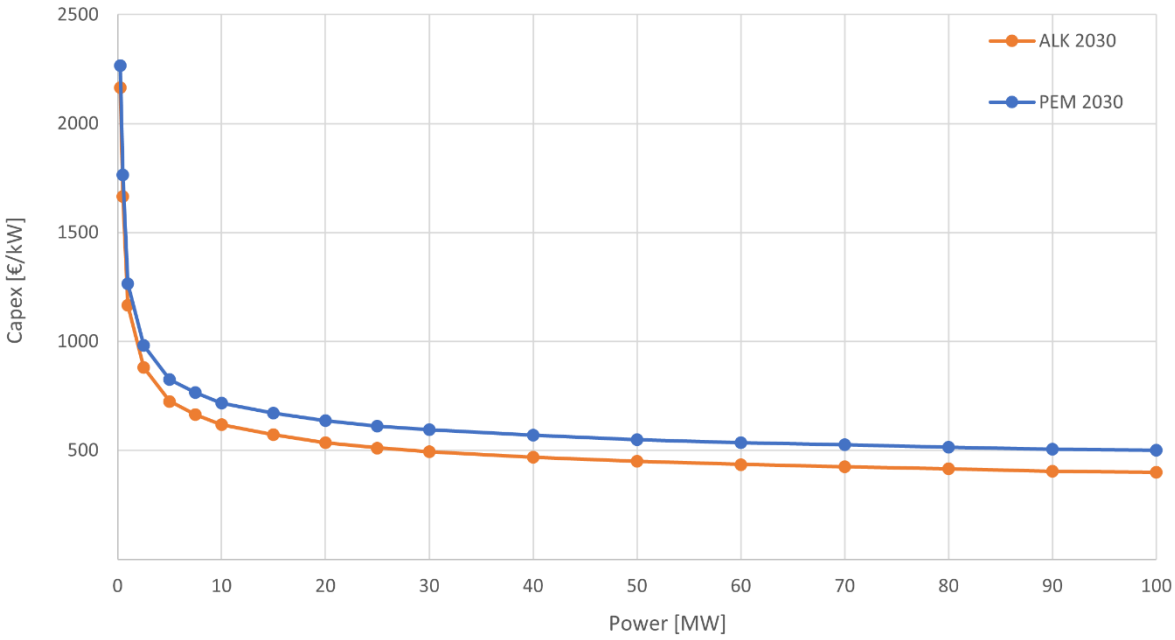

Figure 53: 2030 specific Capex curves for ALK and PEM electrolyzers

Oxygen valorization scenario

The valorization of oxygen could be included as indirect incentive in the WTP logic, hence a second term of $C_{inc}[€/kg_{H_2}]$ is added, knowing oxygen selling price and the O_2-to-H_2 mass ratio equal to 8 kg_{O_2}/kg_{H_2}. Furthermore, if oxygen needs to be compressed, its specific work must be added at denominator of WTP equation. Finally, for the economic assessment, additional possible equipment to reach oxygen requirements, according to the end application, must be accounted in the Capex.

To include this scenario a concrete end use of oxygen should be present, such as wastewater treatment, oxygen gasification, hospital oxygen as well as oxygen feeding to the boiler to improve efficiency. In this case study the two main exploitable options are the use in the boiler and the use for wastewater treatment since both processes are present in the industrial site. However, oxygen feeding to the boiler was evaluated in the past by the company and it turned out that temperature was too high for biomass combustion as well as NO_x generation. While the current demand of oxygen in the wastewater treatment is satisfied by oxygenated water that release oxygen during the process. Even if direct use of oxygen could be evaluated, the yearly amount required is so low that does not make sense to have any extra fixed or variable cost. Therefore, the model does not include oxygen valorization despite it can be inserted in future studies.

Final notes

The hydrogen production via electrolysis is divided in three main sub-case:

1. Techno-performance analysis varying size and reference year
2. Comparison between techno-economic performance of ALK and PEM electrolyzers
3. Sensitivity analysis for most relevant parameters:
    - Total Capex due to uncertainty related to its estimation and the cost reduction in 2030
    - Electricity and natural gas prices due to high variability and difficult forecasts about these markets
    - Electrolyzer efficiency since the uncertainty related to the achievement of 2030 targets.

The sensitivity analysis, even on electricity and NG prices, is carried out similarly to gasification configuration. However, a peculiarity is added since, in contrast with gasification, hydrogen production via electrolysis depends on hourly electricity prices, Therefore, to keep track of daily trend of electricity price as well as other features of the market, the price is not set constant equal to the average value; instead, the hourly prices are applied, scaling them according to the ratio between average price for the sensitivity analysis and average DAM price for the reference year (2018). Hence, each hourly price of reference year is divided for average value of 2018, and afterward it is multiplied for the average electricity price for which the sensitivity analysis is carried out. This approach assumes constant trends of electricity market, hence the profile is stretched or compressed according to average electricity cost. However, it is important to keep in mind that this assumption leads to accentuated electricity price peaks. While nowadays' (2022) high electricity price shows a different trend, i.e., for the hours of a typical day, all prices move to very high values, nevertheless the peaks are still present, but they are much less pronounced. On the other side, for natural gas price is considered the average value since the market is daily based and typically it does not have significant variation day by day as well as according to the season, except for some not ordinary events.

3.3. Economic evaluation

As explained in "Case study" chapter, cost of electricity for a firm in the industrial district could be well approximated by the price on DAM. Therefore, hourly prices from Italian market organizer are used in the model [58]. In the next paragraphs hydrogen price trends as well as possible incentives are discussed, and economic parameters to evaluate the investment are explained.

Hydrogen price and incentives

First of all, three different end applications are analyzed for green hydrogen:

1. **H_2 injection in the natural gas grid**, hence the objective is to provide mainly heat and it competes with natural gas.
2. **Industrial use**, where hydrogen is meant as a feedstock, hence it is needed to carry out reactions/processes as well as to provide heat. For instance, refineries, ammonia production, steel production, but even green fuels production. For this application green hydrogen competes with grey one.
3. **Transport use**, where hydrogen is adopted as fuel for vehicles, hence it competes with fossil fuels that are different according to considered transportation.

Therefore, three different hydrogen prices are estimated since different end consumers have different willingness to pay hydrogen due to different substitutes of green hydrogen. This approach is useful to understand for the case study if there is an industry where hydrogen is already competitive, and/or which are the required incentives to make investment profitable according to the end application. Furthermore, examples of possible incentives for each application are analyzed and estimated.

The sale price of hydrogen for injection in NG grid is estimated via energy equivalence with natural gas by Eq. 31, since H_2 as well as NG would be paid according to the energy that it can provide:

$$P_{H_2}^{case1}\left[€/kg_{H_2}\right] = P_{NG}\,[€/MWh] \cdot \frac{LHV_{H_2}\,[MJ/kg]}{3600} \qquad \text{Eq. 31}$$

A possible incentive related to this end use is the CIC mechanism currently used in Italy for biomethane. CIC means "Certificati di Immissione in Consumo di biocarburanti", i.e., "injection certificates for biofuels consumption". Since 2006, fossil fuels producers for transport application are obliged to supply a percentage of biofuels. Therefore, these firms can decide to directly provide the amount or buying CIC from other companies that sell biofuels at national level, for instance biomethane producers. Incentive for hydrogen is computed in analogy with biomethane incentive. Biomethane producers receives one CIC each five Gcal injected into the grid. A CIC quote in the free market can be currently valorized between 150 and 400 €/CIC according to demand and supply curves, but even a minimum CIC price of 375 /CIC could be guaranteed for the first 10 years. If CIC value will

remain in the same range, hydrogen incentive can vary between 0.86 to 2.29 €/kg, with a mean value of 1.58 €/kg. However, there are not a lot of information available about CIC market.

Hydrogen price for industrial sector depends mainly on hydrogen production process and CO_2 cost, since industries are typically included in the emission trading scheme (ETS). An empirical formula given from an Italian refinery is adopted to estimated hydrogen price. The Eq. 32 links H_2 price with natural gas price since most of the hydrogen (>76%), while it does not consider variation in carbon tax. Therefore, price will be slightly underestimated if assumed that in the future CO_2 cost will not decrease anymore at very low level as before pandemic.

$$P_{H_2}^{case2}\left[€/t_{H_2}\right] = 3.8 \cdot P_{NG}[€/t_{NG}] + 80 + \frac{255{,}555}{400} \qquad \text{Eq. 32}$$

For industrial applications just an indirect incentive is considered. The use of green hydrogen, instead of grey one, gives an advantage for industrial firms in ETS sector, since it is not associated to them CO_2 equivalent emission from hydrogen production. Therefore, the company can buy green hydrogen at a price equal to the one for grey H_2 plus the avoided cost related to CO_2 emissions. Furthermore, the company has other side advantages since it will look better to costumers' eyes. Greenhouse gases (GHG) emission related to grey hydrogen are about 10 t_{CO_2}/t_{H_2} according to international energy agency [2]. However, a detailed discussion that accounts also for methane leakages before the steam reforming process are present in literature [5]–[7]. The forecast on CO_2 cost is complex, but assuming an average value of 70 $€/t_{CO_2}$ with 45 $€/t_{CO_2}$ *and* 95 $€/t_{CO_2}$, as lower and upper limits, the indirect incentives for green hydrogen are comprised between 0.45 and 0.95 €/kg.

Finally, **hydrogen price for transport** is evaluated through a cost for kilometer equivalence between diesel heavy-duty trucks and fuel cell ones since the main target of fuel cell electric vehicles (FCEV) is the heavy-duty transportation. It is assumed that in future, as nowadays, the excises on hydrogen for transportation are not charged (at least for green H_2), hence it represents an indirect incentive. Therefore, known the diesel price and the consumption of diesel and hydrogen trucks is possible to perform the equivalence. Diesel consumption is in the range of 24-33 *l*/100km, while hydrogen consumption is between 5 and 9 kg/100km [60], [61]. The lower limits of both ranges are taken since they are the most likely values in the next future. Furthermore, it is taken into account that the final H_2 price must contain the cost related to the hydrogen refueling station (HRS). The price related to HRS roughly account for 36.4% of total LCOH according to [62], [63], while transportation costs are assumed to be close to zero thanks to the strategic position of the industrial site. Therefore, hydrogen price for transport sector is scaled considering that only 63.6% of total costumer price corresponds to cost sustained for processes inside the industrial site.

Beyond the exception from excises, green hydrogen for transports can be further incentivize with a logic like CIC mechanism. Since, instead of buying CIC certificates on the market, a firm could provide the required amount of biofuels even via green hydrogen production.

Natural gas daily prices are taken from [58], while the diesel prices derive from [64]. In Table 16 the average prices of electricity, natural gas and biomass for the past four years are reported as reference, despite hourly electricity price and daily natural gas price are used in the model.

Table 16: Electricity, natural gas and biomass average market prices for 2018-2021

Year	E el [€/MWhe]	NG [€/MWh HHV]	Biomass [€/t]
2018	60.71	24.24	69.33
2019	51.25	16.07	70.28
2020	37.80	10.42	63.18
2021	125.20	46.30	69.15

In Table 17 average prices of natural gas and diesel for the previous four years as well as the associated hydrogen prices are reported. However, in the model daily prices of hydrogen are calculated according to daily NG and diesel prices.

Table 17: Hydrogen price vs end application

Year		2018	2019	2020	2021
$P_{NG}[€/MWh]$		24.24	16.07	10.42	46.30
$P_{diesel}[€/l]$		1.49	1.48	1.32	1.49
$P_{H_2}\left[€/kg_{H_2}\right]$	NG grid injection	0.81	0.54	0.35	1.54
	Industrial	1.92	1.52	1.24	3.02
	Transport	3.73	3.71	3.31	3.73

While examples about incentives on green hydrogen with mean value as well as lower and upper limits are reported in Table 18, according to what explain previously in this section. Despite incentives on H_2 could use a similar mechanism to one adopted for current renewables, they will be made by policy makers according technology characteristics and features of industry where it will be used, in order to shape and set in a better way the mechanism. It is even more interesting see in the results how much should be the incentive to make green hydrogen competitive according to final application and production technology.

Table 18: Example of incentives for green H_2 vs end use

End use	Injection in NG grid	Industrial	Transport
Incentive type	CIC mechanism	Avoided CO2 emissions	CIC mechanism
Value [€/kg]	0.86-1.58-2.29	0.45-0.7-0.95	0.86-1.58-2.29

Economic indicators

The **levelized cost of hydrogen** (LCOH) represents the cost of hydrogen production, assuming an identical annual operation along the plant lifetime, and taking into account all financial factors as inflation and capital cost. Therefore, it is equivalent to the sale price of hydrogen that would lead to reach an NPV equal to zero.

$$\text{LCOH}\left[\frac{€}{\text{kg}}\right] = \frac{Capex + \sum_{t=1}^{T} \frac{c_{el} + Opex}{(1+r)^t}}{\sum_{t=1}^{T} \frac{H_{2\,prod}}{(1+r)^t}} \qquad \text{Eq. 33}$$

The formula to evaluate LCOH is reported in Eq. 33, where:

- T the investment duration assumed equal to 20 years
- Capex the total investment cost [€]
- c_{el} the yearly cost of electricity [€/y]
- $Opex$ the yearly operative cost, except of electricity consumption [€/y]
- $H_{2\,prod}$ the yearly hydrogen production [kg/y]
- r the exponent to actualize costs in different year. It considers inflation and cost of capital. It is assumed equal to 6%, but it should be assessed by a proper analysis.

The **net present value** (NPV) is an index to represent the project value at a selected year. Hence considering the end of the investment, it shows whether it results economically feasible (NPV>0) or not (NPV<0). As shown in Eq. 34, it is given by the sum of yearly actualized net cash flow (NCF) over the investment duration. NCF for a year represents the difference between revenues, given according to produced hydrogen, the selling price and possible incentive, and costs over the year, as reported in Eq. 35. In addition, Capex is even present and not equal to zero only for year zero or when a component is substituted, as the electrolyzer stack.

Finally, the project could have a terminal value (TV). In this case study is utilized in the electrolysis configuration to consider the value associated to the stack if it still has useful

lifetime. For instance, it could happen when stack is substituted just few years before the end of investment time horizon, hence TV is evaluated according to remaining lifetime by Eq. 36. TV approach could be used just when stack is substituted or even if the first stack does not come to life end, as done in this case study. In the latter approach TV is slightly overestimated in scenarios when electrolyzer is used just few hours in 20 years, since it would have a quite high terminal value despite the stack is 20 years old, hence some degradation occurred even if the stack is not exploited at its potential. However, it does not affect the results because if the electrolyzer is not exploited for enough hours during each year the NPV turns to be strongly negative in any case.

$$NPV\ [€] = \sum_{t=0}^{T} \frac{NCF\,(t)}{(1+r)^t} + \frac{TV}{(1+r)^T} \qquad \text{Eq. 34}$$

$$NCF(t)[€/y] = Revenues(t) - C_{el}(t) - Opex(t) - Capex(t) \qquad \text{Eq. 35}$$

$$TV\ [€] = \left(1 - \frac{OH_{stack}}{LT_{stack}}\right) \cdot\ Capex_{stack} \qquad \text{Eq. 36}$$

Where $OH_{stack}\ [h]\ and\ LT_{stack}[h]$ are respectively the operated hours and the lifetime of the stack.

The NPV method considers just differential costs respect the base case, defined as the situation in which just Sices boiler and De Pretto turbine work at nominal level in order to satisfy all the energy demands. The latter, beyond modifications described in "Case study" chapter, are assumed to be unchanged. Finally, in the base case the excess of electricity is immitted into the national grid, but there are not any incentives since they will end in 2026.

Therefore, if the energy is used for hydrogen production in the industrial area there is not any change for the power generation firm, since electricity is always paid according to price on DAM, as already explained in section 2.2. In addition to that, for the configuration based on gasification a differential cost is represented by the gasified biomass cost and the avoided cost thanks to NG substitution with tail gas. The latter is accounted directly in Opex voice of Eq. 35.

The **payback period** (PBP) is the time after which a firm reach a breakeven point for the investment, hence the first year with NPV equal or higher than zero. The model checks year by year if NPV is equal or greater than zero until this condition is satisfied. The PBP is a relevant parameter to evaluate an investment from companies' perspective since they want to reach recover the invested capital as soon as possible.

Finally, the **profitability index** (PI) shows in a relative way the return on investment. Compared to NPV that is an absolute index, it gives a further information, since compared the NPV with invested capital.

As reported in Eq. 37, the PI is defined as the ratio of NPV and actualized Capex.

$$PI\,[\%] = \frac{NPV}{Capex_{act}} \cdot 100 \qquad \text{Eq. 37}$$

Where $Capex_{act}$ considers cost actualization for investment cost for years different from the starting one, therefore when the electrolyzer stack is substituted.

4 Results and critical analysis

4.1. Gasification

Techno-economic performance vs Size

In this paragraph economies of scale effects in gasification plant and its techno-economic assessment are presented. The biomasses mix is equally distributed between the three biomasses currently fed to the Idrotermici boilers, hence grape pomace, residual wood, and grape skin. The latter is assumed dried with no additional cost, given the high quantity of low temperature heat recoverable from the hydrogen production plant. The aim of this section is to understand how performances change according to the plant magnitude, in order to evaluate which size may be better for the case study.

A larger plant implicates a higher amount of tail gas to be valorized, as shown in Figure 54. It is a by-product of hydrogen production via gasification, but it is crucial to exploit it in a proper way, given the valuable composition and the high energy associated to it, as explained in section 3.1.

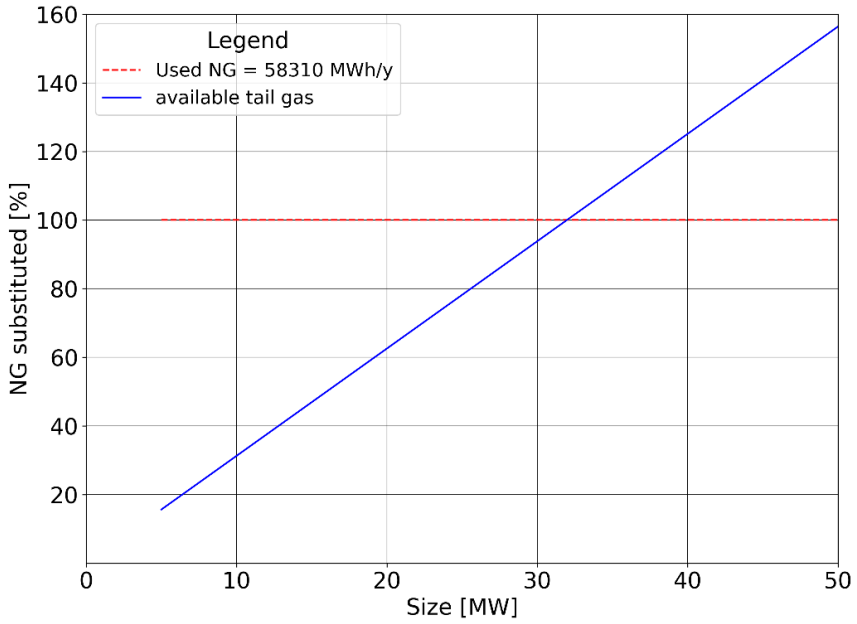

Figure 54: NG substitution capability as function of plant size

By increasing the plant size, it is possible to substitute with tail gas a higher percentage of natural gas utilized in the industrial area nowadays, leading to a cost reduction and more independency of the industrial site from the gas grid. All the natural gas is substituted for a size of about 32 MW_{th}, hence the extra tail gas of bigger plants is assumed to have zero economic value. However, other uses can be assessed in further studies in order not to waste the energy related to the portion of tail gas considered as extra.

The electricity consumption as well as the related cost are linearly dependent on the size of the plant according to the assumptions and modeling done. The higher is the electricity price the steeper is the curve, as reported in Figure 55.

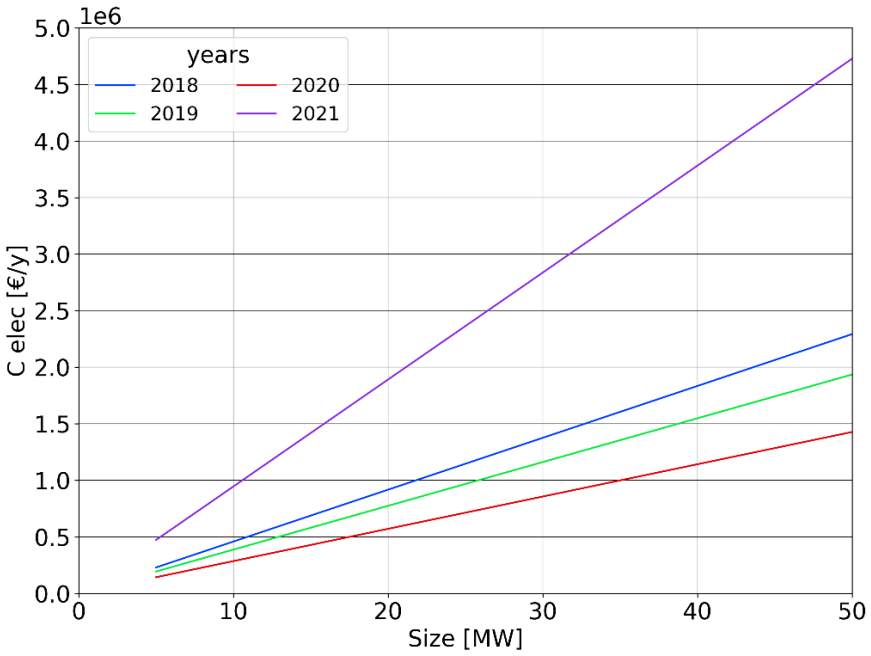

Figure 55: Yearly electricity cost vs Size of gasification plant and year

Furthermore, relevant economies of scale are present for hydrogen production via gasification, as it can be noticed in Figure 56. The latter figure, together with Figure 54 and Figure 55, explains the trend of the LCOH as well as economic KPIs. The information given by the diagrams are completed by Table 16 in which the average prices of electricity, natural gas and biomass for the past four years are reported.

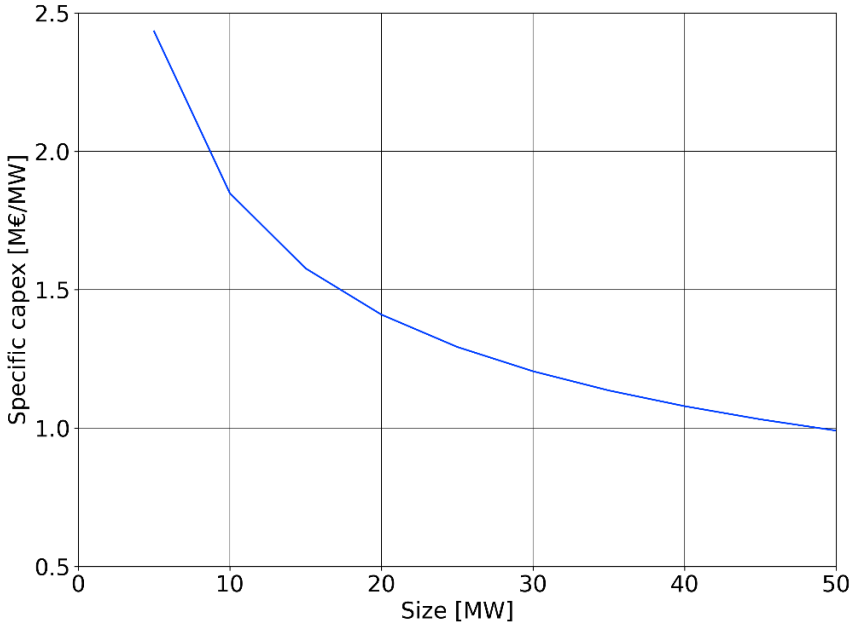

Figure 56: Specific Capex of gasification plant as a function of size

The levelized cost of hydrogen is reported in Figure 57. Looking at one year, the LCOH shows a strong hydrogen cost decrease until the 30 MW_{th} plant size. This is given by the economy of scale of the plant components and thanks to the full valorization of the produced tail gas; the greater amount of tail gas produced for bigger sizes is not valorized, as mentioned before, so it does not contribute to a significant further decrease in LCOH. It must be mentioned that there is no effect deriving from processes efficiency change, since efficiencies are assumed constant, although the size increase could likely lead to slight improvements.

The comparison between several years according to electricity, NG and biomasses prices gives back interesting results. In terms of LCOH the results are comprised in a small range of values. This trend derives from the fact that the electricity price and the NG avoided cost both increase, thus balancing each other, while the cost of biomasses mix remains quite constant throughout the four years considered. This aspect will be further analyzed later in this section, but it is important to notice how this configuration is not much dependent on electricity and NG prices as long as these two markets are linked, and the biomasses market is not relevantly affected by them. Above 32 MW_{th} size, since part of the tail gas is not valorized, the LCOH curves for the different years slightly diverge because to an electricity cost increase does not correspond a greater NG avoided cost, given that all the NG demand is already substituted. Therefore, the years with higher cost of electricity have a flatter LCOH curve.

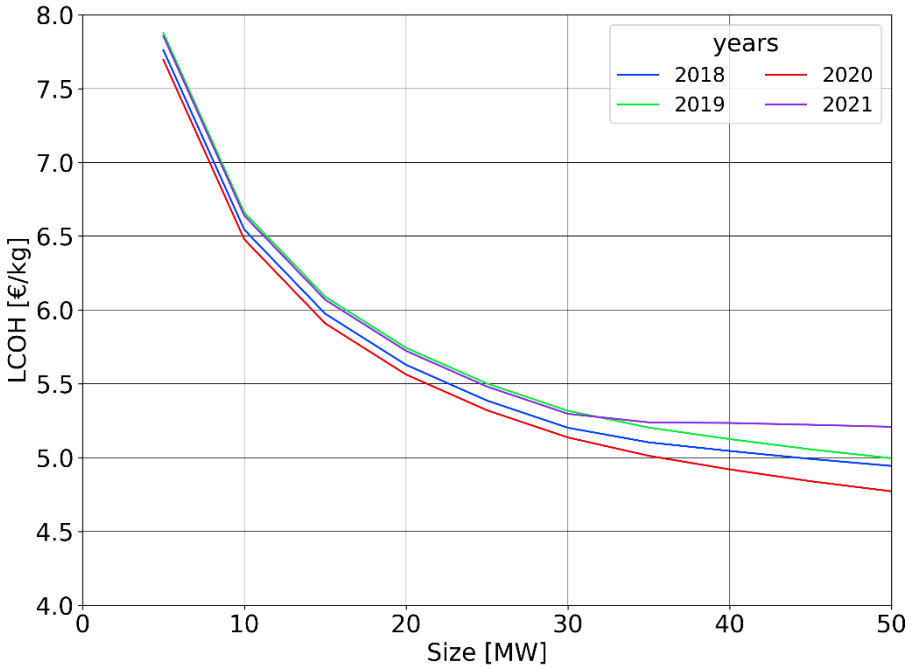

Figure 57: Gasification configuration LCOH vs Size and year

LCOH does not depend on the hydrogen price because the gasifier is continuously operated at nominal conditions without choosing when to produce hydrogen or not. Therefore, once set electricity, NG and biomass prices, as well as the size of the reactor, the LCOH represents the H_2 selling price to have NPV equal to zero. By comparing the obtained LCOH with reference prices for hydrogen according to the end application in Table 17, it is evident that there is no possibility to have hydrogen production via biomass gasification without an incentive. This could be roughly evaluated as the difference between the LCOH and the reference price for the specific end application, at which it should be added a small increase, to make the investment interesting for companies. An example for a plant of 30 MW_{th} is reported in Table 19.

Table 19: Incentive values to reach NPV=0 for a reference size of 30 MW_{th} in 2018

End use	Injection in NG grid	Industrial	Transport
Incentive 2018 [€/kg_{H2}]	4.39	3.28	1.47

The potential hydrogen production and the additional electric power needed to operate the hydrogen production process via gasification are summarized in Table 20 for a plant size ranging from 5 to 50 MW_{th}. It is relevant to underline that the estimated electric power demand of hydrogen production process based on gasification is about 9.4% of the plant

size, i.e., of the biomass thermal input to the gasification section. The additional power required to run the gasification process can be compared with the surplus electricity produced in the industrial site by the CHP plants (Figure 48). Some point values are also reported in Table 21 to allow a better comparison with electric power demand of the process.

Table 20: Yearly H_2 production and additional P_{el} required to run the gasification process vs Size of gasification plant

Size [MW_{th}]	H_2 production [t/y]	P_{el} add [MW_e]
5	426	0.47
10	852	0.94
15	1,279	1.42
20	1,705	1.89
25	2,131	2.36
30	2,558	2.83
35	2,984	3.30
40	3,410	3.78
45	3,837	4.25
50	4,263	4.72

Table 21: Comparison between load duration curve data and electric power demand

Yearly hours [h/y]	P_{el_min} [MW_e]	Size [MW_{th}]
7,727	1.89	20
7,361	2.36	25
6,726	2.83	30

It is important to check if the extra electricity available in the industrial site is enough to run the hydrogen production plant without requiring electricity from the national grid, since it would imply additional costs. Data from the load duration curve shows that sizes

above 30 MW_{th} should not be considered since the additional electricity demand would be too high, hence for a considerable number of hours it would be necessary to procure electricity from the national grid.

A plant of 20 MW_{th} can operate for 7,727 hours without drawing electricity for outside of industrial area, hence for this size it is reasonable to assume that the hydrogen production process is entirely run with electricity from the CHP plant, if the goal is to operate 8,000 h/y. whereas by increasing the plant size up to 30 MW_{th} the hours during which the plant could operate independently are fewer, but still the majority of the operating hours (Table 21). Nevertheless, the plant should take some electricity from the grid as already occur for few hours per year in the industrial site.

To sum up, a plant magnitude up to 30 MW_{th} can be considered for this case study, according to the following reasons:

1. Relevant economies of scales up to 30 MW_{th} plant (as shown in Figure 56)

2. Increase in natural gas substitution, hence cost reduction and higher independency of industrial area from external factors.

3. 8,000 hours of yearly operating hours is a goal for next generation plant, but it is more likely that plant works between 7,000 and 8,000 hours per year, therefore the electricity needed from national grid is likely lower compared to estimation.

To conclude, the suggested plant size for the case study is between 20 and 30 MW_{th}. Since Idrotermici boilers will not be fed by biomasses from 2023, as explained in section 2.2, it is interesting to underline that, if the gasification plant receives the same quantity of biomasses currently processed by Idrotermici boilers, the equivalent plant size would be around 28.8 MW_{th}.

Cost breakdown structure

In this paragraph cost structure is analyzed in order to understand which are the main parameters that affect H_2 production cost, hence where there is room for improvements to lower the LCOH of the configuration based on gasification.

The results presented in this section refer to a size of 30 MW_{th}, hydrogen delivery pressure of 200 bar and electricity, natural gas and biomass costs of 2018 (Table 16). Furthermore, the biomass mix is assumed to be equally distributed between grape pomace, dried grape skin, and residual wood.

The Capex breakdown structure in Figure 58 shows that 77.9% of the investment cost is related to the gasification section, while only 22.1% is related to the upgrading and purification process. This is an expected result since the gasification section comprises several components, as already mentioned, like biomass feeders, two fluidized bed reactors, filters, and heat exchangers that work as steam generator and air preheater.

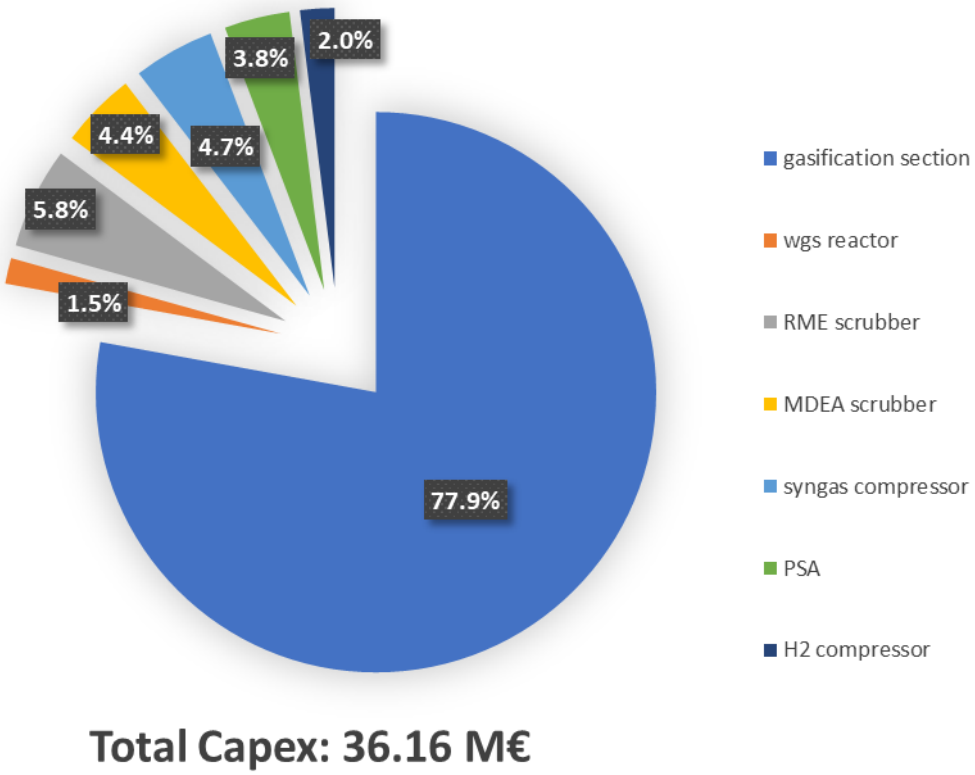

Figure 58: Capex breakdown structure for a 30 MW_{th} gasification plant

The scrubbers and the PSA unit are modeled with the same cost function, but they have different costs, because the volumetric flow rate decreases along the process from the RME scrubber to the MDEA scrubber and then to the PSA unit. In fact, in the RME scrubber section also water is separated from the flow, while in the MDEA scrubber section CO_2 is

captured. Similarly, the syngas compressor has higher Capex due to the higher flow rate and pressure ratio compared to the hydrogen compressor, although the specific consumption for H_2 compression is higher. The WGS reactor represents the unit operation with the lowest cost since it is a relatively simple process composed just by one fixed bed reactor.

As regards the variable costs, shown in Figure 59, it is relevant to notice how the total yearly Opex is high compared with the Capex and represents more than 30% of it. Therefore, although capital costs reduction is important, the abatement of operative costs as well can significantly lower the production cost of hydrogen via gasification.

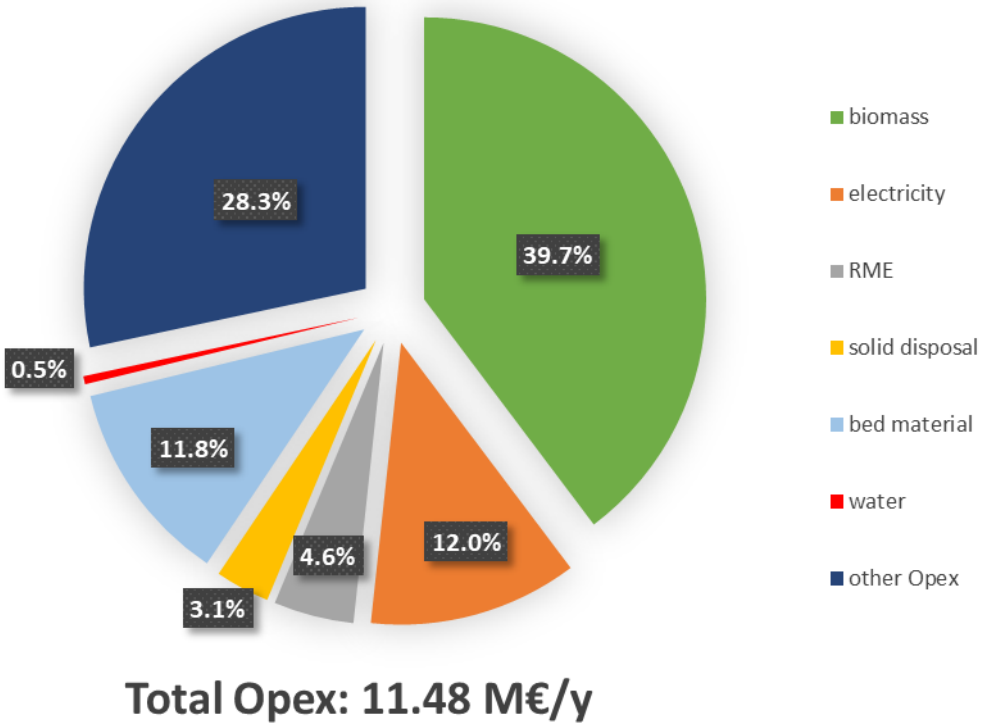

Figure 59: 2018 Opex breakdown structure for a 30 MW_{th} gasification plant

The main variable cost is the biomass from which hydrogen is produced. Biomass cost varies according to the type of biomass, ranging from less than 10 €/t to much more than 100 €/t. Furthermore, with increasing CO_2 and fossil fuels costs, it is expected to have a rise also in the cost of biomass. Therefore, it is crucial to have a flexible system that is able to operate with cheap biomass as M&B meal, manure, sewage sludge, residual or waste biomasses, since it is one of the most feasible ways to reduce the LCOH from gasification. However, the use of cheap biomasses typically leads to have additional challenges to face. This aspect will be further analyzed later in this section.

The second variable cost of relevance is "other Opex" that could be further decomposed in 56% related to maintenance (15.9% of total Opex), 34% related to insurance and operating supply (9.6% of total Opex) and 10% related to plant overhead (2.8% of total Opex). A cost

reduction could be expected for maintenance, since some of the units have components that may have relevant developments in the next years, such as the syngas and hydrogen compressors, the gasification section, and the RME scrubber.

The cost related to electricity consumption accounts for 12.0%, hence it is still considerable, but as discussed, the LCOH does not strongly depend on the electricity price. A similar fraction is covered by the fresh bed material to feed to the gasifier, due to its consumption. The cost of the bed material in the model is considered always equal to that of limestone, therefore it accounts for a relevant part of operative costs, given its high consumption rate. If olivine is used as bed material, it would give a slightly lower H_2 yield and higher tar content in the syngas, but it would significantly reduce the cost related to bed material consumption, given a consumption rate 17.6 times lower than that of limestone. For the mentioned case, limestone consumption accounts for 1,351,000 €, while olivine use would require 79,747 € only. For this reason, currently operating gasification plants typically use olivine. However, even in this field there are possible technological developments; for instance, nickel enriched olivine has the same attrition resistance of olivine, but higher catalytic activity.

Finally, there are less relevant entries, such as RME cost, that accounts for 4.6%, solid disposal cost, which depends on biomasses ash content and it covers a fraction of 3.1%, and water consumption that is less than 1% of the total variable cost.

The total Opex for each year (2018-2021) is summarized in Table 22, while Figure 60, shows the fraction of each variable cost, taking also into account the avoided cost deriving from natural gas substitution with tail gas.

Table 22: Gasification variable cost values for 2018-2021

Year	2018	2019	2020	2021
Total variable cost [M€/y]	10.16	10.45	9.99	10.40

Figure 60 allows to explain how a sort of balance is created between electricity and NG avoided cost, the letter being negative, hence, de facto, a reduction in total costs. It is possible to notice how the total variable cost does not change relevantly over the years, since in Italy nowadays the electricity and NG markets are positively correlated. In fact, the LCOH for 30 MW_{th} plant remained in a small range, between 5.14 and 5.32 €/kg, despite the relevant differences in electricity and NG prices.

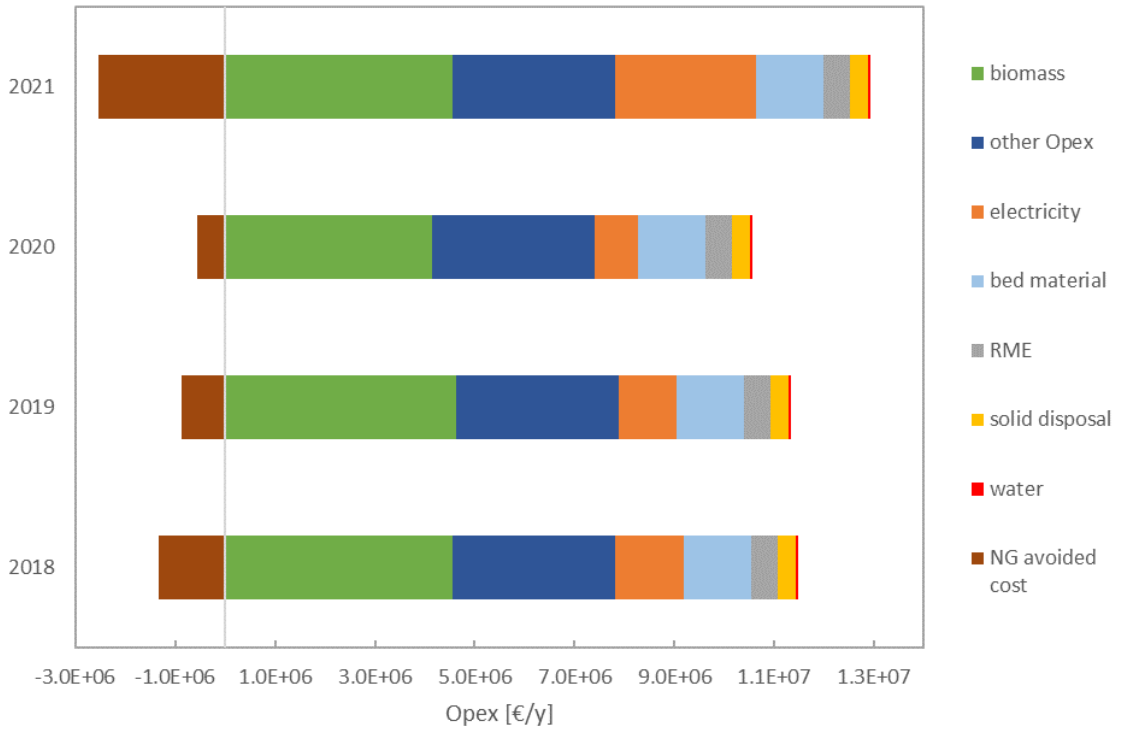

Figure 60: Gasification variable costs for 2018-2021

To conclude there are three main strategies to abate LCOH from gasification:

- Utilize cheap biomasses
- Choose bed material by an optimization between cost and performance
- Valorize the high value tail gas generated as by-product from the process

Finally, the development and commercialization of each plant component could lead to lower both Capex and maintenance costs.

Individual biomasses results

In this paragraph the techno-economic performance for the gasification of each biomass is reported in order to underline characteristics and consequences of the process that can vary significantly depending on the type of feedstock chosen.

First, a note about technical performances must be done. Experimental data from different gasifiers are difficult to compare due to the different operating conditions applied, such as steam-to biomass ratio or temperature, and, in some cases, different bed material. If gasification temperature and SB ratio should be optimized according to biomass characteristics, the bed material should be the same in order to have a proper comparison. Therefore, the obtained values do not have to be meant as a pure consequence of the

biomass type since other parameters that affect the process are also changed, as reported in Table 12. Hence, results must be evaluated according to all the assumptions presented in chapter 3.1. Economic results are of course affected by technical reasons, however the operative costs depend mostly on the gasified biomass, while Capex values depend on the biomass characteristics, its flow rate and the associated SB.

Table 23 reports the reference cost of each biomass provided by the company, which are used to perform this comparison. The results presented in Table 24 and Figure 61 are related to a plant size of 30 MW_{th} fuel input and they are referred to 2018 electricity and natural gas prices.

Table 23: Reference price for each biomass

Biomass	Grape pomace	Dried grape skin	Residual wood	M&B meal
Cost [€/t]	100.0	80.0	60.0	3.2

Table 24: Techno-economic results for individual biomasses

Biomass	Grape pomace	Dried grape skin	Residual wood	M&B meal
H_2 production [kg/h]	288.00	302.87	367.03	297.38
H_2 yield $[g_{H_2}/kg_{dry}]$	48.03	49.07	44.92	53.20
CGE_{H_2} [%]	32.00%	33.65%	40.78%	33.04%
η_{tot} [%]	56.30%	51.25%	54.38%	56.25%
LCOH [€/kg]	6.06	5.40	5.03	3.92
Capex [M€]	35.59	35.56	36.12	35.72
Variable cost [M€/y]	10.86	9.99	11.63	6.20

H_2 yield, H_2 efficiency (CGE_{H_2}) and total efficiency (η_{tot}) are evaluated by following formulas:

$$H_2\ yield\left[\frac{g_{H_2}}{kg_{dry}}\right] = \frac{m_{H_2}[kg/h]}{m_{biomass}[kg/h]\cdot(1-RH)} \qquad \text{Eq. 38}$$

$$CGE_{H_2} = \frac{m_{H_2}[kg/s] \cdot LHV_{H_2}\ [MJ/kg]}{E_{Biomass\ input}[MW_{th}]} \quad \text{Eq. 39}$$

$$\eta_{tot} = \frac{m_{H_2}[kg/s] \cdot LHV_{H_2}\ [MJ/kg] + m_{tg}[kg/s] \cdot LHV_{tg}\ [MJ/kg]}{E_{Biomass\ input}[MW_{th}]} \quad \text{Eq. 40}$$

The m and LHV are, respectively, the mass flow rate and the lower heating value of the tail gas (tg), hydrogen (H_2) and "as received" biomass (biomass). While $E_{Biomass\ input}$ is the thermal power input to the gasification plant.

The hydrogen yield and the efficiencies reported in Table 24 depend mainly on the model assumptions. In fact, keeping constant the thermal input to the plant, the lower the biomass LHV the higher is the biomass flow rate, hence the syngas flow rate and, consequently, the hydrogen produced. For instance, the residual wood has a smaller LHV because of the higher water content and intrinsic biomass characteristics, therefore, even the dry flow rate is higher compared to other biomasses. However, the higher biomass flow rate is balanced partially by the greater hydrogen production. For these reasons the hydrogen yield results smaller, while the H_2 efficiency higher. In addition, a note must be done about varying biomass flow rate feeding the gasifier. This should not lead to technical problems; no issues are reported in pilot plants using significantly varying feeding mass flow rates[25], [26]. Variable biomass flow rates could affect Capex cost, but this is not directly considered since Capex is modeled according to biomass thermal input. However, this can be indirectly accounted in the high uncertainty associated to gasification section cost function.

Besides changes in the operative parameters, set according to the experimental data from literature, the following variations are detected from the model as the input biomass is changed:

- Biomass flow rate, changing according to biomass LHV, assumed constant thermal input
- Syngas yield and composition
- Biomass cost
- Biomass ash content
- Tail gas composition and its availability

The change in biomass flow rate and syngas yield lead to different flow rates in the upgrading and purification section, and the cost of each unit operation, as well as the heat and electricity consumption of amine scrubber and compressor, change accordingly. Biomasses ash content influences the cost associated to solid disposal, hence it increases when the ash content is greater. In general, cheaper biomasses lead to significantly lower variable costs since the feedstock cost is the most relevant Opex.

Looking at the Capex in Table 24 it is possible to observe that just slight changes occur from one biomass to the other. The equipment is sized according to maximum flow rate and energy requirements only, therefore the main differences are related to variable costs, as depicted in Figure 61. As already mentioned, the biomass cost plays the most crucial role.

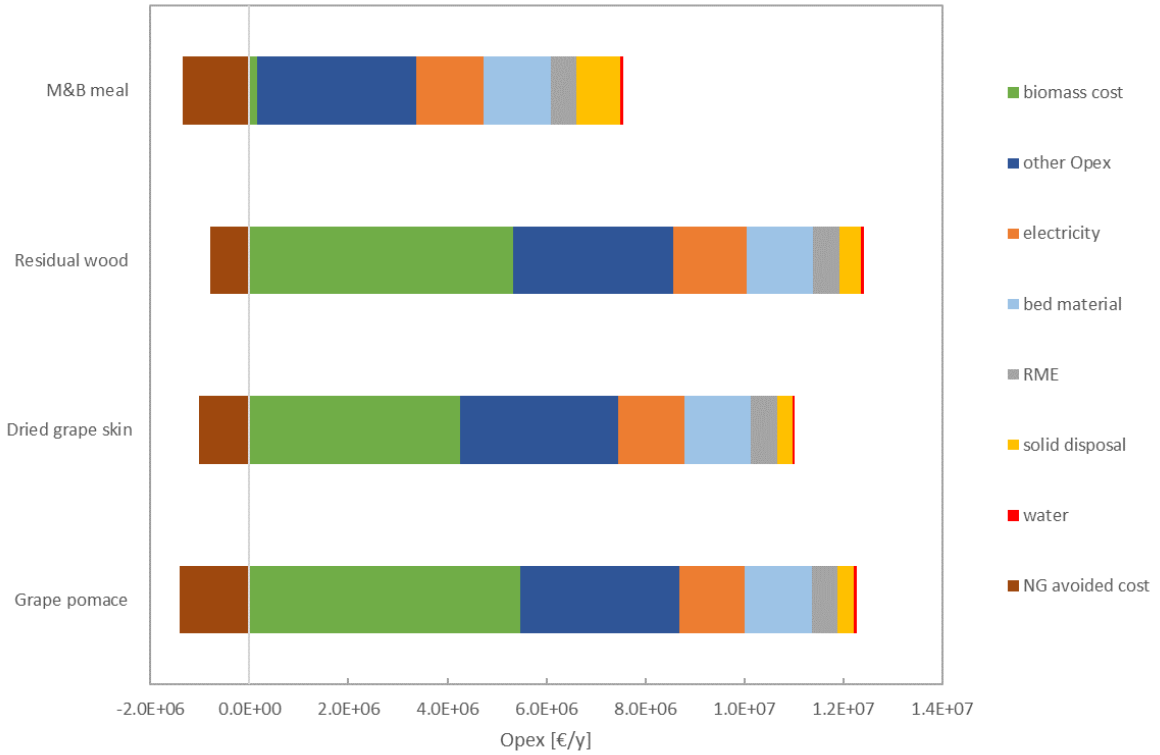

Figure 61: Variable costs for different biomasses

For instance, the LCOH related to M&B meal is drastically reduced to 3.92 €/kg since the very low biomass cost, despite the solid disposal cost is more than double with respect to other biomasses. Hence, as general rule it is possible to assume that the lower the biomass cost the lower is the LCOH. In fact, the residual wood, grape skin and grape pomace present a LCOH between 5.03 and 6.06 €/kg, as reported in Table 24.

A final note about meat and bone meal must be done, since it has a very high nitrogen content compared to other biomasses. Due to lack of specific data, meat and bone meal is modeled by using chicken manure experimental data. Chicken manure has, typically, a N content of about 6% while for M&B meal it is about 12%. Therefore, the ammonia content in the outgoing syngas is most likely higher, thus decreasing accordingly the hydrogen yield. However, the model assumes same hydrogen yield due to lack of experimental data. Moreover, it is assumed that produced ammonia is easily manageable, since a small part of it remains in the condensed water, while the largest part is separated in the PSA unit. At the end, it goes in the tail gas that is afterward burned thus generating high content NO_x exhaust gas. If high nitrogen content biomasses were chosen to feed the gasifier, a detailed evaluation of ammonia management would be required.

Sensitivity analysis

In this paragraph sensitivity analysis results are described with the aim of understanding how relevantly main parameters affect the process, hence, to be able to estimate techno-economic performance of the gasification plant even if input parameters change.

The reference case inputs are reported in Table 25 and it corresponds to technical calculations performed using dried grape skin as reference biomass. The results related to the reference case are shown in Table 26, while sensitivity analysis results, presented in Figure 62 and Figure 63, are given as percentage change with respect to that base case.

Table 25: Reference inputs for gasification sensitivity analysis

Size [MW_{th}]	$C_{biomass}$ [€/t]	OH [h/y]	Bed material	DAM price [€/MWh]	NG price [€/MWh]	other Opex [% Capex]	P_{H2} [€/kg]
30	70	8,000	100% limestone	130	50	9	3.0

Table 26: Reference results for gasification sensitivity analysis

LCOH [€/kg]	NPV [M€]	PI [%]	Incentive [€/kg]	H_2 production [t/y]
5.36	-65.6	-184.50%	2.36	2,423

Looking at LCOH variation according to input parameters it is possible to recognize the relevance of each parameter on LCOH. The reduction of operative hours leads to the greatest increase in cost of hydrogen. A 20% reduction of operative hours correspond to only 6,400 h/y; a more likely decrease of 10% would result in a LCOH increase of 5.41%. Capex cost variation represents the second input parameter that influences more LCOH. The estimation of its value has a high uncertainty, likely ±30%, due to few available data in literature, no information from manufacturers and possible developments in next future. A relevant result in the LCOH is shown by the effect of using a bed material mix 20% limestone and 80% olivine instead of 100% limestone. This solution is actually feasible, and it can lead to great advantages in terms of LCOH reduction. This shows the reason why nowadays all the operating gasification plants are using olivine only, leading to much lower operative costs.

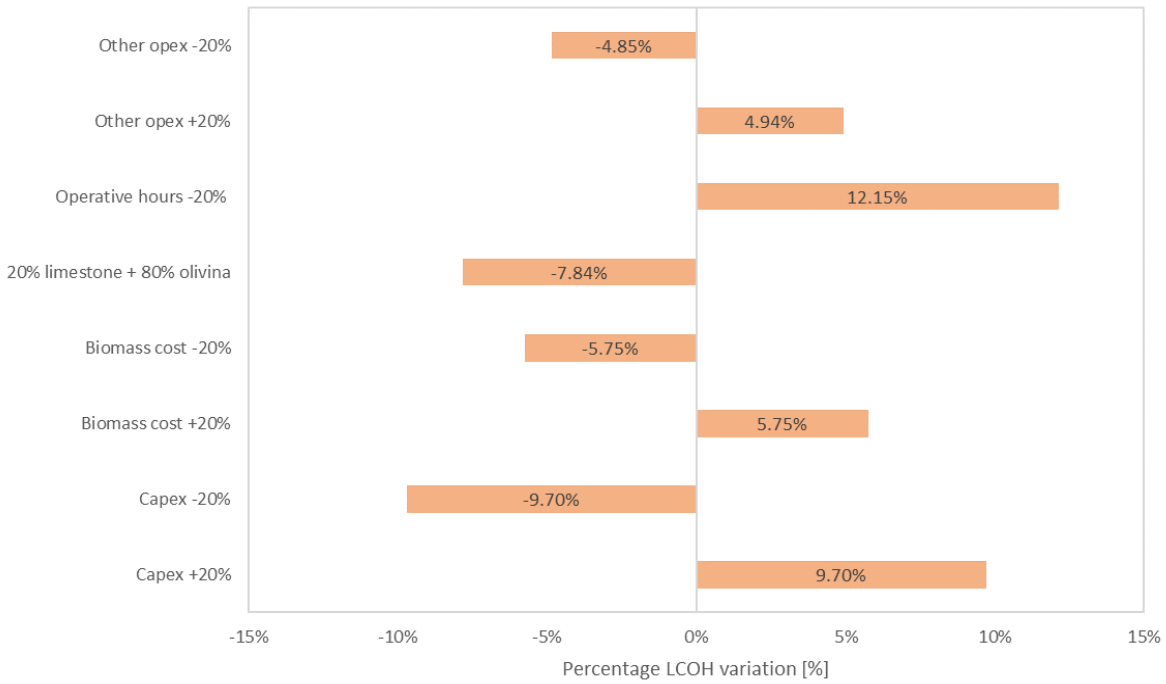

Figure 62: Gasification sensitivity analysis results. Effect of key parameters on LCOH

The biomass cost variation leads to less relevant change in LCOH compared to previously mentioned parameters, only ±5.75% considering a ±20% biomass price change. However, this parameter could have enormous changes according to biomass type and biomasses markets. As previously widely discussed, biomass cost is one of the most influencing factors for the process, although with the same percentage variation other parameters may look more relevant.

Finally, "other Opex" cost, which includes maintenance, insurance, operating supply, and plant overhead, looks like the parameter with the lowest relevance, since the LCOH variation of about ±4.9% compared to an "other Opex" change of ±20%. Nevertheless, the "other Opex" has a high uncertainty due to few values and wide range in literature, hence it could vary up to ±50% with respect to the reference value (9% of Capex). This is translated in maximum LCOH variation around 12.3%.

As regards the effect of the considered parameters on economic parameters like Net Present Value and, equivalently Profitability Index, in Figure 63 it is possible to notice different trends. Besides likely ranges for parameters variation, considering an equal change for all of them, the highest influence is given by the investment cost. Afterward, the use of 20%/80% limestone/olivine mix instead of using just limestone is confirmed as one of the main choices that can strongly affect the NPV, PI and LCOH, hence the plant performance. The biomass cost affects more NPV and PI than LCOH, and it represents a crucial parameter anyway, for what discussed previously. The reduction in operating hours seems to have just a very low effect on NPV and PI. However, this result depends on the reference case chosen, since the assumed hydrogen price is lower than the obtained LCOH. Therefore,

analyzing the yearly cash flow for the reference case and when OH are reduced, it is noticed that with a hydrogen price set to 3 €/kg, a reduction of OH lead just to a slight decrease in the cash flow since the lost revenues due to lower hydrogen production balance with the avoided variable cost related to H_2 production. If a reference case with higher hydrogen price or an incentive that makes the investment profitable is assumed, the change on NPV and PI will be much more relevant.

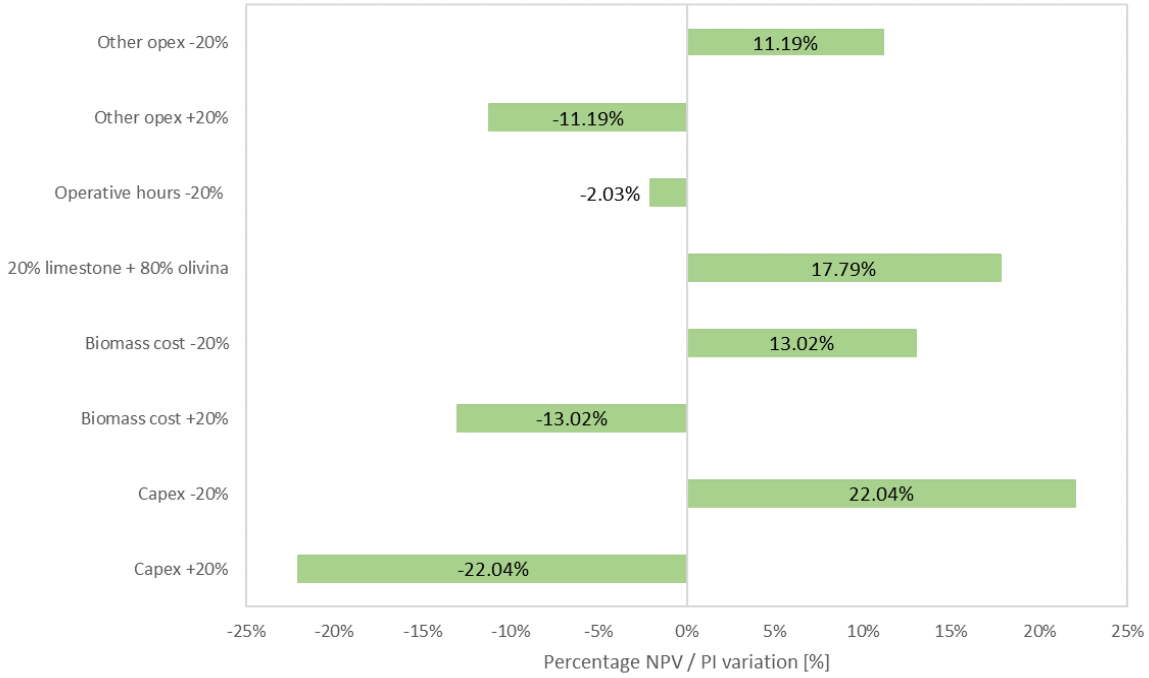

Figure 63: Gasification sensitivity analysis results. Effect of key parameters on NPV and PI

As general concept, NPV and PI are more influenced by the input parameters than LCOH.

The sensitivity analysis for electricity and natural gas prices is presented in Table 27, analyzing the effects on LCOH, and Table 28, on the profitability index. In both tables the first column shows variation of electricity price from 50 to 400 €/MWh, while on the first row the natural gas cost is reported. Table 28 also reports the hydrogen price according to the NG cost, since it also influences the profitability index. NG cost varies from 10 to 200 €/MWh, while the corresponding hydrogen price goes from 1.22 to 10.64 €/kg.

Starting from LCOH results, it is possible to notice three main trends:

- Set an electricity price, the higher the natural gas cost, the lower will be the LCOH, thanks to a greater cost saving related to NG substitution with tail gas.

- Set NG cost, the higher the electricity price the higher will be the LCOH due to the increase in variable costs.

- If NG as well as electricity price increase, the effects on techno-economic performance somehow balance, at least partially. Hence, this is translated in a LCOH that fluctuates in a very small range when both prices increase, i.e.,

gasification LCOH shows low sensitivity to electricity and NG prices if they are positively correlated.

The profitability index (Table 28) gives additional information, since it allows to understand when the investment is profitable, i.e., when hydrogen price is either equal or higher than the LCOH. Furthermore, it shows numerically how the expected return on investment changes with electricity and natural gas prices. The pink area in the table evidence for which couples of electricity and NG prices the investment is not profitable, hence the PI is lower than zero; the graduated colored area shows when the PI is greater than zero and for which couples of NG and electricity prices the profitability index increases.

In addition to the LCOH trend, a further effect on PI is present when natural gas cost increases. In fact, a greater NG cost leads to higher hydrogen price, therefore increased revenues from H_2 sales and to a higher NG avoided cost thanks to the substitution with tail gas. This double effect and the typically low dependency of variable costs from electricity price are translated into a greater influence of natural gas cost on PI compared to electricity price.

The investment in hydrogen production via biomass gasification is profitable for high natural gas and so H_2 prices and relatively low electricity cost. However, it is interesting to notice how for NG and H_2 prices respectively above 120 €/MWh and 6.67 €/kg, the investment is economically feasible for any considered electricity price. Therefore, it would be profitable to invest on this configuration without any incentives if it is assumed that current prices of NG and electricity will not change significantly in the next years. In fact, the 2022 average values until the end of July are respectively 110.97 €/MWh and 280.40 €/MWh, even though they increased relevantly in the last months.

Table 27: Gasification LCOH as a function of electricity and NG prices

E_el [€/MWh] \ NG [€/MWh]	10	20	30	40	50	60	70	80	90	100	110	120	130	140	150	160	170	180	190	200
50	5.33	5.16	4.98	4.81	4.64	4.46	4.29	4.11	3.94	3.76	3.59	3.42	3.24	3.07	2.89	2.72	2.54	2.37	2.20	2.02
60	5.42	5.25	5.08	4.90	4.73	4.55	4.38	4.20	4.03	3.85	3.68	3.51	3.33	3.16	2.98	2.81	2.63	2.46	2.29	2.11
70	5.51	5.34	5.17	4.99	4.82	4.64	4.47	4.29	4.12	3.95	3.77	3.60	3.42	3.25	3.07	2.90	2.72	2.55	2.38	2.20
80	5.61	5.43	5.26	5.08	4.91	4.73	4.56	4.38	4.21	4.04	3.86	3.69	3.51	3.34	3.16	2.99	2.82	2.64	2.47	2.29
90	5.70	5.52	5.35	5.17	5.00	4.82	4.65	4.48	4.30	4.13	3.95	3.78	3.60	3.43	3.25	3.08	2.91	2.73	2.56	2.38
100	5.79	5.61	5.44	5.26	5.09	4.91	4.74	4.57	4.39	4.22	4.04	3.87	3.69	3.52	3.35	3.17	3.00	2.82	2.65	2.47
110	5.88	5.70	5.53	5.35	5.18	5.00	4.83	4.66	4.48	4.31	4.13	3.96	3.78	3.61	3.44	3.26	3.09	2.91	2.74	2.56
120	5.97	5.79	5.62	5.44	5.27	5.10	4.92	4.75	4.57	4.40	4.22	4.05	3.88	3.70	3.53	3.35	3.18	3.00	2.83	2.65
130	6.06	5.88	5.71	5.53	5.36	5.19	5.01	4.84	4.66	4.49	4.31	4.14	3.97	3.79	3.62	3.44	3.27	3.09	2.92	2.75
140	6.15	5.97	5.80	5.63	5.45	5.28	5.10	4.93	4.75	4.58	4.40	4.23	4.06	3.88	3.71	3.53	3.36	3.18	3.01	2.84
150	6.24	6.06	5.89	5.72	5.54	5.37	5.19	5.02	4.84	4.67	4.50	4.32	4.15	3.97	3.80	3.62	3.45	3.27	3.10	2.93
160	6.33	6.16	5.98	5.81	5.63	5.46	5.28	5.11	4.93	4.76	4.59	4.41	4.24	4.06	3.89	3.71	3.54	3.37	3.19	3.02
170	6.42	6.25	6.07	5.90	5.72	5.55	5.37	5.20	5.03	4.85	4.68	4.50	4.33	4.15	3.98	3.80	3.63	3.46	3.28	3.11
180	6.51	6.34	6.16	5.99	5.81	5.64	5.46	5.29	5.12	4.94	4.77	4.59	4.42	4.24	4.07	3.90	3.72	3.55	3.37	3.20
190	6.60	6.43	6.25	6.08	5.90	5.73	5.56	5.38	5.21	5.03	4.86	4.68	4.51	4.33	4.16	3.99	3.81	3.64	3.46	3.29
200	6.69	6.52	6.34	6.17	5.99	5.82	5.65	5.47	5.30	5.12	4.95	4.77	4.60	4.43	4.25	4.08	3.90	3.73	3.55	3.38
210	6.78	6.61	6.43	6.26	6.08	5.91	5.74	5.56	5.39	5.21	5.04	4.86	4.69	4.52	4.34	4.17	3.99	3.82	3.64	3.47
220	6.87	6.70	6.52	6.35	6.18	6.00	5.83	5.65	5.48	5.30	5.13	4.95	4.78	4.61	4.43	4.26	4.08	3.91	3.73	3.56
230	6.96	6.79	6.61	6.44	6.27	6.09	5.92	5.74	5.57	5.39	5.22	5.05	4.87	4.70	4.52	4.35	4.17	4.00	3.82	3.65
240	7.05	6.88	6.71	6.53	6.36	6.18	6.01	5.83	5.66	5.48	5.31	5.14	4.96	4.79	4.61	4.44	4.26	4.09	3.92	3.74
250	7.14	6.97	6.80	6.62	6.45	6.27	6.10	5.92	5.75	5.58	5.40	5.23	5.05	4.88	4.70	4.53	4.35	4.18	4.01	3.83
260	7.24	7.06	6.89	6.71	6.54	6.36	6.19	6.01	5.84	5.67	5.49	5.32	5.14	4.97	4.79	4.62	4.45	4.27	4.10	3.92
270	7.33	7.15	6.98	6.80	6.63	6.45	6.28	6.11	5.93	5.76	5.58	5.41	5.23	5.06	4.88	4.71	4.54	4.36	4.19	4.01
280	7.42	7.24	7.07	6.89	6.72	6.54	6.37	6.20	6.02	5.85	5.67	5.50	5.32	5.15	4.98	4.80	4.63	4.45	4.28	4.10
290	7.51	7.33	7.16	6.98	6.81	6.63	6.46	6.29	6.11	5.94	5.76	5.59	5.41	5.24	5.07	4.89	4.72	4.54	4.37	4.19
300	7.60	7.42	7.25	7.07	6.90	6.73	6.55	6.38	6.20	6.03	5.85	5.68	5.50	5.33	5.16	4.98	4.81	4.63	4.46	4.28
310	7.69	7.51	7.34	7.16	6.99	6.82	6.64	6.47	6.29	6.12	5.94	5.77	5.60	5.42	5.25	5.07	4.90	4.72	4.55	4.37
320	7.78	7.60	7.43	7.26	7.08	6.91	6.73	6.56	6.38	6.21	6.03	5.86	5.69	5.51	5.34	5.16	4.99	4.81	4.64	4.47
330	7.87	7.69	7.52	7.35	7.17	7.00	6.82	6.65	6.47	6.30	6.13	5.95	5.78	5.60	5.43	5.25	5.08	4.90	4.73	4.56
340	7.96	7.79	7.61	7.44	7.26	7.09	6.91	6.74	6.56	6.39	6.22	6.04	5.87	5.69	5.52	5.34	5.17	5.00	4.82	4.65
350	8.05	7.88	7.70	7.53	7.35	7.18	7.00	6.83	6.66	6.48	6.31	6.13	5.96	5.78	5.61	5.43	5.26	5.09	4.91	4.74
360	8.14	7.97	7.79	7.62	7.44	7.27	7.09	6.92	6.75	6.57	6.40	6.22	6.05	5.87	5.70	5.53	5.35	5.18	5.00	4.83
370	8.23	8.06	7.88	7.71	7.53	7.36	7.18	7.01	6.84	6.66	6.49	6.31	6.14	5.96	5.79	5.62	5.44	5.27	5.09	4.92
380	8.32	8.15	7.97	7.80	7.62	7.45	7.28	7.10	6.93	6.75	6.58	6.40	6.23	6.05	5.88	5.71	5.53	5.36	5.18	5.01
390	8.41	8.24	8.06	7.89	7.71	7.54	7.37	7.19	7.02	6.84	6.67	6.49	6.32	6.15	5.97	5.80	5.62	5.45	5.27	5.10
400	8.50	8.33	8.15	7.98	7.81	7.63	7.46	7.28	7.11	6.93	6.76	6.58	6.41	6.24	6.06	5.89	5.71	5.54	5.36	5.19

Table 28: Gasification PI as a function of electricity and NG prices

P H2 [€/kg]	1.22	1.71	2.21	2.70	3.20	3.70	4.19	4.69	5.19	5.68	6.18	6.67	7.17	7.67	8.16	8.66	9.16	9.65	10.15	10.64
NG [€/MWh] / E_el [€/MWh]	10	20	30	40	50	60	70	80	90	100	110	120	130	140	150	160	170	180	190	200
50	-322	-269	-217	-165	-112	-60	-7	45	97	150	202	255	307	359	412	464	517	569	621	674
60	-329	-276	-224	-172	-119	-67	-14	38	90	143	195	248	300	352	405	457	510	562	614	667
70	-336	-284	-231	-179	-126	-74	-22	31	83	136	188	240	293	345	398	450	503	555	607	660
80	-343	-291	-238	-186	-133	-81	-29	24	76	129	181	233	286	338	391	443	495	548	600	653
90	-350	-298	-245	-193	-141	-88	-36	17	69	122	174	226	279	331	384	436	488	541	593	646
100	-357	-305	-252	-200	-148	-95	-43	10	62	114	167	219	272	324	376	429	481	534	586	639
110	-364	-312	-259	-207	-155	-102	-50	3	55	107	160	212	265	317	369	422	474	527	579	631
120	-371	-319	-267	-214	-162	-109	-57	-5	48	100	153	205	258	310	362	415	467	520	572	624
130	-378	-326	-274	-221	-169	-116	-64	-12	41	93	146	198	250	303	355	408	460	512	565	617
140	-386	-333	-281	-228	-176	-123	-71	-19	34	86	139	191	243	296	348	401	453	505	558	610
150	-393	-340	-288	-235	-183	-131	-78	-26	27	79	131	184	236	289	341	394	446	498	551	603
160	-400	-347	-295	-242	-190	-138	-85	-33	20	72	124	177	229	282	334	386	439	491	544	596
170	-407	-354	-302	-250	-197	-145	-92	-40	13	65	117	170	222	275	327	379	432	484	537	589
180	-414	-361	-309	-257	-204	-152	-99	-47	5	58	110	163	215	267	320	372	425	477	530	582
190	-421	-368	-316	-264	-211	-159	-106	-54	-2	51	103	156	208	260	313	365	418	470	522	575
200	-428	-376	-323	-271	-218	-166	-114	-61	-9	44	96	149	201	253	306	358	411	463	515	568
210	-435	-383	-330	-278	-225	-173	-121	-68	-16	37	89	141	194	246	299	351	403	456	508	561
220	-442	-390	-337	-285	-232	-180	-128	-75	-23	30	82	134	187	239	292	344	396	449	501	554
230	-449	-397	-344	-292	-240	-187	-135	-82	-30	22	75	127	180	232	285	337	389	442	494	547
240	-456	-404	-351	-299	-247	-194	-142	-89	-37	15	68	120	173	225	277	330	382	435	487	539
250	-463	-411	-359	-306	-254	-201	-149	-96	-44	8	61	113	166	218	270	323	375	428	480	532
260	-470	-418	-366	-313	-261	-208	-156	-104	-51	1	54	106	158	211	263	316	368	420	473	525
270	-477	-425	-373	-320	-268	-215	-163	-111	-58	-6	47	99	151	204	256	309	361	413	466	518
280	-485	-432	-380	-327	-275	-223	-170	-118	-65	-13	39	92	144	197	249	302	354	406	459	511
290	-492	-439	-387	-334	-282	-230	-177	-125	-72	-20	32	85	137	190	242	294	347	399	452	504
300	-499	-446	-394	-341	-289	-237	-184	-132	-79	-27	25	78	130	183	235	287	340	392	445	497
310	-506	-453	-401	-349	-296	-244	-191	-139	-87	-34	18	71	123	175	228	280	333	385	438	490
320	-513	-460	-408	-356	-303	-251	-198	-146	-94	-41	11	64	116	168	221	273	326	378	430	483
330	-520	-468	-415	-363	-310	-258	-206	-153	-101	-48	4	57	109	161	214	266	319	371	423	476
340	-527	-475	-422	-370	-317	-265	-213	-160	-108	-55	-3	49	102	154	207	259	311	364	416	469
350	-534	-482	-429	-377	-324	-272	-220	-167	-115	-62	-10	42	95	147	200	252	304	357	409	462
360	-541	-489	-436	-384	-332	-279	-227	-174	-122	-70	-17	35	88	140	193	245	297	350	402	455
370	-548	-496	-443	-391	-339	-286	-234	-181	-129	-77	-24	28	81	133	185	238	290	343	395	447
380	-555	-503	-451	-398	-346	-293	-241	-188	-136	-84	-31	21	74	126	178	231	283	336	388	440
390	-562	-510	-458	-405	-353	-300	-248	-196	-143	-91	-38	14	66	119	171	224	276	329	381	433
400	-569	-517	-465	-412	-360	-307	-255	-203	-150	-98	-45	7	59	112	164	217	269	321	374	426

4.2. Electrolysis

Techno-economic performance vs Size

The objective of this section is to underline trends according to the size and the reference year, in order to individuate the optimal electrolyzer and compressor sizes for the case study.

Contrary to gasification configuration operating hours changes according to electricity and hydrogen prices following the WTP hourly logic. Therefore, hydrogen production as well as economic KPIs of electrolysis configuration depend strongly on the control logic. Since the H_2 price changes according to the end application, different LCOH are obtained. However, set the electricity cost, there is just an equivalent hydrogen price to reach NPV=0. Therefore, incentives to reach that objective change according to the end use. For these reasons following diagrams are only reported for "Transport" application and not for all of them, since similar trends according to the size are present, they are just shifted to different values according to operating hours. Moreover, it is the only application for which the estimated hydrogen price is high enough to have profitable investment without any incentive. Finally, the results are related to an alkaline electrolyzer since it gives the best techno-economic performance, however a comparison between the two technologies is carried out later in this section (Table 31).

The capacity factor (C_f) is a relevant parameters that shows how much the electrolyzer is exploited compared to its potential. As reported in Eq. 41, it is defined as the ratio between the fraction of hours per year, that an electrolyzer operating at nominal power (P_{nom}), would require to process the actual electricity input over the year (E_{el_input}), and the total amount of yearly hours equal to 8,760 h/y.

$$C_f\ [\%] = \frac{E_{el\_input}\,[MWh/y]}{P_{nom}[MW] \cdot 8{,}760[h_{tot}/y]} \cdot 100 \qquad \text{Eq. 41}$$

Yearly operating hours have the same trend of capacity factor in Figure 64, and they are firstly related to electricity and hydrogen prices' trends over the year. In fact, set these two parameters, the hours during which hydrogen production is profitable are defined. However, operating hours are also influenced by the minimum load of the electrolyzer. Hence, the latter is not operated for some hours because the available electric power is below the minimum load, even though it would be profitable to produce hydrogen. This effect is clearly shown in Figure 64, where increasing the size, the capacity factor decreases due to this phenomenon. Compared to operating hours, the C_f presents an additional factor which influences its trend. Set a year, it shows a decreasing trend when electrolyzer size goes up even because a bigger electrolyzer works more hours at part loads, hence the higher the hours during which electrolyzer works at part loads, the lower is the capacity factor. The small reduction until a size of 3.5 MW_e and the great decrease for bigger sizes is

explained comparing size and minimum load of the electrolyzer with the load duration curve of available electricity in Figure 48.

Looking at differences between several year, it is necessary to remember the average values of electricity and hydrogen prices presented in Table 16 and Table 17. Firstly, it must be noticed how in the considered year diesel market had less volatility, hence the price changes in a narrower range compared to NG price. Furthermore, the operating hours between 2018 and 2021 drastically change, even though average diesel price is equal the two years. This is due mainly to the great increase in electricity price in the second half 2021, while diesel price on which H_2 price is estimated, also had a slight increase during those months. This graph shows that the current relation between electricity and natural gas markets does not advantage hydrogen production via electrolysis. In fact, capacity factor decreases when prices increase, despite a greater NG price leads to an increase of both, hydrogen and electricity prices. Since differences between curves of different years depend just on operating hours they will not further discussed in the following figures.

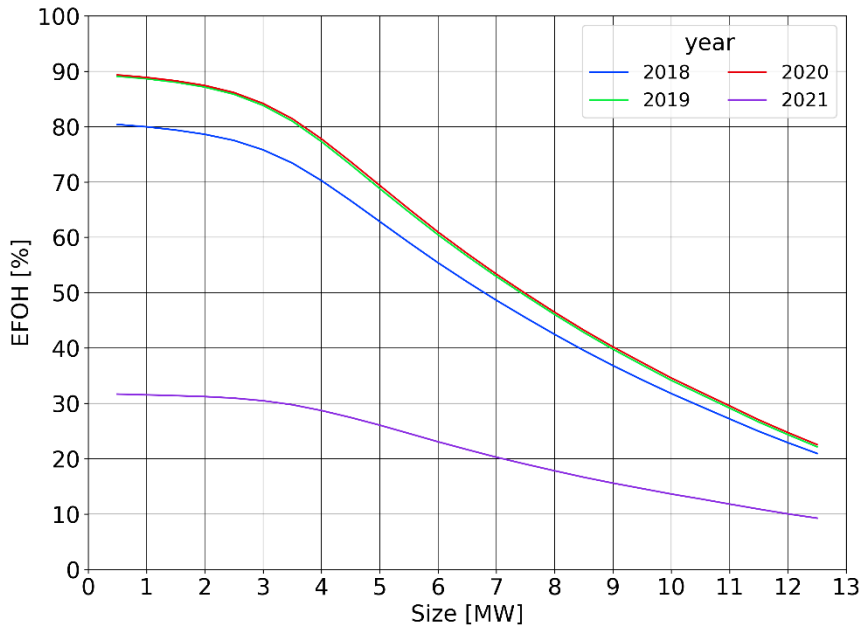

Figure 64: Electrolyzer EFOH as function of size

Yearly hydrogen production presented in Figure 65 depends mainly on two factors, the operating hours, and the energy exploitable in those hours. Set a reference year, H_2 production strongly increases up to a 4 MW_e size since to a size increase corresponds a greater exploitable electricity. Afterward it grows in a less relevant way until the maximum that is reached for an electrolyzer of about 7.5 MW_e. Finally, for bigger sizes the hydrogen production decreases until the maximum analyzed size of 12.5 MW_e. This trend is due to two aspects that occur for sizes above 4 MW_e:

- The higher the size, the lower the number of hours with available power equal to nominal size of electrolyzer. Therefore, bigger sizes lead to just a small increase in the electricity processed during the year, according to the load duration curve (Figure 48).
- The hours during which electrolyzer does not operate due to an electric power lower than minimum load increases with the size.

Therefore, there is no reason to select an ALK electrolyzer of size higher than 7.5 MW.

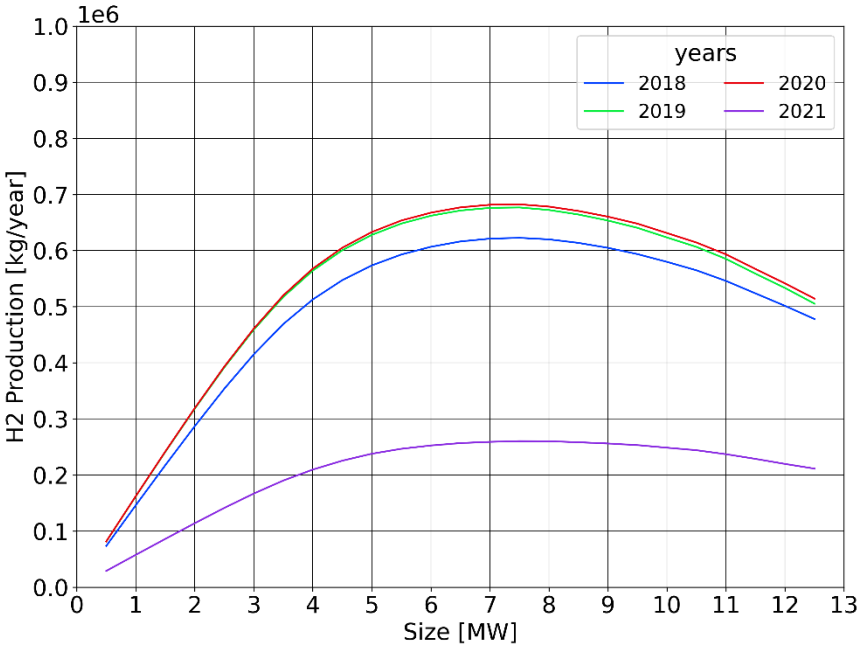

Figure 65: Electrolyzer hydrogen production as function of size

LCOH obtained via water electrolysis is reported in Figure 66. Chosen a year, going from low to intermediate sizes, the trend shows a decrease in LCOH since H_2 production relevantly increases and the specific investment cost decreases thanks to economies of scale. A minimum hydrogen production cost is achieved for electrolyzer size about 4-4.5 MW_e according to the reference year. Vice versa, moving to bigger sizes there is a new increase of LCOH, because H_2 production reaches slowly a maximum and after it decreases, as shown in Figure 65, while absolute investment cost becomes greater.

Different years imply different operating hours as well as different electricity cost. Therefore, chosen a size, the changes in electricity cost and secondly in hydrogen price lead to relevant variation in LCOH obtained in different years.

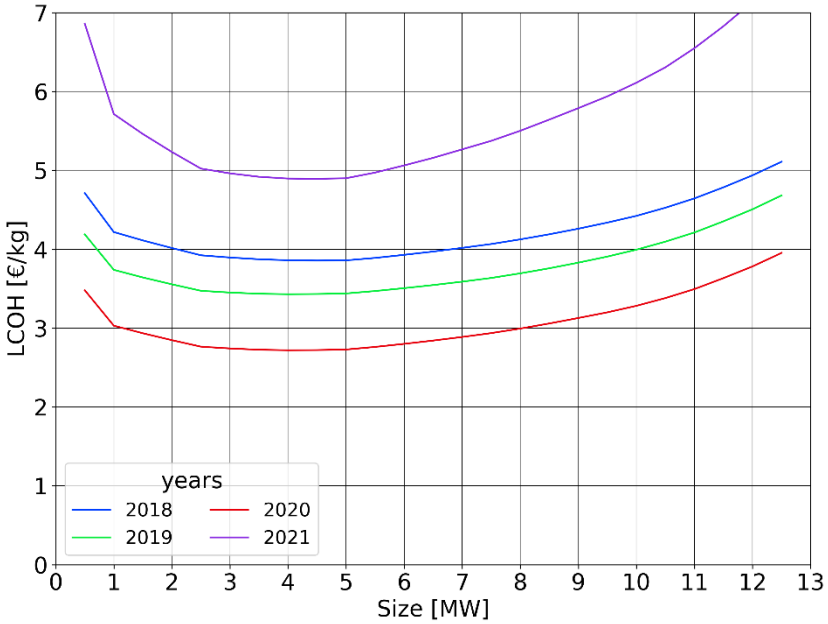

Figure 66: Electrolysis LCOH as function of size

Finally, Figure 66 gives the optimal size for the case study, i.e., the size at which corresponds the minimum LCOH and the maximum profitability index. It varies according to the reference year between 4.0 and 4.5 MW_e. Known the optimal size, it is interesting to underline the correspondent hydrogen production. It varies between 500 and 600 t/y according to selected year, as depicted in Figure 65.

For the considered case, hence ALK electrolyzer that produces hydrogen to serve heavy-duty vehicles, the achievable pay-back periods for the optimal size are reported in Table 29 according to the years between 2018 and 2021.

Table 29: PBP for optimal size and transport application vs Year

Year	2018	2019	2020	2021
PBP [y]	16	8	6	NPV<0

Assuming no delivery pressure differences between end uses and set the size equal to 4.5 MW_e. Considering a reference year, hence setting electricity and H_2 prices, it exists only an H_2 equivalent price that leads to achieve NPV=0 at the end of the investment period. Therefore, incentives to reach green H_2 competitiveness depends on the likely hydrogen selling price of each end application. For the analyzed case the hydrogen equivalent price is 3.63 €/kg, hence incentives needed in 2018 are reported in Table 30.

Table 30: 2018 incentives for NPV=0 vs H_2 end use

End use	Injection in NG grid	Industrial	Transport
H_2 price [€/kg]	0.81	1.92	3.73
Incentive [€/kg]	2.82	1.71	0.00

Nevertheless, between end application other small changes should be accounted beyond hydrogen price for both configurations (electrolysis and gasification). In fact, hydrogen injection into the NG grid, compared to other end uses, requires lower delivery pressure, 100-115 bar respect to 200-700 bar. Therefore, smaller Capex and lower electricity consumption related to intercooled compressors. However, it does not represent an important voice of cost with both technologies, hence in first approximation might be neglected.

Cost structure

A detailed cost breakdown structure of the electrolyzer is presented in the "state-of-the-art" chapter (section 1.2.2), while here costs composition for the entire plant is presented i.e., electrolyzer and compressor.

The results derive from following assumptions:

- Alkaline electrolyzer
- 2018 as reference year (see Table 16)
- Industrial application hence 2018 H_2 price equal to 1.92 €/kg
- Electrolyzer size = 4.5 MW_e
- Delivery pressure = 200 bar
- Incentive = 2.00 €/kg → H_2 equivalent price is 3.92 €/kg in order to show results when investment is profitable.

The Figure 67 shows how the total investment cost is divided between electrolyzer system and compressor. Moreover, the total Capex for the optimal size is reported equal to 3.970 M€.

Both components are still not at their maximum readiness, therefore total Capex for electrolysis configuration should decrease relevantly in the next decade as well as in the long period, thanks to research and developments and scale production.

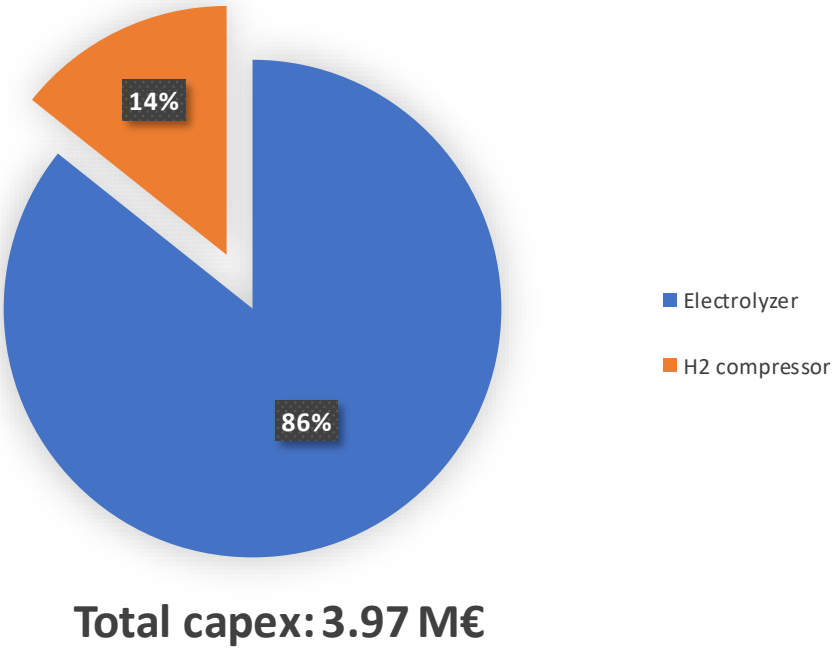

Figure 67: Electrolyzer vs Compressor Capex

Variable cost composition is reported in Figure 68. Firstly, it can be noticed that most of the cost (89%) is related to electrolyzer electricity consumption. In fact, hydrogen compression account on for 2.87% of annual Opex, that corresponds to about 3.2 % of total electricity consumption. Hence, when the plant draw electricity to produce hydrogen the remaining 96.8% is fed to the electrolyzer plant. This information allows even to underline that hydrogen compression at higher pressure until 700 bar will not causes drastic changes in variable cost, since the major Opex is associated to electric consumption of the electrolyzer. However, it can slightly affect the final LCOH because even the compressor Capex increase since another intercooling stage as well as compression stage are required. For instance, according to the assumption of this paragraph, if the delivery pressure goes from 200 to 700 bar, the LCOH will increase from 3.865 to 3.955, hence 2.33% of percentage variation is estimated. Operation and maintenance cost accounts for 6.77% of total Opex, while water consumption does not reach the 1%. For this reason, the possible use of seawater for which further purification processes are needed does not lead to significant variation in term of costs.

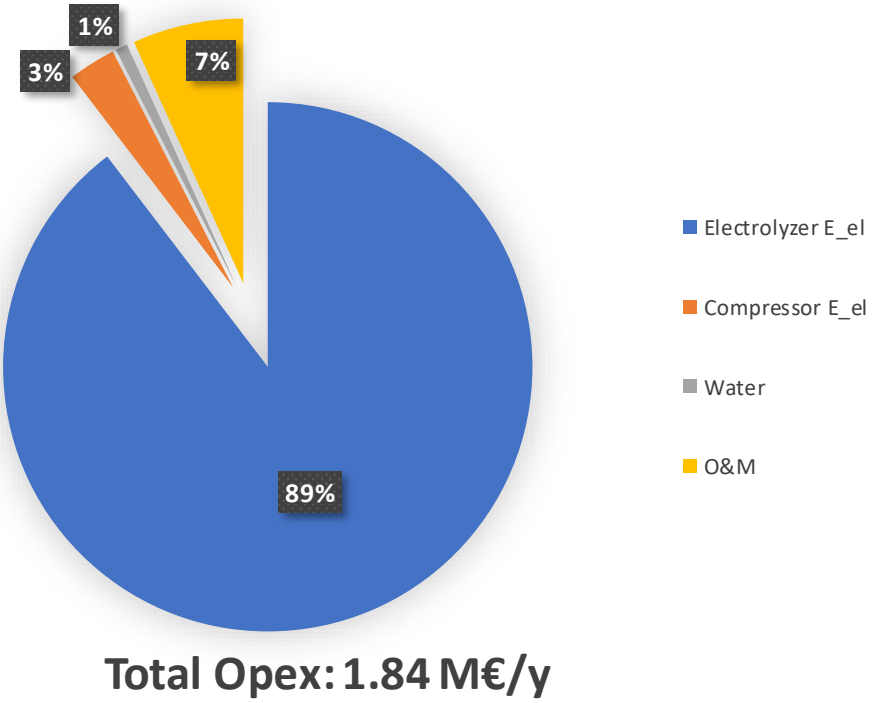

Figure 68: Electrolysis Opex composition

Yearly total Opex represents more than 45% of investment cost, therefore the economic performance strongly depends on electricity cost, that accounts for about 92.50% of total variable cost. However, even Capex plays a crucial role since the electrolyzer typically does not work at its maximum potential. In fact, it is typically used less hours per year compared to its availability, and it works likely at part load for several hours.

To provide good performance, electrolysis required very cheap electricity, hence for the case study there is a limit since it is paid according to price on DAM, even though it also represents an advantage, because if the price was paid according to LCOE of CHP plant, the techno-economic performances would have been worse.

In Figure 69 the changes in Opex composition due to different reference year are shown. In this case results depends on two factors, the electricity and hydrogen prices (Table 16 and Table 17). In fact, production logic leads to have lower operating hours in the years where the electricity cost is too high compared to the hydrogen value. Therefore, current relations between electricity, NG and H_2 markets lead to an operating hours reduction when electricity price increases. This production logic leads to economic losses reduction, however higher LCOH are achieved as described in Figure 66.

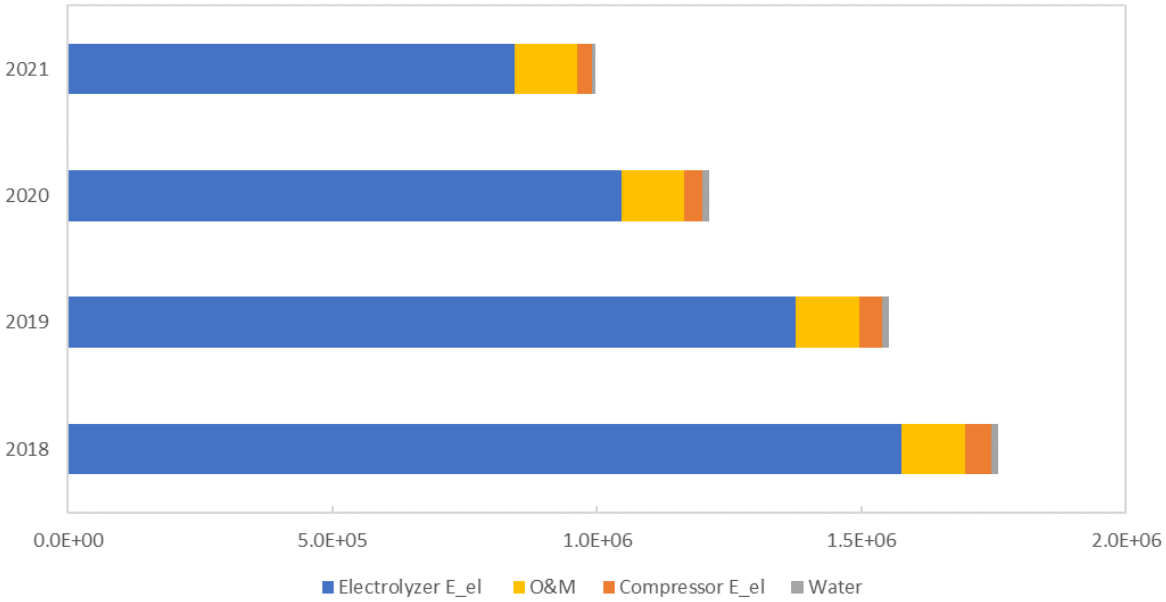

Figure 69: Opex composition as function of year

ALK vs PEM electrolyzers

The presented comparison between ALK and PEM electrolyzer is done according to modeling parameters in Table 15 and with same reference case for which cost structure has been presented, at which corresponds a size of 4.5 MW_e, i.e., in the optimal value range.

Since dynamics is not modeled the differences between the two technologies are:

- Capex cost
- Efficiency
- Minimum load
- Operating pressure
- Stack lifetime

Results are summarized in Table 31. The operating hours as well as the capacity factor depend firstly on WTP, i.e., the value associated to electricity consumed for producing hydrogen. Set hydrogen price, incentive, and delivery pressure, the WTP depends on electrolyzer and compressor specific consumption of electricity. The resulting WTP in the case of ALK electrolyzer is slightly greater (+3.2%) than the case of PEM electrolyzer. This is due to the small difference in electrolyzer efficiency in favor of ALK electrolyzer and lower compressor electricity consumption for PEM electrolysis, given the higher stack operating pressure.

Table 31: Comparison ALK vs PEM electrolyzer

Technology	ALK	PEM
WTP [€/MWh]	78.67	76.22
Operating hours [h/y]	7,272	7,303
H_2 production [t/y]	580.41	548.55
Capex [M€]	3.970	4.238
LCOH [€/kg]	3.86	4.08
Profitability Index [%]	22.61	-4.33

Given the hours during which is economically advantageous, the electrolyzer minimum load additionally influences OH and C_f. In fact, thanks to the possibility of operating down to 10% of nominal load the PEM electrolyzer works for a higher number of hours, despite the WTP is more favorable to ALK electrolysis technology. This phenomenon has been already described at the beginning of section 4.2, and in Figure 70 the difference in operating hours between ALK and PEM electrolyzer is reported according to the size.

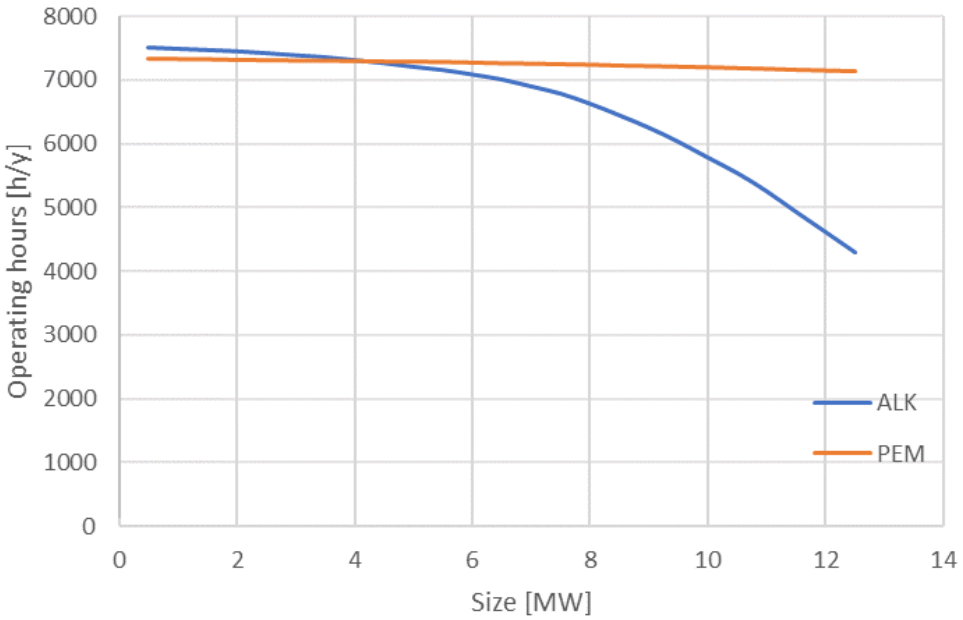

Figure 70: ALK vs PEM electrolyzer operating hours

It is interesting to notice how difference in the efficiency of electrolyzers is not relevant anymore for electrolyzer sizes above the 4 MW_e. In fact, the minimum load becomes the main parameters that affects operating hours. However, the OH referred to a size of 4.5 MW_e are quite similar, as shown in Table 31.

Hydrogen production is affected by operating hours and electrolyzer efficiency, therefore for the refence case of 4.5 MW_e size, hence with a small difference in operating hours, the H_2 production is greater for ALK electrolyzer, given the higher efficiency. Nevertheless, the hydrogen production according to the size for both technologies is reported in Figure 71. It could be noticed how relevant is the limit imposed by minimum load for ALK electrolysis compared to PEM one. In fact, the latter does not show a relevant decrease in hydrogen production, even for big sizes. However, the maximum hydrogen production is achieved for a size of 10 MW_e, since for bigger sizes the extra amount of electricity is typically lower than the one available with electric power below the 1 MW_e.

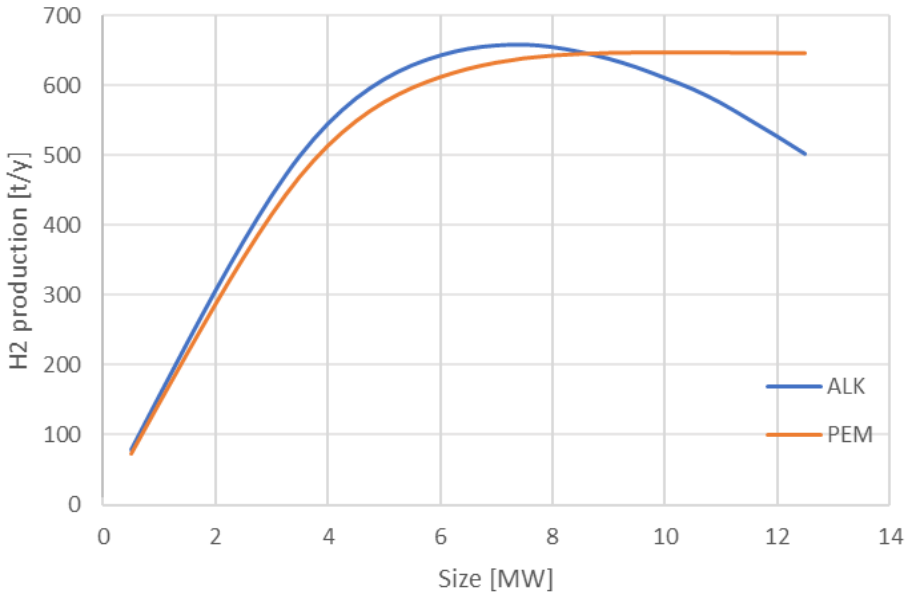

Figure 71: ALK vs PEM electrolyzer hydrogen production

The investment cost is lower for alkaline technology since the lower electrolyzer cost, despite PEM electrolyzer allows to have a cost reduction on compressor. In fact, set an electrolyzer size and H_2 delivery pressure, the compressor size of PEM electrolysis configuration is lower since:

- Maximum H_2 flow rate is lower due to smaller PEM electrolyzer efficiency
- Specific electric consumption of compressor is smaller thanks to higher stack operating pressure

Hydrogen production and Capex values obtained for the reference case leads to a lower LCOH for ALK electrolyzer, as reported in Table 31. This implies the need of higher incentive for making the investment feasible with PEM electrolyzer. In fact, a 2.0 €/kg incentive leads to a profitability index of 22.61% for ALK electrolysis while a -4.33% for PEM. The PI is even influenced by the stack lifetime. Both technologies lead to one stack substitution for 20 years operation for this reference case, however PEM electrolyzer stack is substituted earlier, and it has a higher cost. Furthermore, it has a lower terminal value due to the lower lifetime.

Therefore, it clearly shows that in the short run the ALK electrolyzer leads to better techno-economic performances for this case study, where electricity is generated by a fully dispatchable plant, hence with no drastic and aleatory load changes. However, for other case studies or applications, for instance the coupling with power generation from wind turbine or photovoltaic panel, a PEM electrolyzer might be the best solution since the wider load range and the faster dynamics.

Finally, it must be underlined that, for this case study, optimal size for PEM electrolyzer typically results to be 0.5 MW_e lower compared to ALK electrolyzer, since the different cost features. However, value obtained in Table 31 are really close to the ones achievable with optimal PEM electrolyzer size.

Sensitivity analysis

In this paragraph sensitivity analysis results for hydrogen production via electrolysis are described in order to understand the influence of main input parameters, and to estimate how techno-economic KPIs change according to an input variation.

The base case for sensitivity analysis refers to an ALK electrolyzer of 4.5 MW_e that serves industrial end users with a delivery pressure of 200 bar. Electricity and natural gas average prices are assumed both 80 €/MWh since it corresponds to a case in which the investment is profitable. Input parameters are reported in Table 32 while correspondent results are presented Table 33.

Table 32: References input for electrolysis sensitivity

Technology	Size [MW_e]	DAM price [€/MWh]	NG price [€/MWh]	Efficiency [kWh/kg]
ALK	4.5	80	80	48

Table 33: Reference results for electrolysis sensitivity

LCOH [€/kg]	OH [h/y]	H_2 prod. [t/y]	NPV [M€]	PI [%]
4.75	6,209	501.15	1.11	23.62%

While sensitivity analysis results are summarized in Table 34, as percentage variation compared to the reference case.

Table 34: Electrolysis sensitivity analysis results

Sensitivity parameters	Capex +20%	Capex -20%	Efficiency +20%	Efficiency -20%	Efficiency +6%	Efficiency -6%
LCOH [€/kg]	4%	-4%	-18%	16%	-5.5%	6.0%
OH [h/y]	0%	0%	22%	-39%	10.7%	-11.7%
H_2 prod. [t/y]	0%	0%	50%	-48%	17.2%	-16.4%
NPV [M€]	-108%	108%	710%	-311%	161.7%	-128.3%
PI [%]	-107%	160%	674%	-325%	155.7%	-128.6%

First of all, it must be underlined that these results are strongly affected from the reference case choice. In fact, due to the production logic, the operating hours vary a lot. If a not profitable investment is taken as reference, it has typically low operating hours, hence the Capex influence results extremely high since variable costs are low. In fact, the effect of electrolyzer efficiency change would be small. On the other side, when the investment is advantageous, hence NPV and PI greater than zero, the operating hours are much higher, therefore Capex impact on KPI is less relevant. While electrolyzer efficiency assume more influence with increasing OH since the economic parameters depend more on variable costs. The reference case of this analysis tries to simulate a likely case for an investor that implement this configuration, hence a slightly positive profitability index is present in the reference case.

Investment cost variation does not lead to operating hours and H_2 production changes, while efficiency variation has several effects. From one side it influences the WTP, hence the operating hours. While, on the other side it affects the hydrogen output, since higher efficiency leads to greater H_2 production, set the available electricity profile and the operating hours.

Assumed same input variation, efficiency change strongly affects all economic KPI if compared with Capex influence. However, it is not realistic a variation of $\pm 20\%$ in efficiency, a reasonable assumption could be respectively in the range of 6% for ALK electrolyzer and 10% for PEM electrolyzer. To these variations correspond the results reported in the last two columns of Table 34. The variations are not symmetric since the change of electrolyzer efficiency leads to several consequences. Operating hours change turns into a variation in electric energy utilized over the year. However, it is not directly proportional to OH reduction since the electric power available for each hour is different. In addition, OH variation leads to different year of stack substitution, hence also different terminal value. Finally, set OH and electric load profile, efficiency change modifies hydrogen production.

According to the reference case, the variation on LCOH due to efficiency change is close to the 6% input variation. While the influence on the NPV and PI results to be very relevant,

since the high percentage changes, that correspond to profitability index values of 60.39% and -6.76% compared to the 23.62% of reference case.

On the other side, possible capex variation likely stays in an uncertainty of ±20%, given the assumed Capex trend and the forecasts for 2030 investment cost. Comparing KPIs variations according to most likely ranges for the two input parameters, the electrolyzer efficiency seems to still have a slightly more relevance on LCOH, NPV and PI. Nevertheless, these results might change significantly when reference case is different.

Electricity and natural gas prices are the parameters with the highest uncertainty and the most difficult to forecast. If for electrolyzer Capex and efficiency, target values are clear, there are not equivalent reliable values for electricity and NG prices and forecast on relation between these markets. In addition, it must be done different reasoning according to the country in which the investment would be implemented since different energy mix are adopted.

Table 35 and Table 36 report respectively LCOH and profitability index values according to the couples of electricity and hydrogen prices. As for gasification sensitivity on these parameters, the first column is related to electricity prices, while in the first two rows the natural gas prices and correspondent hydrogen price are reported. Nevertheless, it can also be accounted as normal sensitivity analysis on hydrogen prices since natural gas has no other influences in the electrolyzer configuration.

Starting from Table 35, the LCOH present the following trends:

- Set the electricity cost, increasing the hydrogen price, the LCOH decreases. This is strictly link to the operating hours that increases when the H_2 price becomes greater. In contrast to gasification configuration, electrolysis LCOH depend on hydrogen price due to the hourly production logic adopted in the model. Furthermore, for electricity prices below 100 €/MWh operating hours reaches a plateau before maximum hydrogen price, since a lower price is enough to let the electrolyzer operates all the available hours. This turns into the same trend in LCOH, in fact for low electricity prices the minimum LCOH is achieved before the highest H_2 price and afterward it remains constant with hydrogen price increase.

- Set the hydrogen price, an electricity cost increase is translated to higher LCOH. As for the first point, even this trend is related to operating hours. Hence, they decrease with an electricity cost increase. The latter also represents a greater specific cost for consumed electricity. Finally, it can be noticed how for hydrogen price below 2.70 €/kg and high electricity price the best solution might be to not operate the electrolyzer, so operating hours are equal to zero and the LCOH to infinite.

Due to production logic and electrolyzer features, LCOH is extremely affected by changes in both, electricity and H_2 prices. In addition, it is possible to notice the typical greater influence of electricity cost compared to hydrogen price.

The sensitivity analysis on profitability index (Table 36) has similar trends but with some peculiarities:

- The production logic based on WTP allows to limit possible economic losses when the electricity and hydrogen prices become disadvantageous for H_2 production. In fact, the minimum return on investment is set by the zero operating hours case at which correspond a PI of -123.3%.

- The maximum profitability index is always reached at the highest hydrogen price since revenues from hydrogen sale always grow with greater H_2 price, despite LCOH might reach its minimum already at lower values.

Finally, profitability index shows for which couples of electricity and hydrogen prices is economically feasible to invest in this technology. Electrolysis configuration results to be interesting for couples in the top-right corner of Table 36, hence for high hydrogen prices and relatively low electricity costs. Therefore, it demonstrates how hydrogen production is not profitable according 2018-2021 market conditions and it is even worse for 2022 prices. Hence, incentives are needed and the current link between electricity and NG costs must be changed in order to make green hydrogen production more competitive in the next future.

Table 35: Electrolysis LCOH vs electricity and NG prices

P H2 [€/kg]	1.22	1.71	2.21	2.70	3.20	3.70	4.19	4.69	5.19	5.68	6.18	6.67	7.17	7.67	8.16	8.66	9.16	9.65	10.15	10.64
NG [€/MWh] / E_el [€/MWh]	10	20	30	40	50	60	70	80	90	100	110	120	130	140	150	160	170	180	190	200
50	50.86	9.37	3.96	3.46	3.35	3.36	3.37	3.38	3.38	3.39	3.39	3.39	3.39	3.39	3.39	3.39	3.39	3.39	3.39	3.39
60	116.99	21.97	7.16	4.18	3.92	3.82	3.83	3.86	3.87	3.88	3.88	3.89	3.89	3.89	3.89	3.89	3.89	3.89	3.89	3.89
70	188.62	44.84	14.21	6.25	4.46	4.37	4.29	4.31	4.34	4.36	4.37	4.38	4.38	4.38	4.39	4.39	4.39	4.39	4.39	4.39
80	379.85	95.41	24.36	10.42	6.04	4.79	4.81	4.75	4.78	4.81	4.84	4.86	4.87	4.88	4.88	4.88	4.89	4.89	4.89	4.89
90	448.20	136.32	44.56	17.40	9.07	5.91	5.13	5.24	5.21	5.25	5.28	5.32	5.34	5.36	5.37	5.38	5.38	5.39	5.39	5.39
100	663.43	189.02	87.50	27.16	14.12	8.04	6.08	5.49	5.67	5.65	5.71	5.76	5.78	5.82	5.84	5.86	5.87	5.88	5.88	5.89
110	843.51	313.65	117.75	44.31	20.48	11.38	7.71	6.30	5.85	6.10	6.10	6.15	6.22	6.26	6.30	6.32	6.34	6.35	6.37	6.38
120	1054.19	448.51	150.96	79.59	29.18	16.51	10.56	7.63	6.54	6.22	6.53	6.54	6.60	6.68	6.73	6.76	6.80	6.83	6.84	6.85
130	1830.64	474.39	189.42	103.31	43.72	23.33	13.92	9.72	7.68	6.83	6.60	6.96	6.98	7.05	7.14	7.20	7.24	7.28	7.31	7.33
140	2898.93	663.81	296.42	130.12	75.42	30.24	18.62	12.27	9.18	7.76	7.16	6.97	7.38	7.42	7.50	7.59	7.66	7.71	7.74	7.78
150	6965.29	744.42	411.90	160.08	96.55	38.90	24.73	16.43	11.68	9.04	7.91	7.48	7.34	7.81	7.85	7.94	8.03	8.12	8.18	8.20
160	inf	843.96	448.93	189.82	118.51	69.42	32.38	20.89	14.44	11.01	9.02	8.18	7.82	7.72	8.23	8.29	8.38	8.47	8.58	8.65
170	inf	1054.63	474.80	268.15	137.49	92.60	39.06	26.15	18.32	13.11	10.64	9.19	8.45	8.17	8.10	8.65	8.72	8.82	8.91	9.03
180	inf	1831.05	664.19	380.95	171.04	108.38	66.78	32.97	22.68	16.71	12.75	10.36	9.32	8.73	8.52	8.49	9.07	9.15	9.25	9.36
190	inf	2899.32	744.80	449.24	190.22	130.86	89.00	39.23	27.42	19.84	15.13	12.36	10.33	9.49	9.04	8.89	8.87	9.49	9.58	9.69
200	inf	2899.40	844.32	449.35	255.02	149.85	102.42	61.09	33.57	24.94	18.38	13.96	11.93	10.42	9.71	9.36	9.25	9.25	9.92	10.01
210	inf	6965.74	906.85	475.22	314.82	171.45	119.27	83.30	38.69	28.54	21.76	17.16	13.66	11.71	10.56	9.94	9.70	9.62	9.64	10.33
220	inf	6965.81	1055.08	664.57	412.65	190.62	138.22	97.68	59.69	34.42	25.87	19.76	15.87	13.40	11.56	10.75	10.25	10.04	9.99	10.03
230	inf	inf	1831.47	664.67	449.66	255.39	152.52	113.63	81.48	38.68	30.14	23.31	18.54	14.79	13.05	11.63	10.97	10.55	10.39	10.36
240	inf	inf	1831.55	844.69	475.52	315.18	171.87	125.37	93.75	58.30	35.19	27.19	21.06	17.25	14.58	12.83	11.74	11.18	10.86	10.74
250	inf	inf	2899.79	844.78	475.63	412.97	191.02	138.66	105.22	78.41	39.10	30.93	24.42	19.86	16.54	14.37	12.82	11.89	11.42	11.18
260	inf	inf	2899.87	907.30	664.95	413.08	255.76	161.61	120.04	92.98	58.68	35.62	28.08	22.34	18.84	15.66	14.10	12.79	12.12	11.68
270	inf	inf	6966.18	1055.52	665.05	450.07	297.97	184.49	132.04	100.28	76.90	39.37	32.45	26.54	21.17	17.75	15.46	14.02	12.90	12.35
280	inf	inf	6966.26	1831.88	745.63	475.94	382.05	191.42	150.99	114.40	90.50	57.02	36.22	28.93	23.78	20.27	17.26	15.36	13.93	13.05
290	inf	inf	inf	1831.96	845.14	476.04	413.40	256.13	162.03	126.12	98.81	72.64	39.78	33.11	27.24	22.28	19.52	16.54	15.25	13.98
300	inf	inf	inf	2900.19	845.23	476.14	450.39	298.32	184.89	139.38	108.09	84.83	55.66	36.82	29.88	25.18	21.42	18.37	16.34	15.08
310	inf	inf	inf	2900.26	907.75	665.43	450.49	315.99	191.82	151.41	120.80	94.90	70.53	39.98	33.93	28.24	23.37	20.57	17.62	16.33
320	inf	inf	inf	2900.34	1055.96	746.00	476.35	413.72	256.51	172.96	132.78	104.34	83.02	56.04	37.24	30.92	27.26	22.55	20.01	17.37
330	inf	inf	inf	6966.63	1832.29	845.50	476.45	413.83	298.68	185.30	139.82	117.64	95.22	69.50	40.39	34.65	29.22	24.89	21.73	19.03
340	inf	inf	inf	6966.70	1832.38	845.59	476.55	450.80	316.35	192.22	154.08	126.88	101.41	83.37	55.95	37.85	31.99	28.15	23.51	20.98
350	inf	inf	inf	inf	1832.46	908.11	665.81	450.91	414.04	244.72	173.38	136.58	111.04	91.66	67.21	40.81	36.29	30.04	26.14	22.78
360	inf	inf	inf	inf	2900.66	908.20	746.38	476.76	414.15	270.48	192.49	152.13	121.56	99.02	81.42	55.86	38.45	33.12	28.85	24.39
370	inf	inf	inf	inf	2900.74	1056.41	746.47	476.86	451.12	316.70	192.62	163.15	133.53	107.12	91.99	64.25	41.23	37.04	30.79	27.03
380	inf	inf	inf	inf	2900.81	1340.06	845.96	476.96	451.22	383.16	245.10	173.79	140.55	118.41	96.05	78.83	55.79	39.06	33.66	29.61
390	inf	inf	inf	inf	6967.08	1832.79	846.05	666.19	477.07	414.47	270.84	192.89	152.55	127.63	103.55	86.36	63.48	41.64	37.46	31.65
400	inf	inf	inf	inf	6967.15	1832.87	908.56	666.29	477.17	414.58	317.05	193.02	163.57	133.97	116.26	96.37	79.18	55.73	39.85	35.02

Table 36: Electrolysis PI vs electricity and NG prices

P H2 [€/kg]	1.22	1.71	2.21	2.70	3.20	3.70	4.19	4.69	5.19	5.68	6.18	6.67	7.17	7.67	8.16	8.66	9.16	9.65	10.15	10.64
NG [€/MWh] / E_el [€/MWh]	10	20	30	40	50	60	70	80	90	100	110	120	130	140	150	160	170	180	190	200
50	-123.0	-120.4	-106.3	-59.0	0.8	74.2	152.3	231.5	311.2	391.1	471.0	551.0	631.0	710.9	790.9	870.9	950.9	1030.9	1110.8	1190.8
60	-123.1	-122.1	-116.8	-97.7	-49.5	8.0	80.1	155.6	234.3	313.6	393.4	473.2	553.1	633.1	713.1	793.0	873.0	953.0	1033.0	1113.0
70	-123.2	-122.8	-120.2	-112.0	-88.7	-40.4	15.3	85.1	159.2	237.3	316.3	395.7	475.5	555.3	635.2	715.2	795.1	875.1	955.1	1035.1
80	-123.3	-122.9	-121.7	-117.6	-106.0	-79.4	-31.2	23.6	90.4	163.5	240.6	319.2	398.4	477.9	557.6	637.4	717.3	797.3	877.2	957.2
90	-123.3	-123.1	-122.4	-120.1	-114.0	-99.5	-69.9	-21.7	31.4	96.2	170.1	244.3	322.3	401.2	480.4	560.0	639.7	719.5	799.4	879.3
100	-123.3	-123.2	-122.7	-121.4	-117.7	-109.6	-91.9	-60.3	-12.5	39.5	103.8	175.1	248.4	325.7	404.1	483.2	562.5	642.1	721.9	801.7
110	-123.3	-123.2	-122.9	-122.1	-119.8	-114.8	-104.3	-84.0	-50.6	-3.4	48.6	110.5	180.3	255.5	329.3	407.3	486.1	565.2	644.6	724.2
120	-123.3	-123.2	-123.0	-122.4	-121.0	-117.7	-111.1	-98.4	-75.7	-40.8	5.8	57.0	117.4	185.8	260.2	333.3	410.7	489.1	568.0	647.2
130	-123.3	-123.3	-123.1	-122.6	-121.8	-119.5	-115.2	-107.0	-92.0	-67.0	-31.1	15.0	65.5	124.6	191.6	265.1	340.9	414.3	492.4	571.0
140	-123.3	-123.3	-123.1	-122.8	-122.2	-120.7	-117.6	-112.0	-102.2	-85.1	-58.2	-21.2	24.1	75.1	133.6	197.5	270.2	345.4	418.2	495.8
150	-123.3	-123.3	-123.2	-122.9	-122.4	-121.5	-119.2	-115.3	-108.4	-96.8	-77.8	-49.2	-11.3	34.0	83.7	141.2	206.1	275.6	350.2	422.4
160	-123.3	-123.3	-123.2	-123.0	-122.6	-121.9	-120.4	-117.4	-112.5	-104.3	-90.8	-70.0	-40.0	-1.4	43.2	92.4	148.9	212.7	281.2	355.1
170	-123.3	-123.3	-123.2	-123.1	-122.7	-122.2	-121.2	-118.9	-115.3	-109.3	-99.7	-84.5	-62.0	-30.8	8.5	52.4	101.1	156.8	219.6	286.9
180	-123.3	-123.3	-123.2	-123.1	-122.8	-122.4	-121.6	-120.0	-117.2	-112.7	-105.6	-94.8	-78.0	-53.8	-21.4	18.4	61.6	109.8	164.8	226.6
190	-123.3	-123.3	-123.3	-123.1	-122.9	-122.5	-121.9	-120.9	-118.6	-115.2	-109.9	-101.6	-89.2	-71.0	-45.4	-12.0	28.4	70.8	118.6	174.7
200	-123.3	-123.3	-123.3	-123.2	-123.0	-122.7	-122.1	-121.3	-119.7	-116.9	-112.8	-106.5	-97.2	-83.3	-63.7	-36.6	-2.5	38.3	80.0	127.4
210	-123.3	-123.3	-123.3	-123.2	-123.1	-122.8	-122.3	-121.6	-120.6	-118.3	-115.0	-110.2	-102.9	-92.4	-77.1	-56.1	-27.8	7.1	48.3	89.2
220	-123.3	-123.3	-123.3	-123.2	-123.1	-122.9	-122.5	-121.9	-121.0	-119.4	-116.7	-112.8	-107.2	-98.9	-87.3	-70.6	-48.2	-18.9	16.7	58.3
230	-123.3	-123.3	-123.3	-123.2	-123.1	-122.9	-122.6	-122.1	-121.4	-120.2	-118.0	-114.8	-110.3	-103.8	-94.7	-81.7	-63.9	-40.2	-9.9	26.4
240	-123.3	-123.3	-123.3	-123.3	-123.2	-123.0	-122.7	-122.3	-121.6	-120.8	-119.0	-116.4	-112.7	-107.6	-100.1	-90.0	-75.8	-56.9	-32.0	-0.9
250	-123.3	-123.3	-123.3	-123.3	-123.2	-123.0	-122.8	-122.4	-121.9	-121.1	-119.9	-117.7	-114.6	-110.4	-104.5	-96.2	-85.1	-69.6	-49.6	-23.6
260	-123.3	-123.3	-123.3	-123.3	-123.2	-123.1	-122.9	-122.5	-122.0	-121.4	-120.4	-118.7	-116.1	-112.6	-107.8	-101.0	-92.1	-79.8	-63.2	-42.1
270	-123.3	-123.3	-123.3	-123.3	-123.2	-123.1	-122.9	-122.6	-122.2	-121.6	-120.8	-119.6	-117.4	-114.4	-110.4	-105.0	-97.4	-87.6	-74.1	-56.6
280	-123.3	-123.3	-123.3	-123.3	-123.2	-123.1	-123.0	-122.7	-122.3	-121.8	-121.1	-120.1	-118.4	-115.8	-112.5	-107.9	-101.8	-93.5	-82.7	-68.3
290	-123.3	-123.3	-123.3	-123.3	-123.3	-123.2	-123.0	-122.8	-122.5	-122.0	-121.4	-120.6	-119.2	-117.1	-114.1	-110.3	-105.2	-98.3	-89.4	-77.7
300	-123.3	-123.3	-123.3	-123.3	-123.3	-123.2	-123.0	-122.9	-122.6	-122.1	-121.6	-120.9	-119.8	-118.1	-115.5	-112.3	-107.9	-102.3	-94.6	-85.0
310	-123.3	-123.3	-123.3	-123.3	-123.3	-123.2	-123.1	-122.9	-122.7	-122.3	-121.8	-121.1	-120.3	-118.9	-116.7	-113.9	-110.2	-105.4	-99.1	-90.8
320	-123.3	-123.3	-123.3	-123.3	-123.3	-123.2	-123.1	-122.9	-122.7	-122.4	-121.9	-121.3	-120.6	-119.5	-117.7	-115.2	-112.1	-107.9	-102.6	-95.6
330	-123.3	-123.3	-123.3	-123.3	-123.3	-123.2	-123.1	-123.0	-122.8	-122.5	-122.1	-121.5	-120.9	-120.0	-118.6	-116.4	-113.6	-110.0	-105.4	-99.6
340	-123.3	-123.3	-123.3	-123.3	-123.3	-123.2	-123.2	-123.0	-122.9	-122.6	-122.2	-121.7	-121.1	-120.3	-119.2	-117.4	-114.9	-111.8	-107.8	-102.8
350	-123.3	-123.3	-123.3	-123.3	-123.3	-123.3	-123.2	-123.0	-122.9	-122.7	-122.3	-121.9	-121.3	-120.6	-119.7	-118.3	-116.1	-113.3	-109.9	-105.5
360	-123.3	-123.3	-123.3	-123.3	-123.3	-123.3	-123.2	-123.1	-122.9	-122.7	-122.4	-122.0	-121.5	-120.8	-120.0	-118.9	-117.1	-114.6	-111.6	-107.8
370	-123.3	-123.3	-123.3	-123.3	-123.3	-123.3	-123.2	-123.1	-123.0	-122.8	-122.5	-122.1	-121.7	-121.1	-120.3	-119.4	-117.9	-115.8	-113.0	-109.7
380	-123.3	-123.3	-123.3	-123.3	-123.3	-123.3	-123.2	-123.1	-123.0	-122.8	-122.6	-122.3	-121.8	-121.3	-120.6	-119.8	-118.6	-116.7	-114.3	-111.3
390	-123.3	-123.3	-123.3	-123.3	-123.3	-123.3	-123.2	-123.1	-123.0	-122.9	-122.7	-122.3	-121.9	-121.4	-120.8	-120.1	-119.1	-117.6	-115.4	-112.7
400	-123.3	-123.3	-123.3	-123.3	-123.3	-123.3	-123.3	-123.2	-123.1	-122.9	-122.7	-122.4	-122.1	-121.6	-121.0	-120.3	-119.5	-118.3	-116.4	-114.0

4.3. Configurations comparison

The aim of this section is to compare results from gasification and electrolysis in order to underline peculiarities and differences between the two configurations, as well as to summarize results and give feedback about the analyzed case study.

The two proposed configurations are based on totally different technologies. According to presented results for the case study, the best size of the gasification-based process is in the range of 20-30 MW_{th} of biomass input, while the electrolysis configuration optimal design requires a 4.0-4.5 MW_e electrolyzer. Hence, the following reasonings and data reported in Table 37 refer to a gasification plant size of 30 MW_{th_input} and an electrolyzer of 4.5 MW_e.

Table 37: Comparison between gasification and electrolysis configuration

Configuration	Gasification	ALK electrolyzer
Size	30 MW_{th_input}	4.5 MW_e
Capex [M€]	36.16	3.97
H_2 production [t/y]	2,558	630
Land footprint	Big	Small
Current TRL	7-8	9

The configuration based on gasification presents higher investment costs as well as operative costs, however it guarantees a much greater hydrogen production compared to electrolysis. For instance, gasification system produces 306% more hydrogen than electrolysis configuration, but with an 811% higher investment cost, according to the cases reported in Table 37. Furthermore, it provides a steady hydrogen production over the year since it always works at nominal point, hence just small changes are present according to the gasified biomass. Even though, biomasses are already managed in the industrial site, this configuration has a large land footprint since several unit operations are needed to carry out the hydrogen production.

Biomass gasification is a proven process for syngas production, however there are no operating commercial plants that produce hydrogen nowadays. The TRL of single processes results to be high (8-9), however the readiness of the overall process is still lower. Moreover, additional studies and research must be done in order to implement hydrogen production via steam gasification, especially if, as in the case study, several biomasses with different characteristics are treated. In fact, current commercial gasification plants for syngas production typically process just woody biomasses. However, testing with other fuels is going on since the last years.

Electrolysis configuration has several aspects that differ from the gasification technology. Since the power generation plant is managed by a third part firm, electricity production in the industrial site is independent from hydrogen production because its aim is to satisfy internal energy demands. Therefore, an additional section for producing hydrogen requires the electrolyzer system and a compressor. This turns into a smaller footprint, i.e., the hydrogen production plant would occupy less space and a smaller investment compared to the gasification configuration, as reported in Table 37. Furthermore, also the variable costs are much lower, hence it results the less risky solution. In fact, if electricity and natural gas prices become not favorable for producing hydrogen, the maximum economic loss results to be lower in case of the electrolysis configuration. This happens also thanks to the production logic that can be adopted given the dynamics features of electrolyzers. On the other side, it typically leads to have no H_2 production in some hours of the day or during some periods of the year according to electricity cost trend and hydrogen price.

In contrast with gasification technology, electrolysis provides a lower hydrogen production, since the overall process biomass-to-H_2 has lower efficiency due to the two steps transformation, but even because the overall electrolysis process has a lower energy input. Nevertheless, it results the readiest technology to produce hydrogen since CHP plant fed by biomass is a commercial technology, as well as the alkaline electrolyzer. Furthermore, it allows to overcome problems related to the gasification of several types of biomasses that might be present if gasification is adopted.

LCOH of the two configurations cannot really be compared since gasification LCOH does not depend on H_2 price, while the electrolysis LCOH does, due to WTP production logic. Therefore, it is better to focus only on economic KPIs such as the profitability index that allows to understand when investment in green hydrogen production might be profitable and with which technology.

Table 38 is generated comparing Table 28 and Table 36 that show PI values according to electricity and NG prices, as well as H_2 price since it depends on natural gas cost. This comparison allows to make evident for which couples of electricity and NG prices the investment in hydrogen production is:

- Not feasible (pink area)
- Feasible and better via gasification (green area)
- Feasible and better via electrolysis (light blue area)

For couples of electricity, NG and H_2 prices where profitability indexes are positive for both technologies, the configuration with the higher return on investment is chosen.

Table 38 can be divided in four quadrants according to electricity cost and NG/H_2 cost:

I. Zone 1 = High-High (bottom-right), where gasification configuration is a profitable solution for hydrogen production.

II. Zone 2 = High-Low (bottom-left), where there is not any feasibility to invest in hydrogen production with either technology.

III. Zone 3 = Low-Low (top-left), where gasification is not competitive at all due to high LCOH, while electrolysis could be profitable only for H_2 price above 3 €/kg and electricity cost lower than 70 €/MWh.

IV. Zone 4 = Low-High (top-right), where both technologies are profitable, and electrolysis is preferred for very low electricity cost, while gasification for values above 110 €/MWh.

Furthermore, Table 38 allows to underline some important differences between the two configurations:

- Investment in H_2 production via gasification might be feasible only for relatively high NG price, since relatively high LCOH decreases with NG price increase (Table 27), while the hydrogen sale price increases. Gasification has a low dependency on electricity price if natural gas cost increases as well, since valuable tail gas is used as NG substitute. In fact, for hydrogen price above 6.67 €/kg and NG cost above 120 €/MWh, gasification configuration turns to have a positive NPV and PI for any electricity price.

- Investment in H_2 production via electrolysis is extremely favored by low price electricity since it decreases significantly the LCOH, while its economic performance quickly gets worse with an electricity cost increase. Even though it is possible to sell hydrogen for more than 10 €/kg, the electricity cost must be lower than 120 €/MWh to produce hydrogen competitively. However, it is not likely to have access to cheap electricity since its cost depends on the market (DAM). Moreover, it must be underlined that low-price electricity makes advantageous the H_2 production instead of electricity sale, but, in the analyzed case study, if the electricity price is low, the power generation firm does not have reasons to produce surplus electricity since it would be valorized to a price lower than LCOE of the CHP plant which is typically higher than 120 €/MWh (section 2.1). Hence for low electricity price, although H_2 production looks better than selling surplus electricity (base case) in a differential perspective, both solutions lead to an overall negative profit for the financial group, i.e., the best option would be to do not produce the surplus electricity if possible.

Compared to gasification, electrolysis configuration depends much more on electricity and hydrogen prices, due to production logic that strongly affects operating hours, but also for the intrinsic characteristics of electrolysis, since more than 90% of the variable costs are related to electricity consumption. Therefore, in a real scenario where electricity and hydrogen prices may change year by year, even widely, electrolysis economic performances have more uncertainty than gasification ones.

Considering hydrogen prices according to the end use reported in Table 17 it is possible to notice how prices related to hydrogen injection into the NG grid as well as H_2 for industrial application are extremely low, therefore green hydrogen production with both technologies cannot compete for any of the previous four years. Hydrogen price for transport application, on the other hand, results to be already competitive (compared to base case) just for electrolysis configuration for the years between 2018 and 2020 to which correspond the electricity and natural gas prices in Table 16. However, those prices are not a likely forecast for the next future, since an increase in both, electricity and gas cost occurred since the second half of 2021. Consequently, there is the need of proper incentive mechanisms for green hydrogen since it still is not competitive with H_2 from fossil fuels or other competitors, and it should also cover uncertainty given from the energy markets. Moreover, the incentive must be designed according to technology characteristics and end application to allow investors to enter each market with different technologies. Finally, incentives permits the creation of a real green hydrogen industry, hence a green hydrogen cost reduction thanks to scale in production, learning rate, and research and developments.

Finally, a discussion about which zone or couple of values will be more likely present in the next 20 years must done, even though forecasts are not reliable, also because possible unpredictable events might occur as from 2020. Current trend in the Italian scenario shows a strong link between natural gas and electricity prices since the majority of traditional power generation plants are NG-fired. In fact, 48.2% of electricity production in 2019 used natural gas as fuel. Therefore, to an increase of natural gas cost and so H_2 price, an increase in electricity cost occurs too. The current link between these markets is represented somehow by a thick diagonal from top-left to bottom-right of Table 38. Hence, if markets coupling remains the same in the future, the investment in hydrogen production will be profitable via gasification only for high prices of electricity, natural gas and hydrogen. However, trends might change in the next future. The energy transition requires time, but it has led, and it will lead to changes. For instance, electricity costs profile in a day changed due the strong increase of intermittent renewable energy sources employment in the last 15 years. According to "Net zero" goal of 2050, the forecasts provide an increase in renewables and a lower relevance of NG going towards 2050, even to decrease energy dependency from abroad. Hence, the link between electricity and NG markets should get lower. However, several factors influence energy transition and its speed, such as technology developments, EU incentives, i.e., governments, and grid resilience. To conclude, a sort of partial decoupling between two markets is expected, and this should likely lead to zones 3 or 4, hence relatively low electricity prices on DAM and high or low NG and so H_2 prices according to the natural gas market.

Additionally, even a note about the link between hydrogen and natural gas price is relevant. Nowadays, hydrogen price is strictly linked to natural gas price since the 76% world H_2 production derives from methane steam reforming processes, (see "Introduction" section). However, objectives for next decades push to have a great increase in green hydrogen production through electrolysis, therefore the dependency between hydrogen and natural gas prices might decrease, taking also in account the CO_2 price increase and a greater production of blue hydrogen in the next 20 years.

Table 38: Gasification vs Electrolysis investment comparison, legend: pink area → PI<0 (-), blue area→ electrolysis (E), green area→ gasification (G)

P H2 [€/kg]	1.22	1.71	2.21	2.70	3.20	3.70	4.19	4.69	5.19	5.68	6.18	6.67	7.17	7.67	8.16	8.66	9.16	9.65	10.15	10.64
NG [€/MWh] / E_el [€/MWh]	10	20	30	40	50	60	70	80	90	100	110	120	130	140	150	160	170	180	190	200
50	-	-	-	-	E	E	E	E	E	E	E	E	E	E	E	E	E	E	E	E
60	-	-	-	-	-	E	E	E	E	E	E	E	E	E	E	E	E	E	E	E
70	-	-	-	-	-	-	E	E	E	E	E	E	E	E	E	E	E	E	E	E
80	-	-	-	-	-	-	-	G	E	E	E	E	E	E	E	E	E	E	E	E
90	-	-	-	-	-	-	-	G	G	G	G	E	E	E	E	E	E	E	E	E
100	-	-	-	-	-	-	-	G	G	G	G	G	G	E	E	E	E	E	E	E
110	-	-	-	-	-	-	-	G	G	G	G	G	G	G	G	G	E	E	E	E
120	-	-	-	-	-	-	-	-	G	G	G	G	G	G	G	G	G	G	G	E
130	-	-	-	-	-	-	-	-	G	G	G	G	G	G	G	G	G	G	G	G
140	-	-	-	-	-	-	-	-	G	G	G	G	G	G	G	G	G	G	G	G
150	-	-	-	-	-	-	-	-	G	G	G	G	G	G	G	G	G	G	G	G
160	-	-	-	-	-	-	-	-	G	G	G	G	G	G	G	G	G	G	G	G
170	-	-	-	-	-	-	-	-	G	G	G	G	G	G	G	G	G	G	G	G
180	-	-	-	-	-	-	-	-	G	G	G	G	G	G	G	G	G	G	G	G
190	-	-	-	-	-	-	-	-	-	G	G	G	G	G	G	G	G	G	G	G
200	-	-	-	-	-	-	-	-	-	G	G	G	G	G	G	G	G	G	G	G
210	-	-	-	-	-	-	-	-	-	G	G	G	G	G	G	G	G	G	G	G
220	-	-	-	-	-	-	-	-	-	G	G	G	G	G	G	G	G	G	G	G
230	-	-	-	-	-	-	-	-	-	G	G	G	G	G	G	G	G	G	G	G
240	-	-	-	-	-	-	-	-	-	G	G	G	G	G	G	G	G	G	G	G
250	-	-	-	-	-	-	-	-	-	G	G	G	G	G	G	G	G	G	G	G
260	-	-	-	-	-	-	-	-	-	G	G	G	G	G	G	G	G	G	G	G
270	-	-	-	-	-	-	-	-	-	-	G	G	G	G	G	G	G	G	G	G
280	-	-	-	-	-	-	-	-	-	-	G	G	G	G	G	G	G	G	G	G
290	-	-	-	-	-	-	-	-	-	-	G	G	G	G	G	G	G	G	G	G
300	-	-	-	-	-	-	-	-	-	-	G	G	G	G	G	G	G	G	G	G
310	-	-	-	-	-	-	-	-	-	-	G	G	G	G	G	G	G	G	G	G
320	-	-	-	-	-	-	-	-	-	-	G	G	G	G	G	G	G	G	G	G
330	-	-	-	-	-	-	-	-	-	-	G	G	G	G	G	G	G	G	G	G
340	-	-	-	-	-	-	-	-	-	-	-	G	G	G	G	G	G	G	G	G
350	-	-	-	-	-	-	-	-	-	-	-	G	G	G	G	G	G	G	G	G
360	-	-	-	-	-	-	-	-	-	-	-	G	G	G	G	G	G	G	G	G
370	-	-	-	-	-	-	-	-	-	-	-	G	G	G	G	G	G	G	G	G
380	-	-	-	-	-	-	-	-	-	-	-	G	G	G	G	G	G	G	G	G
390	-	-	-	-	-	-	-	-	-	-	-	G	G	G	G	G	G	G	G	G
400	-	-	-	-	-	-	-	-	-	-	-	G	G	G	G	G	G	G	G	G

5 Conclusions

This thesis developed a techno-economic assessment of hydrogen production systems integrated in a biomass-fed industrial site, comparing the two options of gasification and electrolysis. The work considered an industrial case study, and it focused on exploiting the available surplus of biomass and/or of electricity, aiming at identifying solutions to maximize the return on investment. First, Electrolyzer shows optimal techno-economic performances with the alkaline technology and for sizes between 4.0-4.5 MW_e. While gasification plant optimal size results to be between 20-30 MW_{th} biomass input.

Then, some relevant differences emerged between the two configurations. Gasification process has low dependency on electricity cost compared to electrolysis, and it produces valuable tail gas which substitutes natural gas needed in the industrial site. However, its hydrogen production cost is significantly affected by biomasses costs that depend on their markets and availability, as well as the type of biomass.

Gasification configuration requires a greater investment, nevertheless it guarantees a greater hydrogen production. In fact, a 30 MW_{th} gasification plant can produce up to 2,558 t/y, i.e., much higher than the maximum production of 630 t/y from a 4.5 MW_e ALK electrolyzer. However, electrolysis configuration is the less risky solution given the lower required capital cost and the higher technology readiness. Besides, it also has a relevant smaller land footprint, i.e., the hydrogen production plant would require much less space.

A detailed analysis on profitability of investing in hydrogen production is carried out according to electricity, natural gas and H_2 prices. It shows that current relation of natural gas market with electricity cost as well as hydrogen price does not favor investment in green hydrogen production. Gasification configuration results profitable only for very high electricity and natural gas costs, as it is occurring after March 2022. However, it is an uncertain situation in the long run since these prices cannot be sustained, while lower prices for these energy vectors still disadvantage hydrogen production via gasification due to its high LCOH. The latter turns about 5.0 €/kg for 30 MW_{th} size gasification plant, and it is about constant considering current energy markets links. On the other side, electrolysis configuration can never achieve competitiveness with high electricity and hydrogen prices. In fact, hydrogen production cost via electrolysis mostly depends on electricity price, therefore it may result better than surplus electricity sale only when very low electricity prices and relatively high hydrogen prices are present. Between the performed simulation for both configurations according to last four years markets, hydrogen production results better than base case just via electrolysis for 2018, 2019 and 2020 in one specific case, i.e., when hydrogen is sold for transport application, since the equivalence cost per kilometers

with diesel heavy-duty vehicles gives a much higher H_2 price compared to other applications, such as injection in the natural gas grid and industrial uses. For instance, a LCOH of about 3.5 €/kg is achievable for a 4.5 MW_e electrolyzer, according to electricity and hydrogen prices in 2019.

To conclude, considering the case study from the company's point of view, today's energy markets instability and the absence of an incentive policy do not allow to say whether it will be profitable to invest in green H_2 production in 2030. Therefore, a further evaluation is needed close to that year to complete this work, hoping in more stable energy markets and incentives for either technology. In fact, according to technology characteristics and H_2 end application, proper incentives are needed to invest in one of these two technologies, even to cover uncertainty related to energy markets. However, it can be underlined that hydrogen production via gasification, if profitable, might be the best solution for the case study. Electrolysis results better than surplus electricity sale (current configuration) and/or H_2 production via gasification just for electricity prices lower than LCOE of CHP plants. Therefore, it should not be considered since the best option in that situation would be not to produce surplus electricity. While for electricity price higher than CHP plants LCOE, the investment in green hydrogen production is better via gasification or it is not profitable with either technology.

Finally, further studies on hydrogen production via gasification may include carbon dioxide valorization in order to understand its feasibility and its potential effect on techno-economic assessment, since CO_2 is already separated from the syngas stream, but it is currently considered to be vented in the atmosphere.

Bibliography

[1] "IEA (2021), Hydrogen, IEA, Paris." https://www.iea.org/reports/hydrogen (accessed Aug. 29, 2022).

[2] International Energy Agency- IEA, "The Future of Hydrogen."

[3] D. B. Pal, A. Singh, and A. Bhatnagar, "A review on biomass based hydrogen production technologies", *International Journal of Hydrogen Energy*, vol. 47, no. 3. Elsevier Ltd, pp. 1461–1480, Jan. 08, 2022. doi: 10.1016/j.ijhydene.2021.10.124.

[4] International Renewable Energy Agency, *GREEN HYDROGEN COST REDUCTION SCALING UP ELECTROLYSERS TO MEET THE 1.5°C CLIMATE GOAL*. 2020. [Online]. Available: www.irena.org/publications

[5] R. W. Howarth and M. Z. Jacobson, "How green is blue hydrogen?", *Energy Sci Eng*, vol. 9, no. 10, pp. 1676–1687, Oct. 2021, doi: 10.1002/ese3.956.

[6] M. C. Romano *et al.*, "Comment on 'How green is blue hydrogen?", *Energy Science and Engineering*. John Wiley and Sons Ltd, Jul. 01, 2022. doi: 10.1002/ese3.1126.

[7] R. W. Howarth and M. Z. Jacobson, "Reply to comment on 'How Green is Blue Hydrogen?'", *Energy Science and Engineering*. John Wiley and Sons Ltd, Jul. 01, 2022. doi: 10.1002/ese3.1154.

[8] "POLITECNICO DI MILANO Hydrogen separation and electricity production from product gas generated by biomass gasification", 2012, Master thesis.

[9] T. Lepage, M. Kammoun, Q. Schmetz, and A. Richel, "Biomass-to-hydrogen: A review of main routes production, processes evaluation and techno-economical assessment", *Biomass and Bioenergy*, vol. 144. Elsevier Ltd, Jan. 01, 2021. doi: 10.1016/j.biombioe.2020.105920.

[10] P. Parthasarathy and K. S. Narayanan, "Hydrogen production from steam gasification of biomass: Influence of process parameters on hydrogen yield - A review", *Renewable Energy*, vol. 66. Elsevier Ltd, pp. 570–579, Jul. 01, 2014. doi: 10.1016/j.renene.2013.12.025.

[11] A. Arregi, M. Amutio, G. Lopez, J. Bilbao, and M. Olazar, "Evaluation of thermochemical routes for hydrogen production from biomass: A review", *Energy Conversion and Management*, vol. 165. Elsevier Ltd, pp. 696–719, Jun. 01, 2018. doi: 10.1016/j.enconman.2018.03.089.

[12] A. Ghimire *et al.*, "A review on dark fermentative biohydrogen production from organic biomass: Process parameters and use of by-products", *Applied Energy*, vol. 144. Elsevier Ltd, pp. 73–95, Apr. 05, 2015. doi: 10.1016/j.apenergy.2015.01.045.

[13] Y. Liu, R. Lin, Y. Man, and J. Ren, "Recent developments of hydrogen production from sewage sludge by biological and thermochemical process", *International Journal of Hydrogen Energy*, vol. 44, no. 36. Elsevier Ltd, pp. 19676–19697, Jul. 26, 2019. doi: 10.1016/j.ijhydene.2019.06.044.

[14] G. Kumar *et al.*, "Biomass based hydrogen production by dark fermentation — recent trends and opportunities for greener processes", *Current Opinion in Biotechnology*, vol. 50. Elsevier Ltd, pp. 136–145, Apr. 01, 2018. doi: 10.1016/j.copbio.2017.12.024.

[15] H. Wang, J. Xu, L. Sheng, X. Liu, Y. Lu, and W. Li, "A review on bio-hydrogen production technology", *International Journal of Energy Research*, vol. 42, no. 11. John Wiley and Sons Ltd, pp. 3442–3453, Sep. 01, 2018. doi: 10.1002/er.4044.

[16] "HYDROGEN INNOVATION REPORT 2021 Le sfide per la creazione di un mercato dell'idrogeno." [Online]. Available: www.energystrategy.it

[17] FRAUNHOFER Ise, "COST FORECAST FOR LOW TEMPERATURE ELECTROLYSIS-TECHNOLOGY DRIVEN BOTTOM-UP PROGNOSIS FOR PEM AND ALKALINE WATER ELECTROLYSIS SYSTEMS."

[18] J. Karl and T. Pröll, "Steam gasification of biomass in dual fluidized bed gasifiers: A review", *Renewable and Sustainable Energy Reviews*, vol. 98. Elsevier Ltd, pp. 64–78, Dec. 01, 2018. doi: 10.1016/j.rser.2018.09.010.

[19] "Comparison of biomass gasification & DME production 2018", Master thesis, Politecnico di Milano.

[20] V. Belgiorno, G. de Feo, C. della Rocca, and R. M. A. Napoli, "Energy from gasification of solid wastes", *Waste Management*, vol. 23, no. 1, pp. 1–15, 2003, doi: 10.1016/S0956-053X(02)00149-6.

[21] V. S. Sikarwar, M. Zhao, P. S. Fennell, N. Shah, and E. J. Anthony, "Progress in biofuel production from gasification", *Progress in Energy and Combustion Science*, vol. 61. Elsevier Ltd, pp. 189–248, 2017. doi: 10.1016/j.pecs.2017.04.001.

[22] C. Pfeifer, S. Koppatz, and H. Hofbauer, "Steam gasification of various feedstocks at a dual fluidised bed gasifier: Impacts of operation conditions and bed materials", *Biomass Convers Biorefin*, vol. 1, no. 1, pp. 39–53, Mar. 2011, doi: 10.1007/s13399-011-0007-1.

[23] J. Corella, J. M. Toledo, and G. Molina, "A review on dual fluidized-bed biomass gasifiers", in *Industrial and Engineering Chemistry Research*, Oct. 2007, vol. 46, no. 21, pp. 6831–6839. doi: 10.1021/ie0705507.

[24] M. Binder, M. Kraussler, M. Kuba, and M. Luisser, *Hydrogen from biomass gasification*.

[25] Schmid, J.C., Benedikt, F., Fuchs, J. et al. Syngas for biorefineries from thermochemical gasification of lignocellulosic fuels and residues—5 years'

experience with an advanced dual fluidized bed gasifier design. Biomass Conv. Bioref. 11, 2405–2442 (2021). https://doi.org/10.1007/s13399-019-00486-2

[26] F. Benedikt, J. C. Schmid, J. Fuchs, A. M. Mauerhofer, S. Müller, and H. Hofbauer, "Fuel flexible gasification with an advanced 100 kW dual fluidized bed steam gasification pilot plant", *Energy*, vol. 164, pp. 329–343, Dec. 2018, doi: 10.1016/j.energy.2018.08.146.

[27] V. Krishnamoorthy and S. v. Pisupati, "A critical review of mineral matter related issues during gasification of coal in fixed, fluidized, and entrained flow gasifiers", *Energies*, vol. 8, no. 9. MDPI AG, pp. 10430–10463, 2015. doi: 10.3390/en80910430.

[28] J. Li, Y. Yin, X. Zhang, J. Liu, and R. Yan, "Hydrogen-rich gas production by steam gasification of palm oil wastes over supported tri-metallic catalyst", *Int J Hydrogen Energy*, vol. 34, no. 22, pp. 9108–9115, Nov. 2009, doi: 10.1016/j.ijhydene.2009.09.030.

[29] C. Pfeifer, R. Rauch, and H. Hofbauer, "In-Bed Catalytic Tar Reduction in a Dual Fluidized Bed Biomass Steam Gasifier", *Ind Eng Chem Res*, vol. 43, no. 7, pp. 1634–1640, Mar. 2004, doi: 10.1021/ie030742b.

[30] A. M. Parvez, S. Hafner, M. Hornberger, M. Schmid, and G. Scheffknecht, "Sorption enhanced gasification (SEG) of biomass for tailored syngas production with in-situ CO2 capture: Current status, process scale-up experiences and outlook", *Renewable and Sustainable Energy Reviews*, vol. 141, May 2021, doi: 10.1016/j.rser.2021.110756.

[31] K. Fürsatz, J. Fuchs, F. Benedikt, M. Kuba, and H. Hofbauer, "Effect of biomass fuel ash and bed material on the product gas composition in DFB steam gasification", *Energy*, vol. 219, Mar. 2021, doi: 10.1016/j.energy.2020.119650.

[32] "POLITECNICO DI MILANO Techno-Economic Assessment & Life Cycle Assessment for Methanol Production through Biomass Gasification", 2019, Master thesis.

[33] H. Boerrigter *et al.*, "Tar removal from biomass product gas; development and optimisation of the OLGA tar removal technology T TAR REMOVAL FROM BIOMASS PRODUCT GAS; DEVELOPMENT AND OPTIMISATION OF THE OLGA TAR REMOVAL TECHNOLOGY", 2005. [Online]. Available: www.dahlman.nl

[34] Kraussler Michael - 2018 – "Evaluation of dual fluidized bed biomass gasification plants generating electricity, valuable gases, and district heating", TU Wien, Doctoral thesis.

[35] Hydrogen Europe, "Strategic Research and Innovation Agenda Final Draft" (SRIA), 2020.

[36] A. Buttler and H. Spliethoff, "Current status of water electrolysis for energy storage, grid balancing and sector coupling via power-to-gas and power-to-liquids: A review", *Renewable and Sustainable Energy Reviews*, vol. 82. Elsevier Ltd, pp. 2440–2454, Feb. 01, 2018. doi: 10.1016/j.rser.2017.09.003.

[37] "HYDROGEN INNOVATION REPORT 2021 Le sfide per la creazione di un mercato dell'idrogeno." [Online]. Available: www.energystrategy.it

[38] O. Schmidt, A. Gambhir, I. Staffell, A. Hawkes, J. Nelson, and S. Few, "Future cost and performance of water electrolysis: An expert elicitation study", *Int J Hydrogen Energy*, vol. 42, no. 52, pp. 30470–30492, Dec. 2017, doi: 10.1016/j.ijhydene.2017.10.045.

[39] "STUDY ON EARLY BUSINESS CASES FOR H2 IN ENERGY STORAGE AND MORE BROADLY POWER TO H2 APPLICATIONS", 2017.

[40] A. Patonia and R. Poudineh, "*Cost-competitive green hydrogen: how to lower the cost of electrolysers?*", Oxford Institute for Energy Studies, 2022

[41] C. Kost, S. Shammugam, V. Jülch, H.-T. Nguyen, and T. Schlegl, "LEVELIZED COST OF ELECTRICITY RENEWABLE ENERGY TECHNOLOGIES", 2018. [Online]. Available: www.ise.fraunhofer.de

[42] Trinomics B.V. and Europaïsche Kommission DG ENV - Generaldirektion Umwelt, "*Cost of energy (LCOE) energy costs, taxes and the impact of government interventions on investments: final report*."

[43] International Renewable Energy Agency, "RENEWABLE ENERGY TECHNOLOGIES: COST ANALYSIS SERIES Biomass for Power Generation Acknowledgement", 2012. [Online]. Available: www.irena.org/Publications

[44] S. Mueller, *"Hydrogen from Biomass for Industry-Industrial Application of Hydrogen Production Based on Dual Fluid Gasification."* 2013. [Online]. Available: http://www.ub.tuwien.ac.athttp://www.ub.tuwien.ac.at/eng

[45] G. Guandalini, A. Poluzzi, and M. Romano, "HORIZON 2020 PROGRAMME RESEARCH and INNOVATION ACTION Flexible Dimethyl ether production from biomass gasification with sorption enhanced processes WP 4-Deliverable D4.1: Preliminary process simulations Dissemination level PU Track changes."

[46] "Phyllis biomasses database." https://phyllis.nl/ (accessed Aug. 29, 2022).

[47] A. Larsson, I. Gunnasrsson, and F. Tengberg, "The GoBiGas Project Demonstration of the Production of Biomethane from Biomass via Gasification."

[48] M. Ruth, "Hydrogen Production Cost Estimate Using Biomass Gasification: Independent Review", 2010. [Online]. Available: http://www.osti.gov/bridge

[49] S. Francisco, "Equipment Design and Cost Estimation for Small Modular Biomass Systems, Synthesis Gas Cleanup, and Oxygen Separation Equipment; Task 2: Gas Cleanup Design and Cost Estimates -- Wood Feedstock", 2006. [Online]. Available: http://www.osti.gov/bridge

[50] W. L. Becker, R. J. Braun, M. Penev, and M. Melaina, "Design and technoeconomic performance analysis of a 1 MW solid oxide fuel cell polygeneration system for combined production of heat, hydrogen, and power", *J Power Sources*, vol. 200, pp. 34–44, Feb. 2012, doi: 10.1016/j.jpowsour.2011.10.040.

[51] Università di Bologna, Master thesis "Analisi tecno-economica relativa all'integrazione di un impianto di digestione anaerobica con tecnologie a idrogeno".

[52] F. Bauer, T. Persson, C. Hulteberg, and D. Tamm, "Biogas upgrading - technology overview, comparison and perspectives for the future", *Biofuels, Bioproducts and Biorefining*, vol. 7, no. 5, pp. 499–511, Sep. 2013, doi: 10.1002/bbb.1423.

[53] A. Christensen and A. Co, "Assessment of Hydrogen Production Costs from Electrolysis: United States and Europe."

[54] "Innovative large-scale energy storage technologies and Power-to-Gas concepts after optimisation Report on the costs involved with PtG technologies and their potentials across the EU", 2018.

[55] "H2A Hydrogen Delivery Infrastructure Analysis Models and Conventional Pathway Options Analysis Results", 2008.

[56] F. Mueller-Langer, E. Tzimas, M. Kaltschmitt, and S. Peteves, "Techno-economic assessment of hydrogen production processes for the hydrogen economy for the short and medium term", *Int J Hydrogen Energy*, vol. 32, no. 16, pp. 3797–3810, Nov. 2007, doi: 10.1016/j.ijhydene.2007.05.027.

[57] C. van Leeuwen and M. Mulder, "Power-to-gas in electricity markets dominated by renewables", *Appl Energy*, vol. 232, pp. 258–272, Dec. 2018, doi: 10.1016/j.apenergy.2018.09.217.

[58] "Gestore mercati energetici (GME)." https://www.mercatoelettrico.org/it/ (accessed Aug. 29, 2022).

[59] A. Zauner, H. Böhm, D. C. Rosenfeld, and R. Tichler, "Innovative large-scale energy storage technologies and Power-to-Gas concepts after optimization Analysis on future technology options and on techno-economic optimization", 2019.

[60] O. Delgado *et al.*, "Fuel eFFiciency Technology in european heavy-DuTy vehicles: Baseline anD poTenTial For The 2020-2030 Time Frame", 2017. [Online]. Available: www.theicct.org

[61] "201211 FCH HDTruck - Study Report_final_vs".

[62] "Clean Hydrogen JU SRIA - approved by GB".

[63] "Path to hydrogen competitiveness A cost perspective", 2020. [Online]. Available: www.hydrogencouncil.com.

[64] "MISE website." https://dgsaie.mise.gov.it/open-data (accessed Sep. 04, 2022).

[65] W. Huang, D. Zheng, H. Xie, Y. Li, and W. Wu, "Hybrid physical-chemical absorption process for carbon capture with strategy of high-pressure absorption/medium-pressure desorption", *Appl Energy*, vol. 239, pp. 928–937, Apr. 2019, doi: 10.1016/j.apenergy.2019.02.007.

List of Figures

List of Tables

List of symbols and acronyms

Variable	Description	Unit
AC	Alternated current	-
AEM	Anion exchange membrane	-
AER	Absorption enhanced reforming	-
ALK	Alkaline	-
aMDEA	Activated methyl-diethanolamine	-
BFB	Bubbling fluidized bed	-
BoP	Balance of plant	-
C_f	Capacity factor	%
C_p	Specific heat at P=const.	kJ/kg K
CFB	Circulating fluidized bed	-
CGE	Cold gas efficiency	%
CHP	Combined Heat & Power	-
DAM	Day ahead market	-
DC	Direct current	-
DEA	diethanolamine	-
DFB	Dual fluidized bed	-
E_{el}	Electricity	-
e	Efficiency	MWh_e/kg_{H2}
FCEV	Fuel cell electric vehicle	-
GDL	Gas diffusion layer	-

GHG	Greenhouse gases	-
HRS	Hydrogen refueling station	-
HT	High temperature	-
J	Current density	A/cm^2
KPI	Key performance indicator	-
LCOE	Levelized cost of electricity	€/MWh
LCOH	Levelized cost of hydrogen	€/kg
LHC	Light hydrocarbons	-
LHV	Lower heating value	MJ/kg
LT	Low temperature	-
LT	Lifetime	h
MDEA	methyl-diethanolamine	-
MEA	mono-ethanolamine	-
MEA	Membrane electrode assembly	-
MPL	Microporous layer	-
MTZ	Mass transfer zone	-
NCF	Net cash flow	€
NG	Natural gas	-
NPV	Net present value	€
OH	Yearly operating hours	h/y
PBP	Payback period	y
p	pressure	Pa
P	Price	-
P_{el}	Electric power	MW_e

PEM	Proton exchange membrane	-
PI	Profitability index	-
PTL	Porous transport layer	-
PZ	Piperazine	-
RH	Relative humidity	%
RME	Rapeseed oil methyl ester	-
SB	Steam to Biomass ratio	-
SER	Sorption enhanced reforming	-
SOEL	Solid oxide electrolyzer	-
T	Temperature	K
TRL	Technology readiness level	-
TV	Terminal value	€
WGS	Water gas shift	-
WTP	Willingness to pay	€/MWh
η_{tot}	Biomass-to-H_2 total efficiency including by-products (tail gas)	%

Acknowledgments

Foremost, I would like to thank "Sustainable Energy Center" at Fondazione Bruno Kessler (FBK) that gave me this internship opportunity in a such positive and enriching working environment. I thank all the people met during these six months, especially my sincere gratitude goes to my tutor, Dr. Eleonora Cordioli, for her great support and constant availability.

Furthermore, I would like to express my gratitude to my PoliMi advisor, Dr. Paolo Colbertaldo, for his precious advices which enriched the work developed in this thesis.

Special thanks to all the people met during my university career in the last five years, we have grown sharing great experiences and joys, as well as tough times.

Last but not least, a huge thank to my family which allowed this journey along my studies with love and unconditional support.